Physiological and Behavioral Consequences of Activity-Dependent Agrin Cleavage by Neurotrypsin

Dissertation

zur

Erlangung der naturwissenschaftlichen Doktorwürde

(Dr. sc. nat.)

vorgelegt der

Mathematisch-naturwissenschaftlichen Fakultät

der

Universität Zürich

von

Ewa Sokolowska

aus

Polen

Promotionskomitee:

Prof. Dr. Peter Sonderegger (Vorsitz)

Prof. Dr. David Wolfer

Prof. Dr. Jean-Marc Fritschy

Zurich 2011

Die vorliegende Arbeit wurde von der Mathematisch-naturwissenschaftlichen Fäkultät der Universität Zürich in Herbstsemester 2011 als Dissertation angenommen.

Promotionskomitee: Prof. Dr. Peter Sonderegger (Vorsitz)

Prof. Dr. David Wolfer

Prof. Dr. Jean-Marc fritschy

Abbreviations

AAMR	American Association on Mental Retardation
AChR	acetylcholine receptor
ADHD	attention deficit hyperactivity disorder
AMPAR	α-amino-3-hydroxy-5-methyl-4-isoxazolepropionic acid receptor
ATX	ω-agatoxin
BDNF	brain-derived neurotrophic factor
cAMP	cyclic adenosine monophosphate
CCP	conditioned cue preference
CNQX	6-cyano-7-nitroquinoxaline-2,3-dione
CNS	central nervous system
CR	conditioned response
CREB	cAMP response element-binding
CS	conditioned stimulus
CTX	ω-conotoxin
DLS	dorsolateral striatum
DMS	dorsomedial striatum
DS	Down syndrome
DSM-IV	Diagnostic and Statistical Manual of Mental Disorders IV
FMR1	fragile X mental retardation gene
fMRI	functional magnetic resonance imaging
FMRP	fragile X mental retardation protein
FXS	fragile X chromosome syndrome
IMST	interactive memory systems theory
IQ	intelligence quotient
kDa	kilodalton
LTD	long-term depression
LTP	long-term potentiation

MK801	dizocilpine
MMS	multiple memory systems
MR	mental retardation
NMDAR	N-methy-D-aspartic acid receptor
NMJ	neuromuscular junction
NS	neutral stimulus
NSMR	non-syndromic mental retardation
NT	neurotrypsin
NtA	N-terminal agrin domain
OCD	obsessive-compulsive disorder
PKA	protein kinase A
PKC	protein kinase C
PMR	profound mental retardation
PSD	postsynaptic density
SER	smooth endoplasmic reticulum
SMR	syndromic mental retardation
SRCR	scavenger receptor cystein-rich repeat
TM-agrin	transmembrane agrin
tPA	tissue type-plasminogen activator
uPA	urokinase-plasminogen activator
UR	unconditioned response
US	unconditioned stimulus
VGCC	voltage-gated calcium channels

Publications and abstracts

Publications related with this thesis

Matsumoto-Miyai K., **Sokolowska E**., Zurlinder A., Gee C.E., Lüscher D., Hettwer S., Wölfel J., Ladner A.P., Ster J., Gerber U., Rülicke T., Kunz B. and Sonderegger P. Coincident Pre- and Postsynaptic Activation Induces Dendritic Filopodia via Neurotrypsin-Dependent Agrin Cleavage. Cell 136, 1161-1171, March 20, 2009

Sokolowska E., Molinari F., Kunz B., Wolfer D. and Sonderegger P. Neurotrypsin/agrin interaction and its role in learning and memory (*in preparation*)

Related abstracts

Sokolowska E., Kunz B., Wölfel D. and Sonderegger P. Behavioral Phenotyping of Neurotrypsin-Deficient Mice. (2011) NCCR Neuro Symposium Ittingen, Switzerland (*Meeting abstract*)

Sokolowska E., Matsumoto-Miyai K., Gerber U., Zurlinder A., Kunz B. and Sonderegger P. Studies on the Role of Na/K-ATPase in Neurotrypsin/Agrin-Dependent Formation of Dendritic Filopodia. (2010) NCCR Neuro Symposium Berlingen, Switzerland (*Meeting abstract*)

Sokolowska E., Matsumoto-Miyai K., Wölfel J., Lüscher D., Ladner A.P., Gerber U., Gee C., Rülicke T., Kunz B. and Sonderegger P. LTP-Associated Promotion of Dendritic Filopodia is Regulated by Activity-Dependent Cleavage of Agrin by Neurotrypsin. (2009) NCCR Symposium Berlingen, Switzerland (*Meeting abstract*)

Sokolowska E., Matsumoto-Miyai K., Wölfel J., Lüscher D., Ladner A.P., Gerber U., Gee C., Rülicke T., Kunz B. and Sonderegger P. LTP-Associated Promotion of Dendritic Filopodia is Regulated by Activity-Dependent Cleavage of Agrin by Neurotrypsin. (2008) Neuroscience Centre Symposium Zurich, Switzerland (*Meeting abstract*)

Sokolowska E., Matsumoto-Miyai K., Wölfer J., Lüscher D., Ladner A.P., Gerber U., Gee C., Rülicke T., Kunz B. and Sonderegger P. Long Term Potentiation (LTP)-Associated Promotion of Dendritic Filopodia is Regulated by Activity-Dependent Cleavage of Agrin by Neurotrypsin (2008) 6th FENS Forum of European Neuroscience Geneva, Switzerland (*Meeting abstract*)

Additional publications

Frazzetto G., Di Lorenzo G., Carola V., Proietti L., **Sokolowska E.**, Siracusano A., Gross C. & Troisi A. Early trauma and increase risk for physical aggression during adulthood: moderating role of MAOA genotype. PLoS ONE. 2007 May 30; 2:e 486

Declaration of my own contributions to the projects of my thesis:

I. Activity-Dependent Formation of Dendritic Filopodia

- Exocytosis of NT as a response to presynaptic activation. *****
- Western blot analysis of the agrin cleavage by NT. *****
- Establishment of chemical stimulation protocols. *****
- Western blot analysis (agrin-90) of the response to the postsynaptic inhibition in the P10 whole hippocampi of the wild-type mice.******
- LTP-associated formation of dendritic filopodia in hippocampal slices from wild-type and NT-deficient mice after inhibition of postsynaptic activity.******
- Dendritic filopodia formation analysis after administration of agrin-22.******

II. Behavioral Phenotyping of the Neurotrypsin-Deficient Mice

- All behavioral tests were performed by me, except the1st series of classical Morris water-maze tests, which was performed and analyzed by Dr. Florence Molinari.
- The statistics of the two-cue water-maze, fear extinction, 1st series of classical fear conditioning and 2nd series of classical Morris water-maze was analyzed by Prof. David Wolfer.
- The rest of the statistics was analyzed be me.

* Performed and analyzed by Dr. Kazumasa Matsumoto-Miyai

** Above tests were performed and analyzed be me.

TABLE OF CONTENTS

Summary

The trypsin-like serine protease neurotrypsin is expressed in various tissues including the central nervous system. The most prominent expression of neurotrypsin was found in the cerebral cortex, the hippocampus, and the amygdale, structures engaged in the processing and storage of memories and learned behaviors. Study characterizing a 4 base pair deletion in the neurotrypsin gene as the cause of severe mental retardation indicated that neurotrypsin is involved in neuronal plasticity. Immunoelectron microscopy showed that neurotrypsin is localized within presynaptic terminals and live imagining revealed that its exocytosis is regulated in an activity-dependent manner. Further investigations identified the heparan sulfate proteoglycan agrin as the unique proteolytic substrate for neurotrypsin and revealed that neurotrypsin cleaves agrin at two conserved sides, resulting in the release of a 90 kDa (agrin-90) and 22 kDa (agrin-22) fragments. The overexpression of agrin in rat hippocampal neurons resulted in the formation of filopodia-like protrusions on axons and dendrites. In the first part of my thesis, we studied whether agrin cleavage is involved in activity-dependent generation of filopodia. Induction of long-term potentiation (LTP), using two types of the chemical stimulation, confirmed that cleavage of agrin by externalized neurotrypsin requires postsynaptic activation. In neurotrypsin-deficient mice LTP was intact, but LTP-associated formation of dendritic filopodia was abolished. Administration of agrin-22 restored the LTP-induced increase of filopodia in neurotrypsin-deficient mice.

The second part of my thesis was devoted to the characterization of the behavioral phenotype of neurotrypsin-deficient mice. Experiments in the Morris water-maze revealed the elevated acquisition of spatial orientation skills, which was most pronounced in the so-called reversal learning phase, in which a previously learned solution of a task becomes unsuccessful and has to be replaced by learning of a new solution.

These data, suggest that the neurotrypsin/agrin interaction system serves a homeostasis role in learning and memory. We speculate that the lack of neurotrypsin, thus absence of agrin-22, results in a deficiency of activity-dependent filopodia formation, which in turn may cause a weaker memory trace during the initial acquisition learning phase. Subsequent learning of a distinct solution to the task becomes easier for these mice, because the weaker memory trace established during the initial acquisition phase exerts a lesser impeding effect on the learning and the consolidation of the new solution.

Zusammenfassung

Die Trypsin-ähnliche Serinprotease Neurotrypsin wird in verschiedenen Geweben, einschliesslich des Zentralnervensystems, exprimiert. Die stärkste Expression von Neurotrypsin wurde im zerebralen Kortex, dem Hippokampus und der Amygdala gefunden. Alle diese Strukuturen sind involviert in die Verarbeitung und Speicherung von Erinnerungen und lernfähigen Verhaltensweisen. Eine Studie fand einen kausalen Zusammenhang zwischen dem Verlust von 4 Basenpaaren innerhalb des Neurotrypsingens und schwerwiegender geistiger Behinderung. Dieses Resultat legte den Schluss nahe, dass Neurotrypsin in plastische Vorgänge innerhalb des Gehirns involviert sein könnte. Elektronenmikroskopische Aufnahmen, basierend auf immunologischer Detektion von Neurotrypsin, zeigten, dass die Protease in präsynaptischen Nervenendigungen angereichert ist. Mit Hilfe von Lebendzellmikroskopie konnte weiterhin gezeigt werden, dass die Freisetzung von Neurotrypsin in aktivitätsabhängiger Weise geschieht. Eine daran anschliessende Studie identifizierte das Proteoglycan Agrin als bisher einziges Substrat für Neurotrypsin. Neurotrypsin schneidet Agrin an zwei konservierten Spaltstellen und bewirkt die Freisetzung eines 90 kDa (Agrin-90), sowie eines 22 kDa (Agrin-22)-Fragmentes. Überexpression von Agrin in hippokampalen Neuronen der Ratte, führte zur Bildung von Filopodien-ähnlichen Fortsätzen an Axonen und Dendriten.

Im ersten Teil meiner Doktorarbeit untersuchten wir, ob die proteolytische Spaltung von Agrin und die aktivitätsabhängige Entstehung von Filopodien in einem direkten Zusammenhang stehen. Die Aktivierung von Langzeitpotenzierung (LTP) durch zwei Arten von chemischer Stimulierung bestätigte, dass das Schneiden von Agrin durch präsynaptisch freigesetztes Neurotrypsin eine postsynaptische Aktivierung benötigt. Mäuse mit Neurotrypsin-Defizienz zeigten eine normale LTP, jedoch fehlte bei ihnen die mit LTP verbundene Bildung von Filopodien. Durch Zugabe von Agrin-22 liess sich die LTP-abhängige Zunahme von Filopodien in Mäusen mit Neurotrypsin-Defizienz wiederherstellen.

Der zweite Teil meiner Arbeit befasste sich mit der Charakterisierung von Verhaltensphänotypen bei Mäusen mit Neurotrypsin-Defizienz. In Experimenten mit der Morris water-maze (Morris Wasser-Labyrinth) zeigten Neurotrypsin-defiziente Mäuse eine erhöhte Fähigkeiten zur räumlichen Orientierung, welche sich am deutlichsten während der Phase des Umlernens (sog. „reversal learning phase“) abzeichnete, in welcher eine vorgängig gelernte Lösung einer Aufgabe nicht mehr funktioniert und durch das Erlernen einer neuen Lösung ersetzt werden muss. Basierend auf diesen Daten vermuten wir, dass die Interaktion zwischen Neurotrypsin und Agrin eine homöostatische

Rolle in Lern- und Gedächtnisprozessen spielen könnte. Ein Mangel an Neurotrypsin und das damit verbunden Fehlen von Agrin-22 verhindern die aktivitätsabhängige Bildung von Filopodien, was in der Folge zu einer weniger stark ausgeprägten Gedächtnisspur während der initialen Erfassungsphase (initial acquisition phase) führen könnte. Wir vermuten, dass das verbesserte Umlernen bei Neurotrypsin-Mangel deshalb zustande kommt, weil das Vorliegen einer schwächeren Gedächtnisspur aus der initialen Erfassungsphase den Umlernprozess mit der damit verbundenen Neu-Etablierung einer unterschiedlichen Lösung der Aufgabe weniger stark verzögert.

1 INTRODUCTION

1.1 Mental retardation

Mental retardation (MR) is a significant impairment in cognitive functions with an Intelligence Quotient (IQ) score under 70. It affects 1-3 % of the North American population (Organization 2010). MR is a complex multifactorial disability, often presenting unknown and ambiguous symptoms that make diagnosis difficult. MR is often accompanied by a number of deficits in adaptive behavior such as daily living skills, communication or social skills that have their onset already in childhood. For a comparison, according to scoring developed in 1916 by Lewis Terman, people with normal/average intelligence are characterized by an IQ level of 90-109. Whereas, people with an IQ level above 110 are considered to possess superior intelligence. Terman's tests to measure intellectual capacity were based on language, vocabulary, numeric reasoning, memory and analytical skills (Terman 1916).

1.1.1 Classification

According to the *Diagnostic and Statistical Manual of Mental Disorders* (DSM-IV) created by the *American Psychiatry Association* (Irwin et al) MR is classified into various developmental disabilities. Correct diagnosis has to meet three criteria: IQ below 70 (scored using the *Wechsler Intelligence Score for Children* or for *Adults*), significant limitations in adaptive behavior, and evidence that these limitations became apparent before the age of eighteen (Wines 2006).

There are several methods to categorize MR. One of them is presence of additional disabilities or lack of some basic abilities. According to this classification MR is characterized as non–syndromic (NSMR), which is the most common cognitive dysfunction, with no changes in brain morphology and no other clinical symptoms. In contrast, syndromic MR (SMR) is combined with other physical and/or behavioral changes. The most common classification, however, is based on IQ level. If the child shows problems with motor skills, language learning, or develops slower then their peer's, then parents might suspect MR. In mild MR (50 > IQ < 70) symptoms might be recognized late and in many cases mitigated with appropriate therapy. Mild MR represents about 85% of all cases. People with this degree of MR can become self-sufficient and, even live independently. People with more

severe signs (moderate MR; IQ < 50) need intensive support and supervision during their entire life. They comprise about 10% of all cases. About 3-4% of the MR population is affected by severe MR (SMR), where IQ oscillates between 20 and 40. They are able to develop basic self-care and communication skills. A high percentage of all SMR cases are syndromic. The most severe type of MR is profound MR (PMR) that occurs only in 1-2% of all cases. Patients with PMR are able to develop only very basic self-care skills and need a high level of supervision. A high percentage of both SMR and PMR cases are syndromic (Niemeijer et al 2010).

Another new and widely accepted diagnostic classification was established by the *American Association on Mental Retardation* (AAMR). It is based on the capabilities to self-care. Each category describes a level of support required by a retarded patient. Support needed only occasionally is called *intermittent* and it is characteristic for mildly retarded individuals. Classification goes through *limited* and *extensive* support to the last level, *pervasive* support, which is associated with profound retardation (Pamela 2004).

1.1.2 Environmental and genetic background

There are many different causes of MR, including both biological and environmental, among them:

- Prenatal illnesses and issues
- Childhood illnesses and injuries
- Other environmental factors
- Genetics.

One of the most common prenatal causes of MR is alcohol abuse by pregnant women known as *fetal alcohol syndrome* (Pittenger et al). The first cases were recorded in 1973; for comprehensive review see: (Jones 2003). Children show pre- and postnatal growth deficiency, developmental delay, motor dysfunction and facial dysmorphism. A positive correlation between alcohol abuse and *Attention Deficit Hyperactivity Disorder* (ADHD) was also found (Bradley H. Smith 2002). The presence of alcohol during neuronal development severely affects a child's CNS, often causing neural tube defects (Ornoy & Ergaz 2010).

Numerous studies have shown that accumulation of toxic substances during pregnancy and in early life may affect N-methyl-D-aspartic acid (NMDAR) function resulting in

impairment in hippocampal long-term potentiation (LTP) (Nihei et al 2000; Toscano & Guilarte 2005). Pb^{2+} exposure during gestation and throughout the postnatal period may result in decreased neurogenesis in dentate gyrus (Stern M.). A reduction in the length of apical dendrites in the CA3 region was also observed (Verina et al 2007). Dendrites play an essential role in neuronal signaling. Therefore, any aberration in dendrites morphology may alter their function. Additional prenatal risk factors include maternal infection with rubella virus, cytomegalovirus, or toxoplasmosis (Stern M. 1969).

After birth a child's CNS is functional and almost completely developed, but still exposed to environmental threats. During the early postnatal period, numerous factors can have a high impact on the proper formation of the neural circuit's, influencing appropriate interaction between environmental stimuli and the genes responsible for cell differentiation, amongst others. Animal studies show that early maternal isolation can affect the structure of CA1 pyramidal neurons associated with the physiology of the hippocampus formation. These changes result in a deficit of cognitive processes such as learning and memory (Bartesaghi et al 2003). Other postnatal risk factors are illnesses, i.e., chickenpox, *Haemophilus influenzae* type b (Otmakhov et al) or hyperthyroidism.

Another common risk factor is early infection of the membrane covering the brain (meningitis) causing swelling that, in turn, leads to brain damage and MR. Traumatic brain injuries caused by a blow or a violent shake to the head may also result in brain damage and MR in children.

Genetic factors causing MR can be classified according to the location and size of the mutation (Fig. 1.1). The most frequent form of inherited MR is *fragile X chromosome syndrome* (FXS), characterized by changes in social behavior, anxiety, emotional problems, difficulties in keeping eye contact, and autistic–like behavior (Hall et al 2008; Hessl et al 2009). FXS is caused by an expanded CGG trinucleotide repeat on the long arm of the X chromosome (Xq27.3).

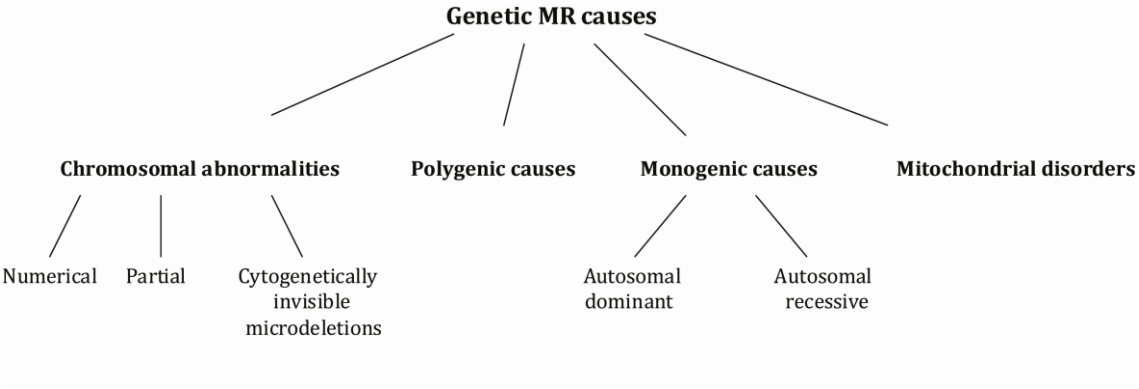

Fig. 1.1 Overview of types of genetic causes of mental retardation

Genetic causes can be divided into four main groups: chromosomal abnormalities, monogenic causes, polygenic causes, and mitochondrial disorders. Adapted from (Winnepenninckx B. 2003).

Methylation of the CpG island suppresses the Fragile X Mental Retardation 1 gene (FMR1), which significantly effects, or causes a complete absence of the fragile X MR protein (FMRP). Lack of FMRP significantly affects various pathways in the developing brain, leading to developmental delay (Schneider et al 2009). Human and mice studies demonstrated that abnormal morphological structure of dendritic spines and lack of its maturation in FXS subjects is directly correlated with cognitive impairment. Most FXS patients present with morphological changes in brain structures; namely reduced amygdale volume, smaller cerebral vermis or enlarged caudate nucleus (Comery et al 1997).

Recently, a number of studies have indicated an important role of serine proteases in the CNS (Molinari et al 2002; Scarisbrick et al 2002). Enzymes containing serine as one of the amino acids at the active site belong to the serine protease family. They seem to have an impact on neuronal development and are crucial in the adult brain as regulators of neuronal survival and plasticity. For instance, plasminogen, after its activation by urokinase-plasminogen activator(uPA) (Thompson & Krupa) and tissue type–plasminogen activator (tPA), becomes responsible for the remodeling of synaptic connections (Gingrich & Traynelis 2000). Another example is neuropsin, a serine protease expressed only in the amygdala and the pyramidal or magnocellular hippocampal neurons. Activity–dependent cleavage of the presynaptic cell adhesion molecule L1 by neuropsin is crucial for early phase LTP (Matsumoto-Miyai et al 2003). Recently, a 4 base pair (bp) deletion in exon 7 of PRSS12 gene coding trypsin-like serine protease, thus neurotrypsin (NT) was found responsible for non syndromic MR. This mutation causes a premature stop codon resulting in a truncated form of NT. The mutation was discovered in four children of an Algerian

family of whom the parents where first-degree cousins, this suggested an autosomal-recessive pattern of heredity (Fig. 1.2) (Molinari et al 2002).

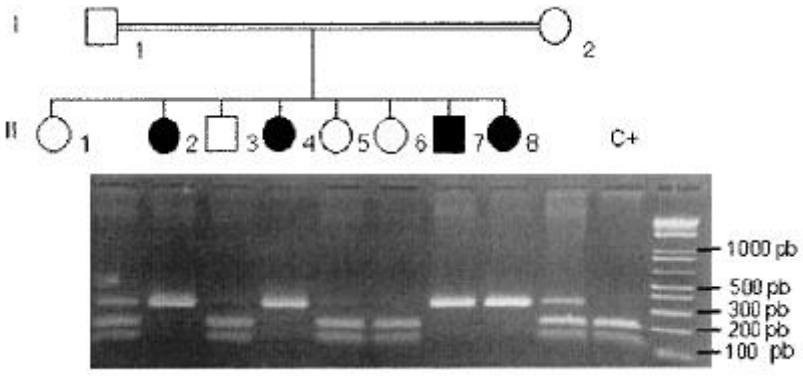

Fig. 1.2 Mutational analysis of neurotrypsin

Simplified pedigree and restriction analysis of the amplified neurotrypsin exon 7. The mutation abolished an Aat II site so that the amplified 370-bp fragment could not be cleaved into the 235-bp and 135-bp fragment. Modified from (Molinari et al 2002)

The affected children develop severe MR, which starts to become evident by the child's second year. We can assume that NT is crucial for adaptive synaptic function rather than synaptogenesis itself. These findings in conjunction with previous studies indicate a significant role of the serine protease family on the CNS.

So, is there a good way to prevent MR? The answer is as complex as the disease. First of all, good prenatal care; mothers should be educated about risk factors. Test such as amniocentesis and ultrasonography can be performed during the prenatal period. After birth, newborn screening and regular pediatric check-ups are highly recommended.

1.2 Characteristics of the neurotrypsin/agrin interaction

1.2.1 Neurotrypsin in the CNS

Neurotrypsin (NT) belongs to the trypsin-like serine protease family. It is a 761 amino acids mosaic protein composed of proline-rich basic segment, followed by a kringle domain, three (in the case of mice), and four (in the case of human) scavenger receptor cystein-rich (SRCR) repeats. The carboxy terminus of NT contains the serine protease domain (Fig. 1.3) (Gschwend et al 1997).

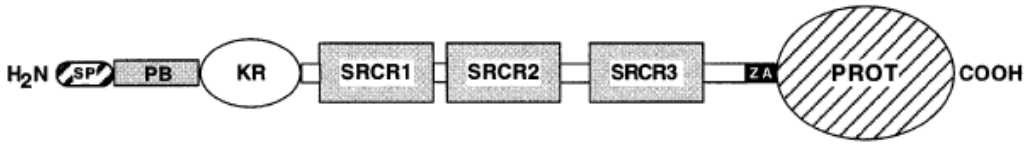

Fig. 1.3 Schematic representation of the domain structure of neurotrypsin

SP, putative signal peptide (aa 1-21); PB, proline-rich basic segment (aa 23-84); KR, kringle domain (aa 85-157); SRCR1 through SRCR3, SRCR domains 1-3 (aa 166-267, aa 273-373, aa 386-487); ZA, segment with homology to zymogen activation region (aa 505-516); PROT, serine protease domain (aa 517-761); open bars mark the segments between the domains. These sequence data are available from EMBL/GenBank under Accession No. Y13192. Figure and text taken and modified from (Gschwend et al 1997).

The specific structure of NT, with the presence of noncatalytic segments with a modular organization, suggests a regulatory function that is typical for several serine proteases. The expression of several extracellular serine proteases was located in the nervous system e.g. tPA and uPA and their function was correlated with developmental changes and neural plasticity. NT is not an exception. The Northern blot analysis of various mice tissues show strong expression in lung, brain and cerebral cortex, whereas a weak signal was detected in intestine and spleen tissue. No NT was found in the liver. Further detailed studies using non radioactive *in situ* hybridization presented strong NT expression in most of the major parts of the CNS, except diencephalon and cerebellum (Gschwend et al 1997). The strongest NT signal can be observed starting from the E 12 to the postnatal P4 in the spinal cord and the peripheral nervous system, and around P4 in the hippocampus (Fig. 1.4) (Wolfer et al 2001). In the adult CNS, NT mRNA is expressed in neurons in the cerebral cortex, hippocampus, amygdala, motor neurons of the brain stem, and the spinal cord.

Strong NT expression in the hippocampus and amygdale (Fig. 1.5) suggests its role in learning and memory formation processes. The recently presented family (described in section 1.1.3) with four severely retarded children who possessed the truncated form of NT confirms that lack of this protein in humans effects establishing and maintaining higher cognitive function (Molinari et al 2002).

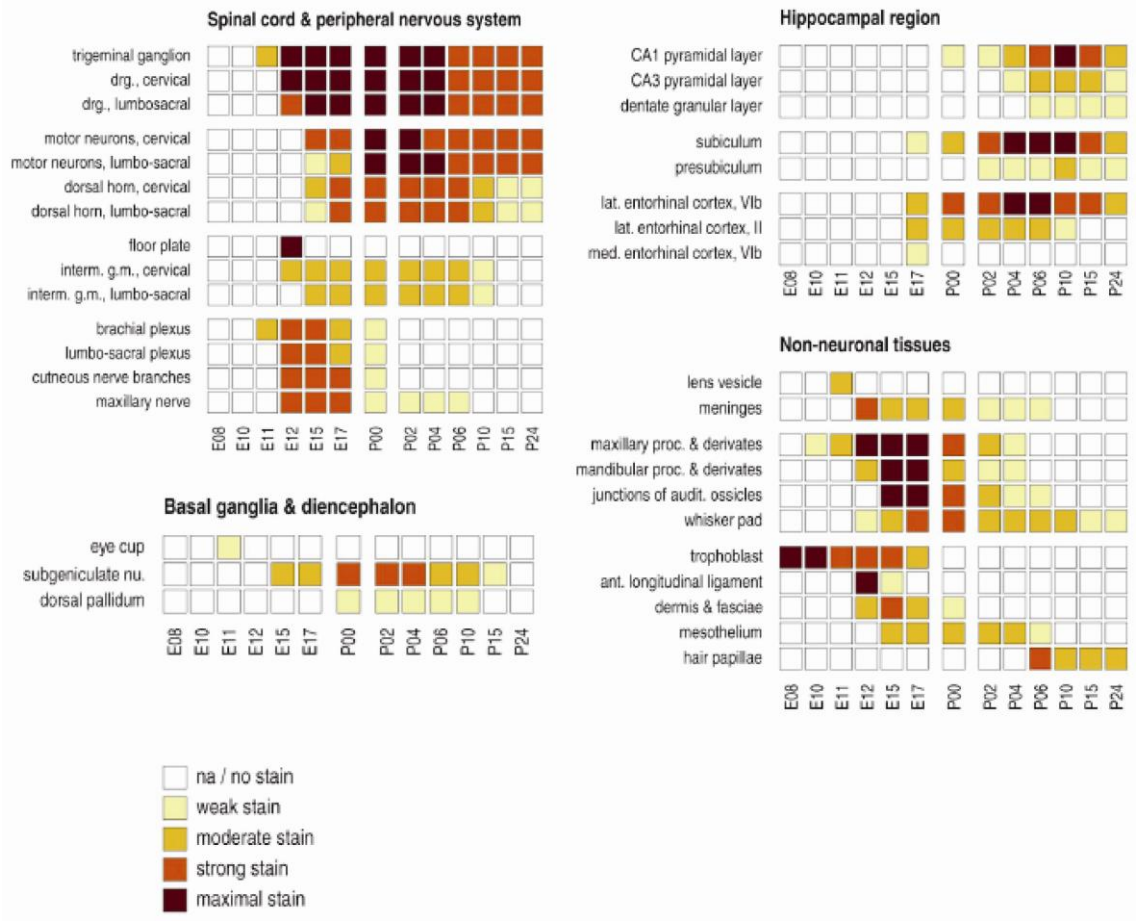

Fig. 1.4 Semiquantitative synopsis of the time course of neurotrypsin mRNA expression in neural and nonneural tissues during pre- and postnatal development

Columns represent development stages. Rows represent cell populations, regions, or tissues. The shading pattern of each box indicates the average signal intensity, assigned to one of the four staining levels listed at the bottom left of the figure. Figure and text taken and modified from (Wolfer et al 2001).

Further studies, using hippocampal cultured neurons expressing pH-sensitive NT (pHluorin) localized protein on the surface and in the internal vesicles of hippocampal synapses. Monitoring of the intra- and extracellular storage of NT in individual synapses

before, during, and after neuron depolarization showed that synaptic exocytosis and refill of the intracellular storage happens in an activity-dependent manner (Frischknecht et al 2008). These results represent a local proteolytic function of NT after its synaptic release.

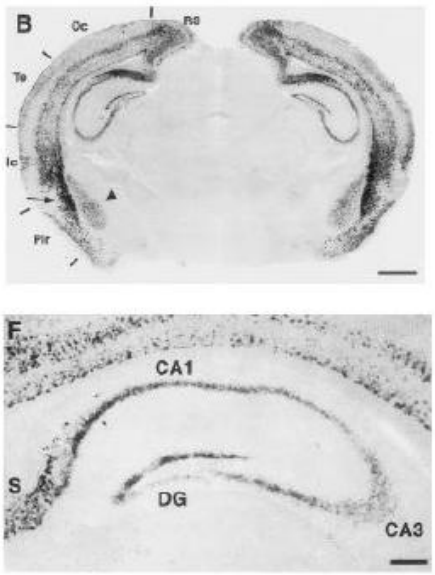

Fig. 1.5 *In situ* hybridization of sections from different CNS regions of adult mice using DIG-labeled NT antisense cRNA

(B) Labeling is seen in distinct layers throughout the neocortex (Te, temporal cortex; Oc, occipital cortex) with a more widespread labeling in the transition zones between iso- and allocortex (Ic, insular cortex; RS, retrospelnial cortex). In the allocortex, labeling is detected in the piriform cortex (Pir), with a strong labeling in the endopiriform nucleus (arrow), and in the hippocampus formation. **(F)** Coronal section of the hippocampus. Labeling is detected in neurons of the subiculum (S), in pyramidal neurons of CA1 and CA3, and in granule neurons of the dentate gyrus (Stern M.). Bar, 300 μm. Figure and text taken and modified from (Gschwend et al 1997).

Further studies performed in our lab using transgenic mice expressing a NT-pHluorin protein in neurons revealed that synaptic exocytosis of neurotrypsin requires presynaptic but not postsynaptic activation. Cell depolarization with extracellular potassium (K^+) increase NT–pHluorin signals, the above signal was identified as a synaptic signal. This increase was abolished after inhibition of the P/Q- and N-type calcium channels with ω-agatoxin (ATX) and ω-conotoxin (CTX), respectively. Inhibition of postsynaptic AMPA and NMDA receptors with a combination of CNQX and MK-801 had no effect. These results confirmed our hypothesis that synaptic exocytosis of NT requires an active potential and activation of presynaptic terminals, but does not rely on postsynaptic glutamate receptors activation (Matsumoto-Miyai et al 2009).

1.2.2 Agrin as a substrate for neurotrypsin

Agrin is a large heparin sulfate proteoglycan, 225 kDa extensive glycosylation increase the molecular mass of agrin to ~600 kDa (Fig. 1.6). Agrin is expressed in the central and peripheral nervous system as well as in the nonneuronal tissues. Agrin was discovered more then 20 years ago in the lab of McMahan. Since then, the function of agrin in the neuromuscular junction (NMJ) has been relatively well established. Observation of the extracellular matrix in the NMJ, and changes of synapses after denervation has allowed agrin to be distinguished as a trophic factor. Further studies have indicated that agrin induces pre- and postsynaptic differentiation (Burden et al 1979; Sanes et al 1978).

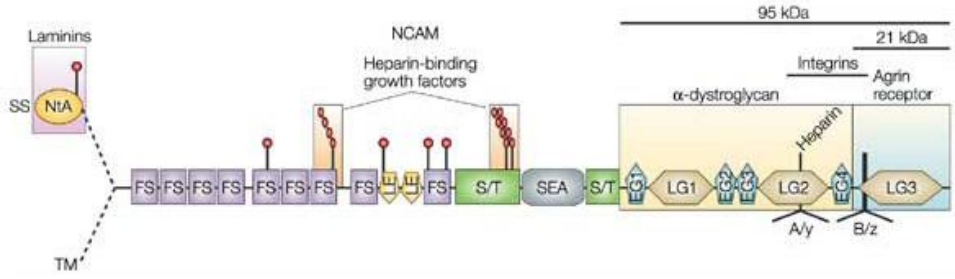

Fig. 1.6 Structural domains of agrin

The signal sequence (SS) and amino (N)-terminal agrin domain (NtA) are presented in an agrin isoform that is localized to the neuromuscular junction (NMJ). These two regions are responsible for the release of agrin (SS) and the binding to the laminins in basal lamina (NtA). The alternatively spliced type II transmembrane segment (TM) of agrin anchors this isoform at place that are devoid of basal lamina such as the brain. The amino-terminal half of agrin is highly glycosylated and this same region is also involved in binding to neural-cell adhesion molecules (NCAM) and heparin-binding growth factor. The carboxy-terminal, 95-kDa part of agrin is fully active in AChR aggregation and contains binding sites for α-dystroglycan, heparin, some integrins and agrin receptor. Figure taken and modified from (Bezakova & Ruegg 2003)

Initially agrin was considered only as a nerve-derived trophic factor responsible for assembly of the postsynaptic apparatus *in vivo*. Twenty years later, the main predictions of this hypothesis have been confirmed. Agrin-deficient mice die at birth, due to breathing failure, caused by lack of breathing muscle innervation (Gautam et al 1996). But agrin can not be considered only in terms of NMJ; the latest studies suggest a crucial role in formation and maintenance of the excitatory synapses in the brain (d'Houtaud et al 2009). Today we know that NtA-agrin is associated with basal lamina and is crucial for the devel-

opment of the neuromuscular connection, whereas TM-agrin remains cell associated and plays a distinct role in the CNS (Burgess et al 2000). The selective expression of agrin in motor neurons in agrin-deficient mice revealed decreased numbers of excitatory synapses, that decreased in length and number of spines (Ksiazek et al 2007). Additional studies performed on cell cultures revealed the role of the transmembrane form of agrin (TM-agrin) in the CNS. Overexpression of TM-agrin in rat hippocampal neurons induces the formation of filopodia-like protrusions on axons and dendrites, while TM-agrin inhibition with RNAi decreases the filopodia number (McCroskery et al 2006). Clustering of TM-agrin by polyclonal anti-agrin antibodies induces the formation of numerous filopodia-like structures in cultured retinal ganglion cells (Annies et al 2006). The above results suggest, for the first time the role of transmembrane agrin in neurite outgrowth and synapse formation.

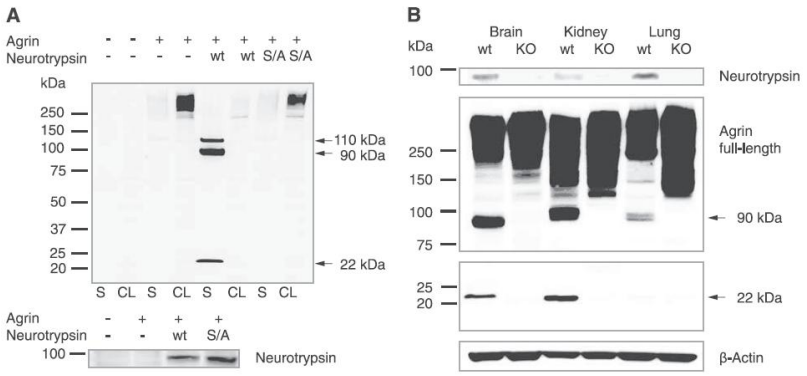

Fig. 1.7 Neurotrypsin cleaves agrin *in vitro* and *in vivo*

(A) Western blot analysis of HeLa cells cotransfected with combinations of membrane-bound agrin (+), wild-type NT (wt), inactive NT (S|A), and empty pcDNA3.1 (-). Supernatants (S) and cell lysates (CL) were analyzed with anti-agrin (R132 and G92) antibodies, directly against the C-terminus of agrin. *(Top)* Transfection of agrin alone resulted in a signal above 250kDa in cell lysate. Upon cotransfection with wild-type NT, full-length agrin was cleaved resulting in fragments running at 22, 90, and 110 kDa in supernatant. No cleavage was found after cotransfection with inactive NT. *Bottom:* Control for NT expression with G93 antibody. **(B)** Western blot analysis of tissue from wild-type (wt) and NT-deficient (KO) mice. The 90 kDa agrin cleavage product was detected in brain, kidney, and lung of wild-type mice but was absent in neurotrypsin-deficient mice. Similar results were obtained from 22 kDa agrin fragment except for lung. B-actin was used as a loading control. Figure and text taken from (Reif et al 2007).

Studies performed in our laboratory have proven that NT cleaves agrin in two conservative cleavage sites *in vitro* and *in vivo.* To test this hypothesis, HeLa cells were transfected with rat agrin (x4y8) alone or in combination with wild-type (Reif et al 2007) or inactive form (S/A) of NT (Fig. 1.7A). Results clearly show that only cotransfection with both proteins released cleavage products of 110 kDa, 95 kDa, and 22 kDa size. The Western blot analysis of the brain tissue (Fig. 1.7B) resulted in similar cleavage products in the case of wild-type mice, but no products in the case of NT-deficient mice (Reif et al 2007). These results indicated that agrin cleavage *in vivo* is strictly NT-dependent. So far agrin is the only known substrate for NT. Further morphological studies indicated proximal location of both proteins. NT is localized to the presynaptic terminals, while agrin is localized to the extracellular space at/or in the vicinity of synapses (Fig. 1.8). Biochemical analysis showed that NT cleaves glycanated agrin exclusively and this cleavage takes place locally at the synapse (Stephan et al 2008).

The developmental course of NT-dependent agrin cleavage showed the highest activity during the fetal and neonatal period, suggesting its involvement in the neuronal development (Wolfer et al 2001). The lower activity in the adult brain can be correlated with reorganization of the existing neural circuits during acquisition of new skills.

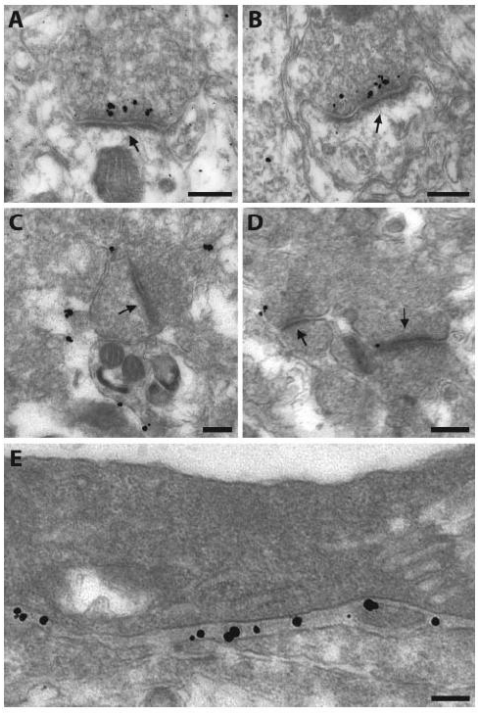

Fig. 1.8 Subcellular localization of neurotrypsin and agrin in hippocampus and cerebral cortex of wild-type mice

(A, B) Immuno-electron microscopy of the neuropil of the hippocampal CA1 area and the cerebral cortex localized NT in presynaptic terminals, close to presynaptic membranes lining the synaptic cleft. Silver-intensified gold particles reporting NT immunoreactivity were accumulated at vesicles close to the presynaptic membrane opposite tot the postsynaptic density (arrows). **(C, D)** Silver-intensified gold particles indicating agrin immunoreactivity were found at perisynaptic, as well as extrasynaptic locations in the neuropil of the hippocampal CA1 area and the cerebral cortex. **(E)** The basal lamina of blood vessels in the stratum radiatum in the CA1 area was strongly labeled with agrin-specific antibodies. The complete absence of gold particles in the adjacent tissue indicates a high specificity of the antibody. The arrow points to postsynaptic densities (A-D). Scale bars = 0.2 µm. Figure taken from (Stephan et al 2008).

Recent studies indicated the C-terminal 22 kDa fragment of agrin as a regulator of presynaptic excitability via inhibition of the α3 subunit of Na^+/K^+-ATPase. Agrin binding results in membrane depolarization and increased action potential in cultured neurons and acute slices. In early response to the agrin binding increase of cytoplasmic Ca^{2+} can be observed. Ca^{2+} is released from intracellular stores or enters the postsynaptic terminal via voltage-gated calcium channels (VGCC) (Hilgenberg et al 2006). Ca^{2+} influx is essential for actin skeleton reconstruction; it activates phosphorylation of calmodulin-dependent protein kinase II (CaMKII) and other Ca^{2+} effectors.

Latest studies in our laboratory concentrated on the neurotrypsin/agrin interaction confirmed previous results showing that agrin cleavage strictly depends on NT. Stimulation of the P10 mice hippocampi (described in Material and Methods, section 5.1.6) were used to monitor NT activity via agrin-90 (90 kDa) release. The agrin-90 fragment (Fig. 1.9A) was clearly visible in the case of wild-type mice and absent in the case of NT-deficient mice (Fig. 1.9B). Further tests show an increase of the agrin-90 signal after the chemical stimulation is abolished if presynaptic activity was inhibited (Fig. 1.9E and F). These results indicate that presynaptic exocytosis of NT is crucial for agrin cleavage (Matsumoto-Miyai et al 2009).

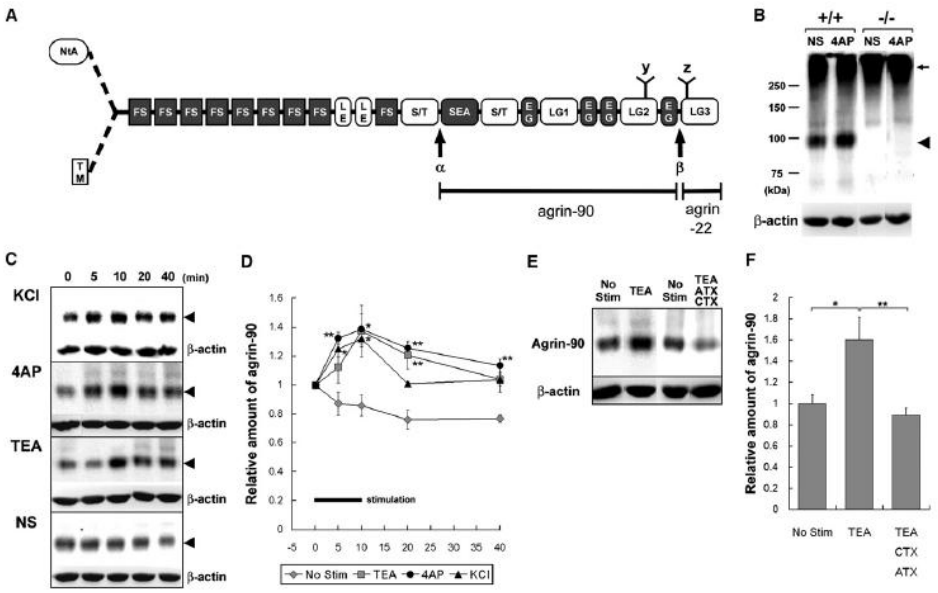

Fig. 1.9 Neuronal activity enhances agrin cleavage by neurotrypsin

NT-dependent cleavage of agrin was studied on Western blots of whole hippocampi from P10 mice after stimulation of neural activity by different protocols. (**A**) Schematic representation of agrin and its neurotrypsin-dependent cleavage sites (arrows α and β). Cleavage of agrin at both sites generates a 22-kDa C-terminal fragment (agrin-22) and a middle 90-kDa fragment (agrin-90). Partial cleavage at the α site only generates a 110-kDa C-terminal fragment (agrin-110). Abbreviations: NtA, N-terminal agrin domain; TM, transmembrane seg-

ment; FS, follistatin-like domain; LE, laminin EGF-like domain; S/T, serine/threonine-rich region; SEA, sperm protein, enterokinase and agrin domain; EG, epidermal growth factor domain; LG, laminin globular domain; y and z, mRNA splicing sites. (**B**) Western blots for agrin from non-stimulated (NS) and 4-aminopyridine-stimulated (4AP) hippocampi from wild-type and NT-deficient mice using anti-agrin antibody R132. Due to differential glycanation, full-length agrin appears as a smear in the range of 200 to 600 kDa (arrow). Agrin-90 is indicated by the arrowhead. β-actin loading controls are shown below. (**C**) Western blots of agrin in KCl, 4AP, TEA-stimulated and non-stimulated hippocampi from P10 mice at various time points after onset of stimulation. Arrowheads indicate agrin-90. β-actin loading controls are shown below. (**D**) Quantification of agrin-90 levels of **C**. Levels of agrin-90 were normalized to β-actin. The average level before stimulation (0 min) was set to 1. The stimulation period is indicated by a black bar. Error bars indicate S.E.M.; *, $p < 0.05$; **, $p < 0.01$ vs non-stimulated controls by ANOVA with Tukey's post hoc test (n = 3-8). (**E**, **F**) Neurotrypsin-dependent agrin cleavage requires activation of presynaptic Ca^{2+} channels. TEA was used to stimulate neurotrypsin-dependent agrin cleavage and the response to blockade of presynaptic P/Q- and N-type Ca^{2+} channels was studied by Western blotting of agrin-90 (**E**). No Stim: control hippocampi without stimulation. Presynaptic P/Q- and N-type Ca^{2+} channels were blocked with ω-agatoxin IVA (ATX) and ω-conotoxin GVIA (CTX), respectively. (**F**) Quantification of agrin-90 levels in **E**. Relative levels of agrin-90 were normalized to β-actin. The average level found without stimulation was set to 1. Error bars indicate S.E.M.; *, $p < 0.05$; **, $p < 0.01$, ANOVA with Tukey's post hoc test (n =4-9). Adapted from (Matsumoto-Miyai et al 2009).

1.3 Dendritic spines

Spines are small protrusions from the dendritic shaft, which receive electrical input, typically from only one excitatory synapse (Fig. 1.10). Spines may be long or short structures with irregular, undulating shapes, ending with smaller or bigger heads facing different directions. The variety of these structures can be observed in the context of total length: 0.2 µm (CA1) to 6.5 µm (CA3), neck diameter: 0.04–1 µm, and head volume (Harris & Kater 1994).

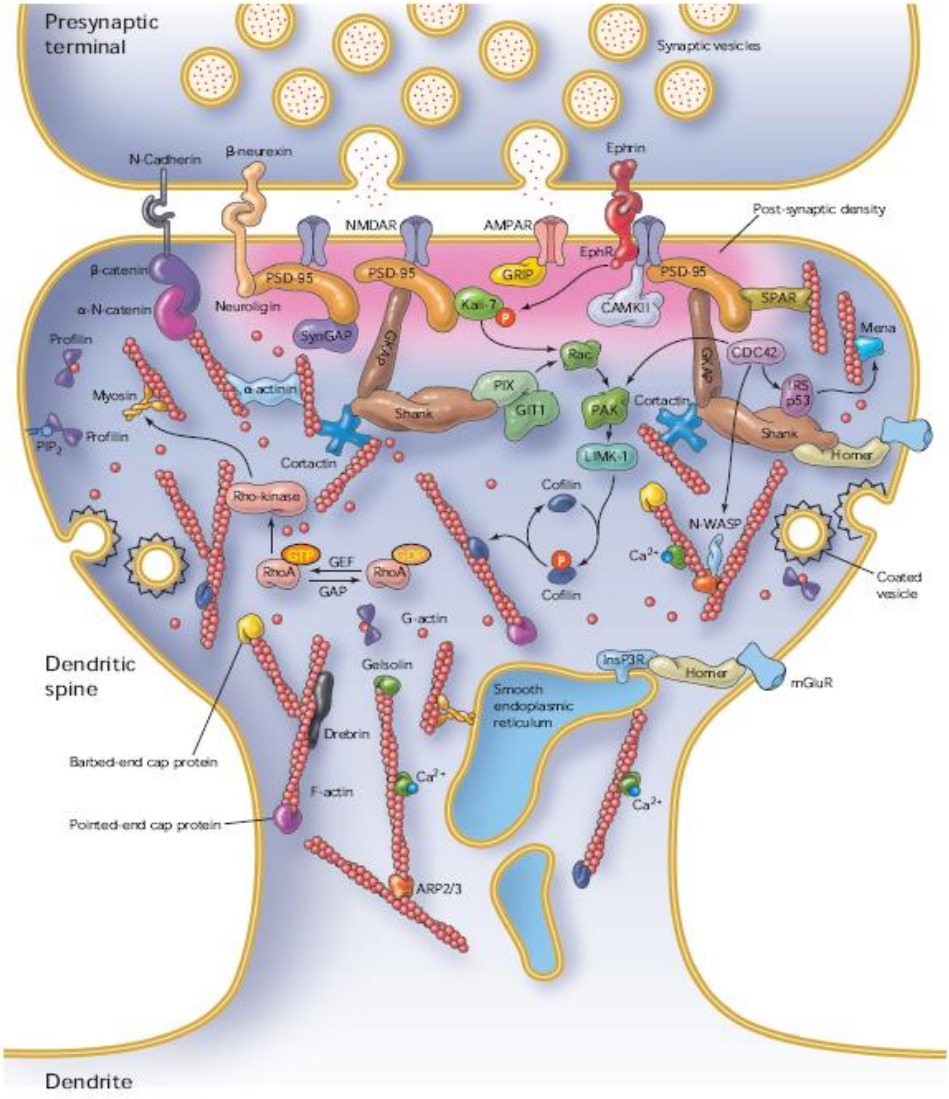

Fig. 1.10 Important components of dendritic spines

Spines are small membrane protrusions at synaptic junctions that use the excitatory neurotransmitter glutamate, which is released from synaptic vesicles clustered in the presynaptic terminal. Across from these glutamate release sites, AMPA and NMDA subtypes of glutamate receptors are clustered at the postsynaptic active zone within a dense matrix called the postsynaptic density (PSD, pink). Beyond the PSD lie subregions of spine membrane that contain G protein-coupled glutamate receptors (mGluR) and endocytic zones for recycling of

membrane proteins. Receptors, in turn, connect to scaffolding molecules, such as PSD-95, which recruit signaling complexes. Actin filaments provide the main structural basis for spine shape. Via a network of protein interactions, actin filaments indirectly link up with the neurotransmitter receptors and other transmembrane proteins that regulate spine shape and development, including Eph receptors, cadherins, and neuroligins. Figure and text taken and modified from (Calabrese et al 2006).

First light microscope techniques allowed Ramon Y Cajal to observe spine-like protrusions (Cajal 1893). These early studies allowed the formulation of theories based on which formatted connections between neurons persisted over the neurons lifetime. The Golgi-staining method revealed this theory showing that protrusions can be formed and eliminated depending on the presence or absence of input. On account of the electron microscope's identification of spines shapes, tracking its changes in response to neuronal activity became possible. Results from these studies for the first time suggested that changes in morphology may affect physiological properties of the spines (Arikkath 2009; Auffret et al 2009). Most recently, 2-photon laser scanning microscopy was adapted for imagining of spines *in vivo* and now allows observation in the depth of living tissue. Currently, morphology of spines and synapses seems to have no further secrets, but what remains unclear is their role in new synapse formation and reorganization of existing neural circuits.

The typical excitatory synapse consists of a pre- and a postsynaptic side, with a cleft in between. Round synaptic vesicles filled with glutamate can be found in the presynaptic terminal, and closely packed neurotransmitters receptors are mounted in the postsynaptic membrane. This dense membrane-associated matrix is call postsynaptic density (PSD). Different types of channels and receptors, cytoskeleton elements and signal transmission systems can be located there. The asymmetric ultrastructure of the PSD is characteristic of excitatory synapses. In addition, nearly half of the CA1 hippocampal spines contain smooth endoplasmic reticulum (SER), which in big spines might transform into the so called *spine apparatus.*

1.3.1 Morphological classification of dendritic spines

Dendritic spines are thin protrusions extending from the dendritic surface, which create functional connection with a presynaptic partner (Garner et al 2002) Detailed observation of spines was possible due to the reconstruction of serial sections from electron microscopy. Dendritic spines of the apical dendrites of the CA1 pyramidal neurons were characterized based on the relative size of head and neck and classified into three main categories: *thin*, *mushroom* and *stubby* (Fig. 1.11) (Peters & Kaiserman-Abramof 1970). Spines are called *thin* when their length is greater then the neck diameter (d_n<<<L) and diameter of head and neck is similar ($d_n \leq d_h$). In contrast, *mushroom* spines possess head with much greater diameter then diameter of the neck (d_n<<<d_h). In addition *mushroom* spines can be characterized by the presence of polyribosomes, enrichment in F-actin and perforated PSD (Nimchinsky et al 2002). When the diameter of the neck is similar to the total spine length it is called *stubby* ($d_n \approx L$) (Harris et al 1992). Some studies consider a *branched* type of spine, characteristic of the hippocampus CA1 region, as an additional category (Sorra et al 1998). These spines have multiple heads that originate from the same neck. Each head can create a connection with an axon, while some heads will stay without a presynaptic partner.

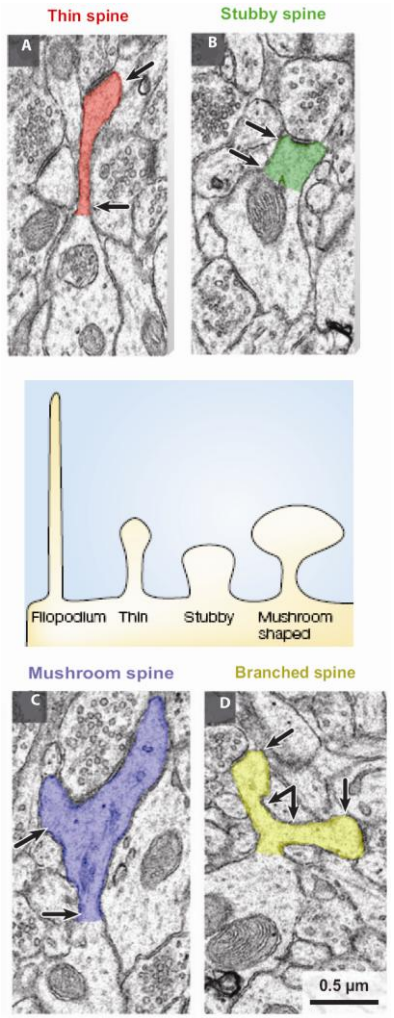

Fig. 1.11 Morphological classification of dendritic spines

Variability in spine shape and size. A three-dimensional reconstruction of a hippocampal dendrite (gray) illustrating different pine shapes including thin (red), stubby (green), mushroom (blue), and branched (yellow). (A) An example of a thin shape (red). (B) An example of a stubby spine (green) with an equal head and neck diameter and an overall length that equals its width. (C) An example of a mushroom spine (blue) with a head diameter exceeding 0.6 microns and a narrow neck. (D) An example of a branched spine (yellow) where both branches are thin spines. The middle figure shows a cartoon version of various spines categories. Scale bar =0.5 µm, and arrows indicating where the head and neck diameters were measured for each spine. Figures were taken and modified from (Bourne & Harris 2008; Hering & Sheng 2001).

As was mentioned previously, spines differ in size and morphological structure, which may indicate their distinct role-, or developmental stage. The size of spines seems to affect their functionality; the number of channels and receptors is closely correlated with the size of the head. Smaller spines are more vulnerable to LTP whereas larger spines show less plasticity. Repetitive glutamate releases can cause permanent effects on small spines and temporarily influence mushroom ones (Matsuzaki et al 2004). The ratio of head to neck diameter influences the dynamic of postsynaptic Ca^{2+} and the influx mediated by NMDA receptors activity (Noguchi et al 2005). The spine head might be considered as a barrier to Ca^{2+} exchange between the spine and dendrite and may play an important role in downstream signaling and regulatory mechanisms.

Filopodia are classified as thin, long, headless structures, extending more then twice the length of the average spine ($L:d_n > 3:1$) (Grutzendler et al 2002; Skoff & Hamburger 1974). In contrast to other spines, filopodia are highly mobile and instable structures. They constantly seek new presynaptic partners in the neuropil to form stable functional connections. Filopodia which do not find an appropriate axonal partner will be retracted. Some of them will create a connection, only a small percentage of them will be selectively stabilized (Lohmann & Bonhoeffer 2008; Xu et al 2009; Yang et al 2009).

1.3.2 Dendritic spines and mental retardation

Numerous clinical studies confirmed an association between morphological changes in spines, a shift in their numbers and maturation with mental disorders (Bartesaghi et al 2003; Verina et al 2007). The first studies showing a correlation between MR and changes in dendrite morphology were published in 1974 by M. Marin-Padil and D. Purpura (Purpura 1974). Unfortunately after 40 years of research results are still inconsistent. Most of the studies focused on pyramidal neurons in the cerebral cortex. There are two main streams; one showing abnormally small and immature spines, mostly as a result of genetic defects in scaffolding and adhesion molecules of PSD. The second is correlated with *Down's syndrome* and *Fragile-X syndrome* with abnormally long and thin spines in different parts of the brain (Irwin et al 2001). The above phenotypes were exacerbated during young age in humans and in animal models. A significant difference in the morphology coincided with a *critical period*, mentioned in section 1.1, in synaptogenesis. The physiological basis for most of those dendritic changes remains unexplained, but appears to be in close correlation with dendritic development. Dendritic development consists of two phases: exploration and consolidation, each depending on different proteins.

Dendritic abnormalities in genetic disorders associated with MR were also observed in cases of: Neurofibromatosis-1, Patau syndrome, Tuberous sclerosis, Williams's syndrome, Phenylketonuria and, Rubinstein-Tybi syndrome.

1.3.3 Brain plasticity

The term plasticity refers to the brain's ability to learn, remember, forget and adapt to environmental stimuli by constant molecular and structural changes (Johnston 2004). High plasticity is a property of a child's brain that enables children to learn faster than adults, react to multiple stimuli from their environment, and adapt to changing situations (Johnston et al 2001). Mechanisms responsible for this enhanced plasticity include increased neurogenesis in some parts of the brain (Toni et al 2007), removal of neurons and synapses through the process of apoptosis and continuous reconstruction of neural circuits (De Paola et al 2006). At the age of two years children have twice as many synapses in their cerebral cortex than adults (Molinari et al 2002). Most of them, in the response to glutamate, are removed or replaced in activity–dependent manner (Johnston 2004). However, high plasticity may also lead to dangerous consequences, i.e. a high sensitivity to any unwanted changes that might occur during brain development. These undesirable changes are often irreversible and can affect quality of life. This crucial time window in a child's brain development, characterized by its high plasticity, is called the *'critical period'*. This period of time displays high sensitivity to certain environmental stimuli. Lack of appropriate stimulus during 'critical period' may disturb proper functioning later in life (Siegler & Svetina 2006).

Brain plasticity is a heterogeneous phenomenon, which consists of structural and functional changes. Differences between them have been discussed in several studies (Butz et al 2009; Weiss et al 2004). Structural plasticity includes morphological changes in synapses, synaptic wiring arising from synapse deletion (Wolff & Missler 1992) or new synapse formation (Knott et al 2006). In contrast, functional plasticity covers changes in synaptic strength, not affected by anatomical connectivity between neurons. Functional MRI study on stroke patients revealed evidences of co-localization of structural and functional plasticity (Schaechter et al 2006).

On the basis of numerous studies, a close correlation between synaptogenesis (Fig. 1.12) and dendritic filopodia formation was proposed, presenting dendritic protrusions, as structures responsible for facilitation of axo-dendritic contact (Knott et al 2006; Maletic-

Savatic et al 1999; Ziv & Smith 1996). The newly formed filopodia are considered as the immature form of synapses, they do not possess the necessary postsynaptic machinery for proper functioning as spines. In a situation when the brain receives a large amount of new stimuli from the environment, and the learning and storing of new information is enhanced the number of filopodia rapidly decrease and the number of stable spines increase. Observation of rat organotypic slices revealed developmental regulation of spine elimination. In the first three months of life, the rate of spine elimination exceeds the rate of formation (Knott et al 2006). In comparison, various examinations of long-term changes, using two-photon microscopy, in young animals detected significant decrease in the ratio of filopodia to spines (Grutzendler et al 2002). This suggested that previously created filopodia were eliminated or transformed into stable spines. Observation of cultured neurons has proven that dendritic spines are formed by stabilization of motile dendritic filopodia (Ziv & Smith 1996). In adult mice this process is not as common as we would expect. Only 0.2% of filopodia are transformed into mushroom spines (Majewska et al 2006), and only 3% of newly formed spines survive one month (Holtmaat et al 2005). However, if a spine persists for at least 4 days, then it always forms a functional synapse with a fully developed postsynaptic density (Knott et al 2006). Process of filopodia formation and its transition in to synapses may be an important contribution to neuronal plasticity by establishment of novel synaptic microcircuits.

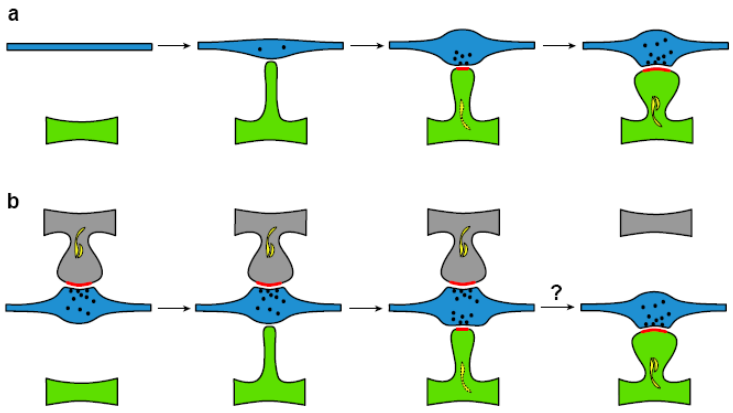

Fig. 1.12 Two models of synapse formation by spine growth

a. A new spine (green) can grow towards an axon (Johnston et al) to make a synapse, resulting in a single-synapse bouton.

b. A new spine often grow towards existing boutons, occupied by another spine (grey), resulting in multi-synapse boutons. The multi-synapse state could be transient. Spine maturation involves an increase in spine volume, synapse (red) formation, and later acquisition of SER (yellow). Taken from (Knott et al 2006).

1.3.3.1 Synaptic plasticity

Studies presented in the above chapter presented evidence confirming existence of structural changes based on dendritic spines interactions with axonal partners. These changes underlie processes of learning and memory. Also molecular mechanisms that underlie these changes are worth of mentioning.

Long-term potentiation (LTP) can be described as increase in synaptic strength, which takes place after high-frequency stimulation. In other words LTP is a long-lasting enhancement in signal transmission between two connected neurons (Cooke & Bliss 2006). In early phase of the LTP induction activation of *N*-methyl *D*-aspartate receptors (NMDA) is required (Lynch 2004; Malenka & Nicoll 1999). This leads to the Ca^{2+} influx through the NMDA receptors and voltage dependent calcium channels (VDCC). Studies performed in the cultured neurons showed that addition of glutamate receptors inhibitors (Collingridge GL 1983) or Ca^{2+} chelator (Malenka et al 1992) inhibited induction of the LTP. Further studies indicated necessity of protein kinases activation, especially calcium/calmodulin-dependent protein kinase II (CaMKII) (Malenka et al 1989; Malinow et al 1989) and protein kinase C (PKC) (Malinow et al 1989). Expression of the LTP mainly depends on autophosphorylation of the CaMKII (Blitzer et al 1995; Giese et al 1998). This way activated CaMKII plays role in the trafficking of α-amino-3-hydroxy-5-methyl-4-isoxazolepropionic acid receptors and (AMPA) its insertion into the postsynaptic membrane (Ju et al 2004; Malenka & Bear 2004). Increased number of AMPA receptors increases postsynaptic response to the presynaptic activation. The next step of the so called long-lasting stage of LTP requires synthesis of new proteins and activation of gen transcription in the postsynaptic cell (Lynch 2004; Pittenger & Kandel 2003). Many proteins of downstream pathway, such like: protein kinase A (PKA), CaMKIV, mitogen-activated protein kinase (MAPK) and cAMP response element binding protein (CREB) will translate neuronal activity to direct gene transcription in nucleus (Lynch 2004; Pittenger & Kandel 2003).

Spines that received stimulation to induce LTP increase in volume and amount of AMPA and NMDA receptors. LTP can affect spine shape promoting its maturation and stabilization (Matsuzaki et al 2004; Yuste & Bonhoeffer 2001). In contrast, induction of the long-term depression (LTD) is linked with reduced spine head diameter (Zhou et al 2004) and weakening of synapses and spines (Nagerl et al 2004) (Fig.1.13).

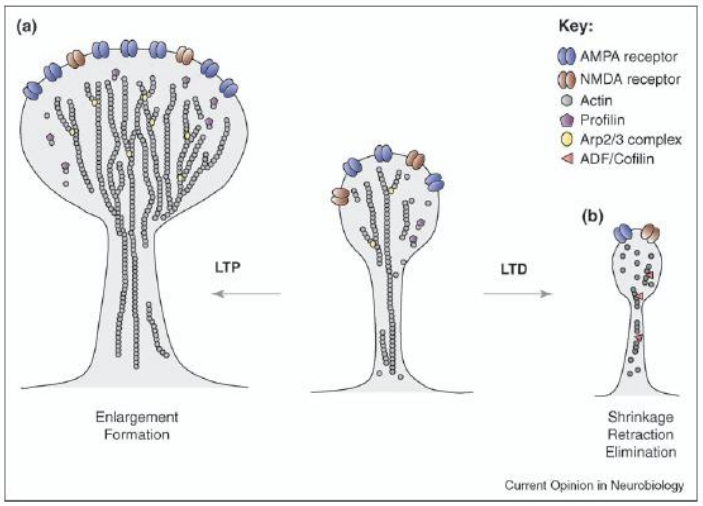

Fig. 1.13 Changes in actin polymerization and spine morphology with LTP and LTD

(a) LTP is associated with a shift of actin equilibrium toward F-actin (F-actin is depicted as linear chains of monomeric G-actin [single circle]) in spines, enlargement of the spine head, and recruitment of more AMPA receptors to the postsynaptic membrane. Profilin promotes actin filament assembly by increasing the availability of actin-ATP for polymerization. The Arp2/3 complex stimulates nucleation of new actin filaments and formation of branches. **(b)** In contrast, LTD stimulation shifts the equilibrium toward actin depolarization, resulting in shrinkage or loss of spines. The actin severing protein ADF/cofilin might be involved in spine shrinkage. Figure and text taken and modified from (Tada & Sheng 2006).

These quick dynamic changes are possible owing to the actin cytoskeleton. Actin can be found in living cells in two states, as monomeric actin (G-actin/globular actin) and as filamentous actin (F-actin). G-actin has the capability to polymerize into F-actin under physiologically salty conditions. This form of actin is a predominant molecule in dendritic spines and creates a skeleton for dendritic structures. The rate of G-actin to F-actin transformation in dendritic spines is regulated in an activity-dependent manner (Okamoto et al 2004), however it might be affected by many molecular mechanisms. The structure of F-actin can be disturbed by GTPases family (Rho, Rac1), which hydrolyze guanosine triphosphate (GTP) modifying actin binding proteins (ABP), resulting in changed morphology. A crucial ABP in neurons is drebrin, encoded by the DBN1 gene (Fig.1.14). It consists of two isoforms, drebrin E that is enriched in the developing brain and drebrin A that is present in the adult brain. These two distinct forms of protein are generated by alternative splicing (Kojima et al 1993). The role of drebrin is to form complexes with actin (DBF-actin) in more mature so called cluster filopodia. In the next stage, drebrin A evokes accumulation of F-actin and PSD-95, the protein responsible for clustering receptors and channels in postsynaptic sites. Accumulation of proteins alone is not sufficient to induce full maturation, and other factors, such as synaptic activity are probably required (Takahashi et al 2003). Overexpression of drebrin A in cultured neurons causes formation of abnormal large protrusions. The lack of head in this structure and absence of MAP2 signal suggests filopodia-like origins (Mizui et al 2005).

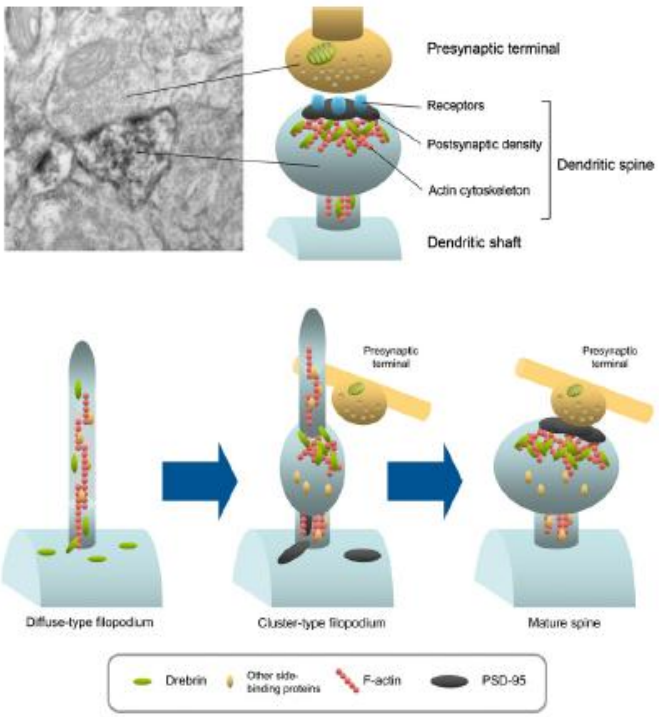

Fig.1.14 Ultrastructure of formation an asymmetric synapse/spine

Upper left panel shows a representative electron microscopic image of an asymmetric synapse immunostained with the anti-drebrin antibody. The right panel is a schematic of an asymmetric synapse. The presynaptic terminal is filed with a number of synaptic vesicles and occasionally with mitochondria. The dendritic spine is composed of an actin cytoskeleton with actin-binding proteins and a PSD structure containing transmitter receptors. Lower panel; during synaptogenesis, dendrites are bristled with many diffuse-type filopodia in which drebrin is diffusely distributed. After an axon terminal establishes contact with filopodia, drebrin clusters with F-actin at a postsynaptic site and forms cluster-type filopodia. PSD-95 cluster formation follows drebrin-actin cluster formation. The drebrin-actin complex tethers the postsynaptic machinery and is crucial for the maturation of dendritic spines. Figure and text taken and modified from (Sekino et al 2007).

The capacity for rapid structural changes and continuous spines remodeling is considered as a possible structural basis for learning and memory. In "The Organization of Behaviour" (1949) Hebb formulated a rule describing basic mechanisms for synaptic plasticity. According to Hebbian rule, if two cells or systems are active at the same time, then they will tend to associate the way that an activity of one facilitates the activity of the other. Thus, Hebb created the basis of the neural network theory. His concept is often paraphrased as: "Neurons that fire together wire together". This links morphological changes with increased synaptic efficacy, like LTP.

Recent studies of motor learning in mice using single seed reaching (Xu et al 2009), and the accelerating rotating rod (Yang et al 2009) demonstrated that extended learning promotes formation and elimination of spines, i.e., remodeling of pre-existing neuronal connections. Both studies showed that by the end of the first two days of training, the number of spines, in the brain region responsible for limb movement, doubled when compared with untrained mice. After consolidation of newly learned abilities, the initial level of spine number returns. In addition, a significantly wider range of reorganization was observed in young animals as a consequence of higher plasticity of the brain. With regard to this ob-

servation, the total pool of spines in the cerebral cortex could be divided into two populations, those created during early postnatal development, persisting throughout adulthood, and those newly formed after induction by novel environmental stimuli. At the lattes, approximately ~60-70% will remain throughout entire life, creating lifelong memories (Yang et al 2009).

1.4 Memory

From a physiological perspective, memory is an organism's ability to format, store, and recall information and experiences according to its needs. The entire process can be divided into three stages: encoding, storage, and retrieval. Worth mentioning is the fact that forgetting information occurs as frequently as memorizing them. Amnesia can be caused by many factors, such as chronic alcoholism (Ling et al 2010), brain tumor (Pyter et al 2010), stroke (Zierath et al 2010), or head injury (Reeves & Panguluri 2011). Loss of memory can present itself in two different ways. The first is called *retrograde amnesia* and is characterized by the loss of memory concerning events before the trauma and the ability to format new memories. The second is called *anterograde amnesia* characterized as an inability to format new memories, whereas those that existed before appear to be intact. In exceptional cases both types of amnesia can occur in the same patient and be correlated with damage to the brain region responsible for episodic memory (M.F. Bear 2007). The concept of memory covers a wide range of phenomena and is hard to define, yet there was a change in the perception of memory at the beginning of the 19th century. The introduction of the term engram/memory trace theory resulted in the "location" of different forms of memory in distinct parts of the brain. In 1824 Marie-Jean-Pierre Flourens introduced ablation experiments based on the lesion of one brain region and observation of the changes of the animal's memory function. His early studies revealed the importance of semicircular canals in the maintenance of posture and balance. Those results indicated that specific parts of the brain control specific functions (M.L.P. 1830).

1.4.1 Classification

Extensive studies allowed to characterization of different types of memory (Hawkins 1897; Izquierdo et al 1998; Wood et al 2000) (Fig. 1.15). The memory of facts and events is called *declarative memory*; it can be created very quickly and can occur even after a single event. Medial temporal lobe and diencephalon are the brain regions involved in the formation of declarative memories. This kind of memory is often referred to as explicit memory because it results from conscious effort. *Nondeclarative memory* often called implicit memory can be divided in to three categories: emotional response, skeletal musculature, and procedural memory. Formation of procedural memory is a slow process that often requires many repetitions over days, months or even years. Typical forms of procedural memory are the capacity of reading, or playing piano. This type of memory enables us to carry out commonly learned tasks without consciously thinking about them (M.F. Bear 2007).

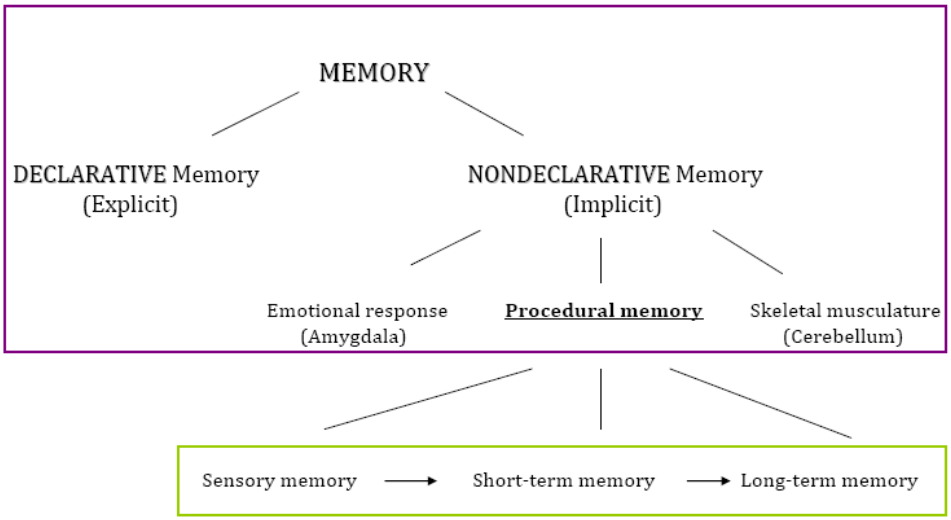

Fig. 1.15 Memory classifications by information type and time

Upper part of the graph (violet box) represents memory classification by information type. Lower section (green box) illustrates memory classification according to duration. Based on the 24th chapter of "Neuroscience Exploring the Brain" (M.F. Bear 2007).

Another characterization can be made based on the time required to create a memory. At the beginning of the process, the first 200-500 milliseconds, we are dealing with *sensory memory*, which involves the temporary form of information storage. This type of memory can not be prolonged with rehearsal. Memories that last on the order of seconds to hours

and are vulnerable to disruption are called *short-term memory;* their capacity is very limited. Multiple studies concerning head trauma led to the hypothesis that newly formed memories are stored in short-term mode and can be selectively converted into a permanent form of *long-term memory* via *memory consolidation*. Consolidation is a process of stabilizing the memory trace after its initial acquisition (M.F. Bear 2007). Results of an active avoidance test indicated the existence of early and late activation phases during long-term memory consolidation. The early phase includes activation of CaMKII, NMDA, AMPA and glutamate receptors. During the late phase the activation of protein kinase A (PKA) and extracellular regulated kinase was reported (Izquierdo et al 2006). Short-term memory is considered as a transient type of memory supported by the frontal lobe, especially the prefrontal cortex, and the parietal lobe. In contrast, long-term memory is maintained by more stable changes in neural connections. For many years it was believed that only the hippocampus was the essential brain structure. However, studies on memory consolidation revealed that the process of procedural memory consolidation depended on various factors such as: post-training intervals (Hauptmann & Karni 2002), sleep (Diekelmann & Born 2010; Diekelmann et al 2009), circadian rhythms, and subject awareness. Most importantly those processes do not depend only on the hippocampus, but also on the striatum (Albouy et al 2008). Functional magnetic resonance imaging (fMRI) during performance of the oculomotor sequence learning task clearly proved that both structures interact during consolidation of the motor task.

1.4.2 Multiple memory systems

Years of studies on memory organization led to the conclusion that memory is not uniform. Different brain systems are responsible for various types of memory and learning. In 1957, Scoville and Milner worked with H.M., a patient with surgical ablation of the medial temporal lobe, who presented amnesia for all events following the surgery and intact memory for events that took place before the surgery. H.M. was subjected to resection of the hippocampus and adjacent structures, most of the amygdala, and the entorhinal cortex to treat otherwise not controllable epileptic seizures. The case of H.M. gave direct evidence for the existence of the interactive memory systems theory (IMST) in the mammalian brain (Scoville & Milner 1957). Further studies showed that, depending on the circumstances, systems can interact with each other in a cooperative or competitive way (McDonald & White 1993; Packard et al 1989; Packard & McGaugh 1996). The concept of multiple memory systems (MMS) was first recognized by the existence of a dual memory system, with the hippocampus as a central structure and other brain areas mediating dif-

ferent, non-hippocampal learning (O'Keefe 1978). These findings appeared as a result of many double irreversible and reversible dissociation studies (Gaffan 1994; Thompson & Krupa 1994). A perfect example of this kind of dissociation is a study on fornix or caudate nucleus bilateral lesion and its effect during a radial maze task. Rats with lesion of the caudate nucleus were impaired in the acquisition of the win-stay task, whereas fimbria-fornix lesions facilitated performance. In contrast, caudate nucleus lesioned rats showed no disturbance in the performance of win-shift tasks, where fimbria-fornix lesions affected the task resulting in poor performance (Packard et al 1989). Most notable was that both of the two systems are able to provide solutions for the one task. A similar situation can be observed during the plus maze task where hippocampus and dorsal striatum can compete with each another during the same learning situation. In this case the early learning phase is mediated by the hippocampus, but this change with extended training. “Place learners” (spatial location/hippocampus) become “response learners” (reinforced response/striatum). Inactivation of the caudate nucleus with lidocaine prevents expression of the response learning and revealed the existence of place learning. These results indicate that existence of two memory systems that can provide a solution to the same task independently and cooperate when necessary (Packard & McGaugh 1996).

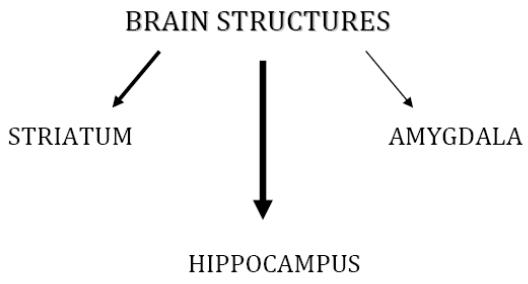

Fig.1.17 Three „central structures" of multiple parallel memory systems

The mammalian brain consists of at least three learning and memory systems with a hippocampus, striatum and amygdale as the three main structures connected with each other. Figure created based on (McDonald et al 2004).

With time it became clear that the MMS is a more complicated structure consisting of diverse interactions. Triple dissociation experiments indicated the existence of at least three main brain structures responsible for different types of learning and memory: hippocampus, amygdala, and striatum (Fig.1.17). Hippocampus is thought to be responsible for formation of episodic and spatial memory (Sutherland 1988), where amygdale is believed to format and store emotional memories (Bagshaw & Benzies 1968).

The amygdala plays an important role in tasks requiring association of the neutral stimuli with the unconditioned one. The stimulus-response learning, habit formation and memory processing depend on the dorsal striatum (Packard et al 1989). Lesions to the dorsal striatum affects motor response in tasks that require reinforcement in the presence of a single cue (Hannon & Bader 1974). Robert J. MacDonald et al. applied three simple behavioral tasks using the radial maze; (win-shift, conditioned cue preference (CCP), and win-stay) to demonstrate the existence of three independent memory systems. Their results indicated the importance of the hippocampus in the win-shift task, which requires association of extra-maze stimuli with each arm of the maze to avoid re-entrance to the same arm. The amygdala and dorsal striatum are not necessary to the correctness of this performance. In contrast, CCP depends only on the amygdala because it requires sensory cue association with the reward. Lesions to the hippocampus or dorsal striatum do not affect acquisition of this task. In the case of the win-stay task, two interesting results can be observed: The first concerns rats with lesion of the dorsal striatum, who clearly present severe impairment in the acquisition of this task, due to the disturbance in stimulus-response association. The second result concerns hippocampus lesion rats, which show enhancement in win-stay performance, probably due to the interference between those two systems. This result might serve as a proof of the competitive nature of the interaction between the hippocampal and striatal systems (McDonald & White 1993).

These results indicate the existence of three independent memory systems, which are activated depending on the demands of the task that should be performed. The hippocampus is important for tasks requiring information about the association between stimuli. The amygdala is responsible for the association between stimuli and reward, and the dorsal striatum is important for tasks requiring reinforced stimulus-response association.

Many recent studies on the MMS suggested that disturbance in function or connectivity between these main structures lies at the base of various psychiatric disorders like; schizophrenia (Hanlon & Sutherland 2000), anxiety (Hariri et al 2002) and depression (Sheline et al 2003). This is quite a new theory which assumes that any change, in one brain structure will alter interactions between different memory/behavioral systems and result in the manifestation of psychiatric disorder symptoms.

1.5 Learning

The phenomenon of learning has fascinated people since antiquity. Many theories that arose during that time are still widely used. One of first examples of the debate on learning is the conflict between Aristotle's *empiricism* and Plato's *nativism*. According to Plato everything what we know is inborn and, therefore, learning is just recalling of knowledge that is already inside of every human. Aristotle, however, claimed that our knowledge is acquired over a life time of experiences (Powell 2009).

A major breakthrough in learning theories and the beginning of behaviorism was the mind-body dualism theory described by Rene Descartes in "Description of the Human Body" 1647 and "Passions of the Soul" 1649. He claimed that our bodies function like machines and are able to produce involuntary reflexes in response to environmental stimuli. On the other hand, he was very emphatic about the fact that we have a mind with a free will, which produces behavior according to our wishes. He suggested that observation of animal behavior might be the source of many answers on reflexes in human behavior (Powell 2009).

1.5.1 Animal behavioral studies

In our behavioral studies we concentrated on the procedural form of learning, especially on the associative part. Procedural learning is based on simple reflex pathways formation. It involves acquisition of a motor response as a reaction to the sensory input. Two main categories can be distinguished in procedural learning. Less significant to our purposes is non-associative learning, described as a change in behavior that occurs with time in response to a single stimulus. In this category, there are two types of learning: habituation and sensitization (Fig. 1.19). Habituation can be characterized as learning to ignore a stimulus that does not carry any meaning, and sensitization is characterized as the intensification of the stimuli that previously did not evoke any reaction.

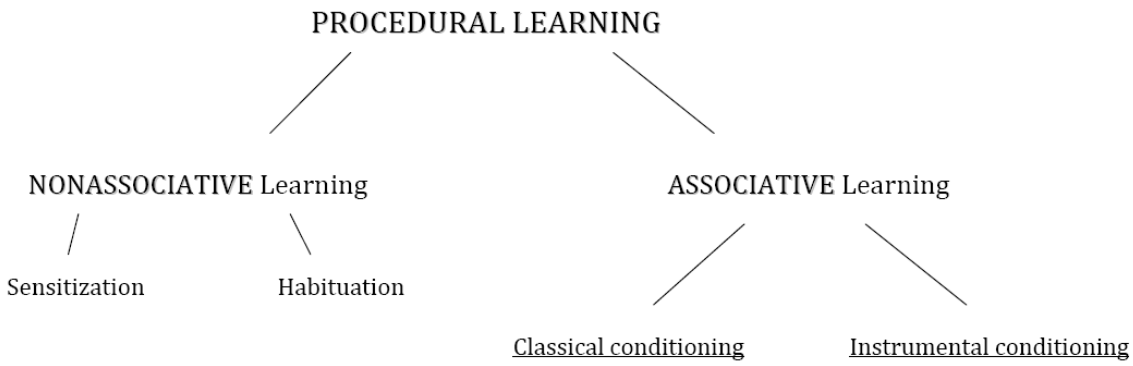

Fig. 1.19 Categories of procedural learning

Created according to chapter 24 of "Neuroscience Exploring the Brain" (M.F. Bear 2007).

1.5.1.1 Classical conditioning

Classical conditioning is a process in which one stimulus that does not elicit a response, (neutral stimulus (NS), is associated with another type of stimulus that does elicit a response, unconditioned stimulus (US). As a result of this association (Fig. 1.20) the NS becomes a conditioned stimulus (CS) and starts to elicit a conditioned response (CR) (Pavlov 1960) (Fig. 1.20).

If we look deeper into the processes underlying classical conditioning, its complex phenomenon can be presented as a *stimulus-response (S-R) model*. According to this concept the NS becomes directly associated with the unconditioned response (UR) and as a result of this association it elicits the same response as the US. This model was extensively studied using the shuttle-box avoidance test, which elicits a conditioned emotional response. In this case a tone/NS was associated with foot shock/US, which resulted in autonomic arousal/CR. This allowed investigation of the physiological structures and sensory pathways of the S-R model (Weinberger 1965). Further studies on rabbits and *Aplysia* indicated the role of the hippocampus, with increased neuronal activity and Ca^{2+} influx as cellular mechanisms of classical conditioning (Berger et al 1976; Hawkins et al 1983).

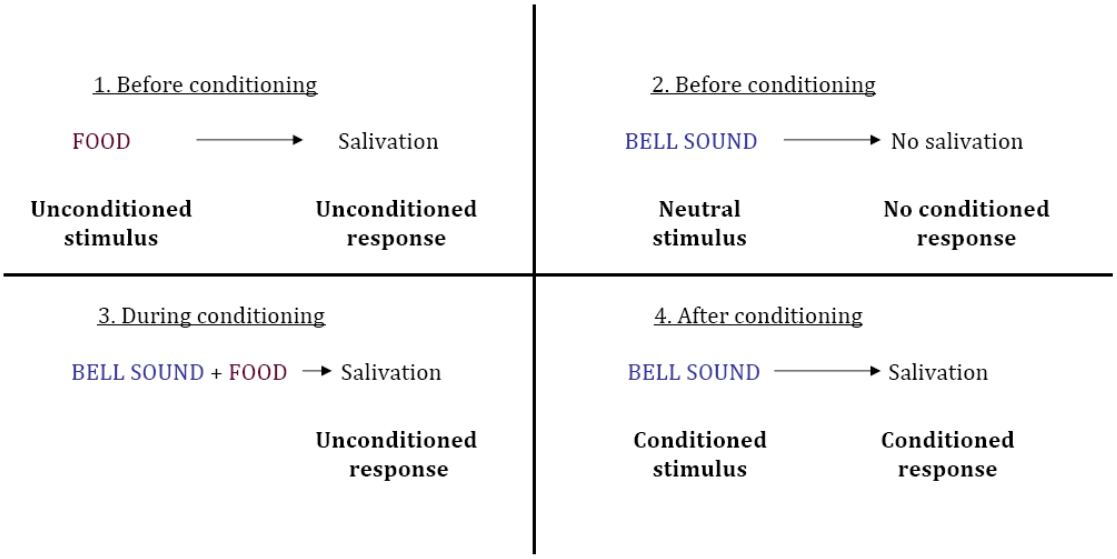

Fig. 1.20 Pavlovian conditioning

Phases of classical conditioning can be described in four main stages. Before conditioning two different stimuli: unconditioned and neutral are presented separately. During the conditioning process both stimuli are presented together, until an association is created. After conditioning, presentation of the stimulus that was previously neutral now becomes CS, due to the association, and now elicits CR. Created according to the 3rd chapter of "Introduction to Learning and Behavior" (Powell 2009).

In my studies I used a fear conditioning paradigm as an example of classical conditioning. During fear conditioning mice learn to predict aversive events. In this paradigm, an electric shock is associated with a neutral stimulus/tone. Repetitive pairing of two stimuli results in expression of the fear response to the neutral stimulus and context.

During his experiments, Pavlov noticed that when he repetitively presented a non-reinforced CS it resulted in learning inhibition that suppressed or replaced the previously acquired association between the CS and US. Today we know that extinction does not erase the original learning but, rather, creates a new one. Many studies on extinction have shown that the extinguished response can recover after a time laps (Robbins 1990) (Devenport et al 1997). There is direct evidence that old memory traces were not destroyed. Similar conclusions can be drawn from rapid reacquisition; presentation of new CS-US after extinction causes rapid reacquisition of the old pairing (Napier et al 1992).

Until the beginning of the 21st century, classical conditioning was used for better understanding and developing treatment of human phobias and drug addiction (Powell 2009). It was also suggested that it can be used to investigate allergy induction (Ader & Cohen 1975; Russell et al 1984).

1.5.1.2 Operant conditioning

Operant conditioning is the type of behavior that is influenced in a positive or negative way by its consequence. This learning paradigm is often called instrumental conditioning because the response is instrumental in producing the consequence. The father of operant conditioning is Edwin L. Thorndike (1874-1949) who was the first to study animal's learning abilities. Based on experiments carried out on cats he was able to formulate the "Law of Effect" (Powell 2009). According to the "Law of Effect", behaviors that lead to satisfaction are strengthened, whereas those connected with dissatisfaction will become weaker with time (Thorndike 1927; 1933).

While the early studies of Thorndike can be considered as a basis for operant conditioning, B.F. Skinner was the one who fully realized the implication of this principle during his rat studies (Fig. 1.21). He designed the apparatus called the operant conditioning chamber, or "Skinner box", in which rats are able to earn food pellets by pressing a lever (Powell 2009). In contrast to Thorndike, he did not consider the strengthening or weakening of an animal's interest in a performance to be the result of its thinking or feelings, but rather as an effect of the consequences on the future probability of the same behavior (Skinner 1935).

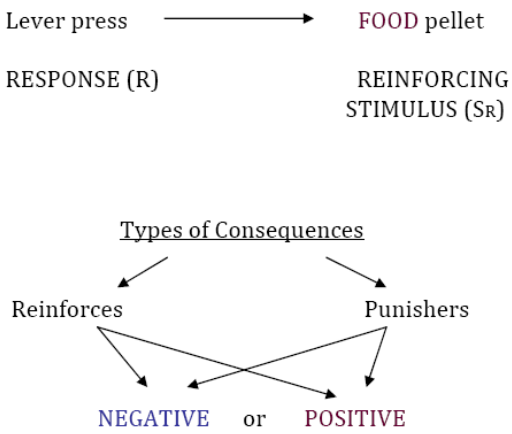

Fig. 1.21 Operant conditioning

During operant conditioning, the lever press described as a response (R) is reinforced by food pellet delivery. Pellets serve as a reinforcing stimulus. Two main types of consequences can be specified in operant conditioning: *reinforces* and *punishers*. They can be further divided in to two subgroups: negative and positive. As a result of this division we have four basic types of contingencies (response-consequence relationships): negative reinforcement, positive reinforcement, negative punisher, and positive punisher. Created according to (Powell 2009).

In contrast to classical conditioning, where performance can be presented as an S-R model, since response is elicited by stimuli, operant conditioning represents an *action-outcome (A-O) model*, at least in its early stage, since organisms are able to encode the specific consequences of their action (Dickinson & Balleine 1994). Detailed studies indicated

the role of the hippocampus and dorsomedial striatum (DMS) in instrumental conditioning. A lesion of the dorsal hippocampus does not affect acquisition of the instrumental response, but influences behavior when the A-O contingency is degraded. After extinction, test rats with lesions to the hippocampus show lever pressing frequency comparable to those before extinction. In the case of sham animals, frequency significantly decreased (Corbit & Balleine 2000). The role of DMS in the acquisition and expression of A-O association in operant conditioning was confirmed both in rats and humans (Yin et al 2005) (O'Doherty et al 2004).

In my studies, as an example of instrumental conditioning, I performed an extended version of the Morris water-maze, where finding the platform hidden under the water was the positive reinforcement. The second example of the operant conditioning was a T-maze test, where a correct turn was rewarded with a sugar pellet.

1.5.2 Motor learning

Motor learning is a process based on constant improvement of motor skills. It consists of the acquisition of new skills and enhancement of those already acquired (Newell 1991). One of the first motor learning theories established by J.A. Adams and R.A. Schmidt concentrated on the idea of how movements are produced and modified as a result of practice and experience (Adams 1971; Schmidt 1976). According to Adams, motor learning consists of a two-stage process. The first is represented with a *memory trace* to select and initiate a movement, and the second *perceptual trace* describes the correctness an image of the movement. Schmidt's theory introduced the concept of the schema as a contribution of recall and recognition to the movement output (Newell 1991).

According to modern thinking, motor skills learning can be divided into three main stages:

- cognitive: during which, cognitive activity is required to determinate appropriate strategy and performance is improved in a short amount of time
- associative: follows the cognitive phase where the task performance has been determined, now enhancement of the task to increase effectiveness is introduced, during this phase further performance improve over long period of time
- autonomous: the last motor skills learning phase which can last several months even years, the task is performed automatically (habit) (Donald 1999).

The modern notion of motor learning relates to human's/animal's ability to acquire new skills through practice and repetitive performance of many single sequences. Studies on implicit motor sequence learning indicate role of the hippocampus (Gheysen et al 2010), parietal, temporal and frontal cortical brain areas, cerebellum (Glickstein 1992), and striatum (Pisani et al 2005). Human studies using serial reaction time (SRT) based on the visuospatial stimulus mapping indicate significant contribution of the left anterior hippocampus to the task performance. Functional magnetic resonance imaging (fMRI) indicates hippocampal involvement during the early encoding phase as well as during the late storing phase (Gheysen et al 2010). Similar results were observed during learning of sequential finger movement test. Based on these results, motor learning was divided into two functional phases for the first time: an initial phase of "fast" learning showing within session improvement, and a "slow" learning phase, characterized by improvement after continued practice (Karni et al 1998).

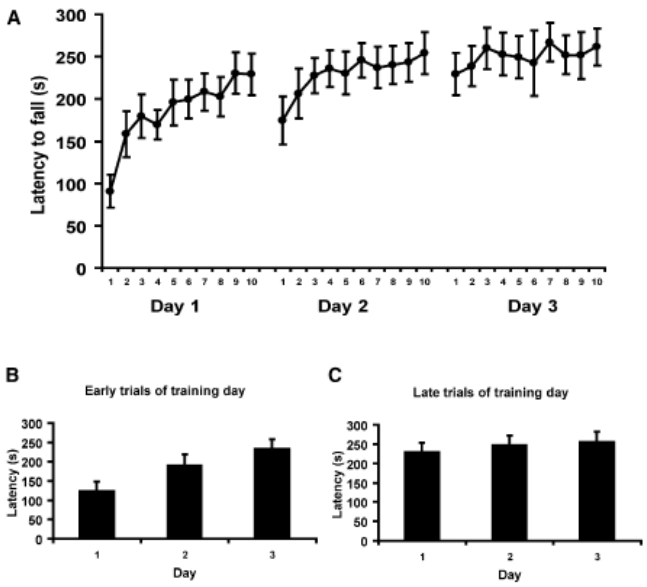

Fig. 1.22 Fast and slow motor skill learning in the accelerated rotarod task.

(A) Animals showed fast learning during the first training day, which slowed down during day 2 and reached plateau during the third day.

(B) Across days, there was a significant change in the latency to fall during the early trials (one and two) of every session. We observed a significant improvement from day 1 to day 2 but no further improvement from day 2 to day 3.

(C) Across days, there was no significant improvement in the latency achieved during the late trials (days nine and ten) of every session indicating that the most substantial improvement occurred during the first training day (Costa et al 2004).

Multielectrode arrays, used to record neuron activity during the accelerated rotarod task, indicated both cortical and striatal neuron activity during different phases of motor learning (Costa et al 2004). Rat performance on the rod clearly showed the existence of two learning phases (Buitrago et al 2004b); within session (intrasession) and between

session (intersession) improvement (Fig. 1.22). Further studies on motor memory consolidation demonstrated different characteristics of the motor learning phases. The fast learning seems to be sensitive to errors but shows poor retention, whereas the slow learning shows robust retention and poor sensitivity to error (Criscimagna-Hemminger & Shadmehr 2008). The latest results on oculomotor sequence learning indicate the functional interaction between the hippocampus and the striatum in offline memory processing (Albouy et al 2008). Extended motor learning process further results in an automatic stage (habit), where the learned behavior requires a minimum level of consciousness and is resistant to disturbance and time. A retention mechanism is considered as responsible for skills that can be performed after a long period of time without additional training (Doyon & Benali 2005).

Because of the NT expression pattern, our studies concentrated on the role of the NT/agrin interaction in motor skills acquisition. During these studies we performed:

- the accelerated rotarod test with the protocol customized for mice
- the staircase test established for measurement of deficits in paw reaching
- the Morris water-maze test, which is a combination of motor and spatial learning
- the T-maze, which allows to study spatial memory and assess preference between hippocampal and striatal spatial response.

1.5.2.1 Habit formation

Constant practicing and improvement of motor skill leads to its automatization and almost unconscious behavior defined as habit. Habits are learned during motor skills acquisition, acquired via experience-dependent plasticity (Graybiel 2008). From an evolutionary perspective, habit formation is an important process that allows learned tasks to be performed unconsciously and thus concentration can be diverted elsewhere. Habits are created as a result of overtraining; its formation depends on the cortico-striatal interaction (Fig. 1.23).

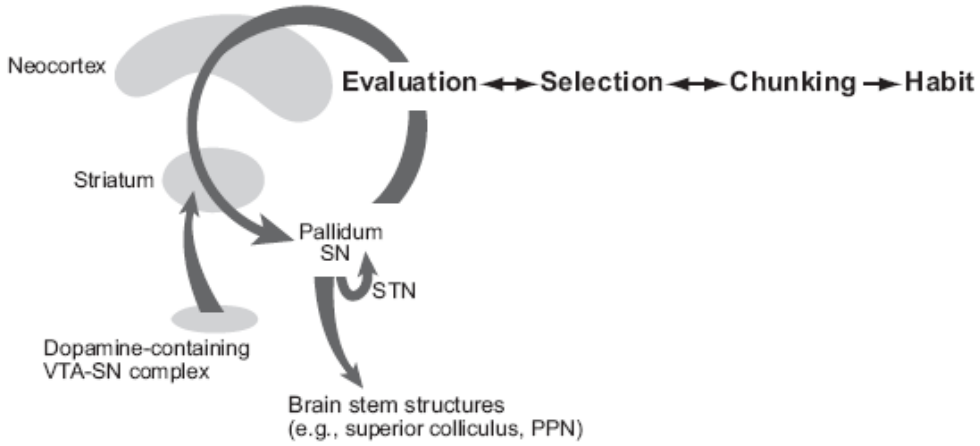

Fig. 1.23 Habit formation.

Schematic representation of the development of habits through interactive action of cortico-basal ganglia circuits. Circuits mediating evaluation of actions gradually lead to selection of particular behaviors that, through the chunking process, become habits. **PPN**, pedunculopontine nucleus; **SN**, substantia nigra; **STN**, subthalamic nucleus; **VTA**, ventral tegmental area (Graybiel 2008).

Studies on two distinct brain areas, namely the hippocampus and caudate nucleus, revealed the existence of two neural systems responsible for different animal reactions. During training in the cross-maze, rats learn to turn into the correct, baited arm of the maze. After a few days of training, the probe trial is performed. Rats start the new trial from the opposite side of the maze. Those animals that choose the arm according to the external cue ended in the correct arm and were rewarded with the food; these are “place learners”. Those that automatically choose the same turn are called “response learners” and finished without a reward. Afterwards, an extended training probe trial was repeated. Rats given a lidocaine injection into the hippocampus did not show a preference for place learning or response learning during the first probe trial, but presented a clear tendency towards response learning during the second probe. This suggested that place learning tendency was blocked by the inactivation of the hippocampus. In contrast, rats that received the injection into the caudate nucleus presented the place learning response during both probe trials. This indicates that the caudate nucleus is responsible for response learning (Packard & McGaugh 1996). Summarizing, the initial place response is overcome with overtraining and results in response-directed learning. With extensive training the initial A-O (goal) tendency shifts into the simple S-R model.

Further research concentrated on the striatal area indicated the distinct role of the dorsolateral (DLS) and dorsomedial (DMS) striatum during the habit formation process. A study on monkey learning and a sequence of button pressing revealed activity of the asso-

ciative DMS during the initial acquisition phase, which decreased with training. Whereas, higher neuronal activity of the sensorimotor DLS was observed during the late, already automated phase (Miyachi et al 2002). These results are consistent with the water-maze studies, which show that the DMS is involved in place learning, whereas the DLS is involved in response learning (Devan et al 1999). The role of the DMS in the acquisition process still remains unclear because of the fact that its lesion contributes to the faster S-R-like habit formation, which is visible even during the early stage of training, thus suggesting that the DMS and the hippocampus belong to the same functional system (Yin et al 2008).

Recently research about habit formation drew great attention from scientists working on addictions and psychiatric disorders, like obsessive-compulsive disorder (OCD) and Tourette syndrome. Constant, repetitive behavior similar to the one observed during the habit formation is a characteristic feature for some of the psychiatric disorders. Extensive work on addiction has led to the conclusion that expression of addictive behavior is driven by the same goal-directed transition as in case of habit formation (Everitt et al 2001; Hyman et al 2006). Further studies concerning processes of habit formation may become extremely useful in the treatment of psychiatric human disorders.

2 Aim of the project

A 4 bp deletion in the PRSS12 gene encoding the trypsin-like serine protease neurotrypsin in humans was found to be responsible for nonsyndromic MR, which starts to become evident by the child's second year. Therefore, we believed that NT is crucial for adaptive synaptic functions. Previous studies have demonstrated that NT cleaves agrin, a large heparin sulfate proteoglycan, at two conservative sites (α and β) *in vitro* and *in vivo*. We know that overexpression of TM-agrin in rat hippocampal neurons induces the formation of filopodia-like protrusions on axons and dendrites. Therefore, we studied whether agrin cleavage is involved in activity-dependent generation of filopodia in the mature hippocampus. Filopodia are transient, short-lived structures that are considered to be immature forms of synapses. To understand NT/agrin interaction and its role in the adult CNS, we applied two chemical stimulations (TEA and PFR) to induce LTP in acute hippocampal slices of wild-type and NT-deficient mice. We applied two techniques: Western blotting, to quantify the agrin-90 fragment released after the chemical stimulation, and 3D reconstruction of the filopodia, to assess new filopodia formation in NT-deficient mice. We hypothesized that NT deficiency will affect structural plasticity in hippocampus. Therefore, our work aimed to detect and quantify the appearance of dendritic filopodia in response to the induction of LTP in wild-type and NT-deficient mice. The extent of filopodia formation could indicate the potential plasticity in the hippocampus region, as it was shown that when the brain receives a large amount of new stimuli and the process of storing new information is enhanced the number of filopodia rapidly decreases and the number of stabile spines increases.

Next, we planned to characterize the behavioral phenotype of the NT-deficient mice, since strong NT expression in the hippocampus and amygdala suggests its role in learning and memory. Furthermore, motor learning studies with mice proved that extended learning promotes elimination and formation of spines, i.e. remodeling of pre-existing neuronal connections. Our studies particularly focused on procedural learning. Initially we mainly concentrated on the motor learning aspects since children with truncated form of NT were not able to learn how to speak; speech learning is a part of procedural learning. We aimed to observe effects of NT/agrin interaction on mice behavior in the context of mental retardation. We strongly believe that further studies on the proteolytic activity of NT could contribute to a better understanding of the molecular and cellular mechanisms underlying learning and memory processes and explain why the lack of NT in humans results in MR.

3 Results

3.1 The neurotrypsin/agrin system as a regulator of activity-dependent synapse formation in the CNS

Results described in chapter 3.1 are part of my research, and were published as a part of the following article:

Cell 136, 1161-1171, 2009

Coincident Pre- and Postsynaptic Activation Induces Dendritic Filopodia via Neurotrypsin-Dependent Agrin Cleavage

Kazumasa Matsumoto-Miyai[1,5], Ewa Sokolowska[1], Andreas Zurlinden[1], Chris Gee[2], Daniel Lüscher[1], Stefan Hettwer[3], Jens Wölfel[1], Ana Paula Ladner[1], Jeanne Ster[2], Urs Gerber[2], Thomas Rülicke[4,6], Beat Kunz[1], and Peter Sonderegger[1,*]

[1] Department of Biochemistry, University of Zurich, CH-8057 Zurich, Switzerland

[2] Brain Research Institute, University of Zurich, CH-8057 Zurich, Switzerland

[3]Neurotune AG, CH-8952 Schlieren, Switzerland

[4] Institute of Laboratory Animal Science, University of Zurich, CH-8057 Zurich, Switzerland

[5] present address: Department of Neurophysiology, Akita University School of Medicine, Akita 010-8543, Japan

[6] present address: Institute of Laboratory Animal Science and Biomodels Austria, University of Veterinäry Medicine Vienna, A-1210 Vienna, Austria

*Corresponding author

3.1.1 Cleavage of agrin by externalized neurotrypsin requires postsynaptic activation

TEA evokes global bursting and produces long-term potentiation (LTP) of synaptic transmission with similar properties as tetanus-induced LTP (Hanse & Gustafsson 1994; Huang & Malenka 1993; Huber et al 1995), indicating the concomitant activation of the pre- and the postsynaptic neuron by TEA, because this is a prerequisite for the induction of LTP (Malenka & Nicoll 1999). We thus tested for a postsynaptic component in TEA-induced neurotrypsin-dependent agrin cleavage. We found that the TEA-induced increase of agrin cleavage was prevented by the AMPA and NMDA-R inhibitors CNQX and MK-801 (Fig. 3.1A, B). In addition, a significant decrease of agrin cleavage was also found with nifedipine, a selective inhibitor of L-type voltage-dependent Ca^{2+} channels (VDCC). Therefore, TEA-induced neurotrypsin-dependent agrin cleavage exhibited a postsynaptic contribution from both NMDA-Rs and L-type VDCCs, as previously reported for the TEA-induced LTP (Hanse & Gustafsson 1994; Huang & Malenka 1993; Huber et al 1995).

We further confirmed this postsynaptic component with another chemical LTP protocol, using the combination of picrotoxin, forskolin, and rolipram at high extracellular Ca^{2+} and no Mg^{2+} (PFR). PFR stimulation induces LTP in the hippocampal CA1 region in an NMDA-R-dependent manner by enhancing neuronal network activity via reduction of GABAergic inhibition in combination with enhancing cAMP-mediated intracellular signaling (Kopec et al 2006; Otmakhov et al 2004). We found that the PFR-induced increase of agrin cleavage was prevented by the AMPA and NMDA-receptor inhibitors CNQX and MK-801 (Fig. 3.1C, D). Only a small, but non-significant reduction of PFR-induced agrin cleavage was found with nifedipine, a blocker of L-type VDCCS (Fig. 3.1.C, D), which is in line with the reported NMDA-R dependence of PFR-induced LTP (Otmakhov et al 2004).

Together, these results indicate that neurotrypsin-dependent agrin cleavage requires activation of presynaptic P/Q- and N-type calcium channels that are essential for presynaptic exocytosis of neurotrypsin. However, in contrast to neurotrypsin exocytosis from presynaptic boutons, neurotrypsin-dependent agrin cleavage also requires the activation of the postsynaptic neuron, with the indispensable activation of NMDA-Rs. These results indicate that neurotrypsin is externalized in an inactive form and that NMDA-R-driven activity of the postsynaptic cell is required for its activation. The dependence of neurotrypsin-dependent agrin cleavage on postsynaptic activation was also found with hippocampal slices from juvenile (4-6 week-old) mice. Therefore, the dependence of neurotrypsin activation on postsynaptic mechanisms was found to be an age-independent process.

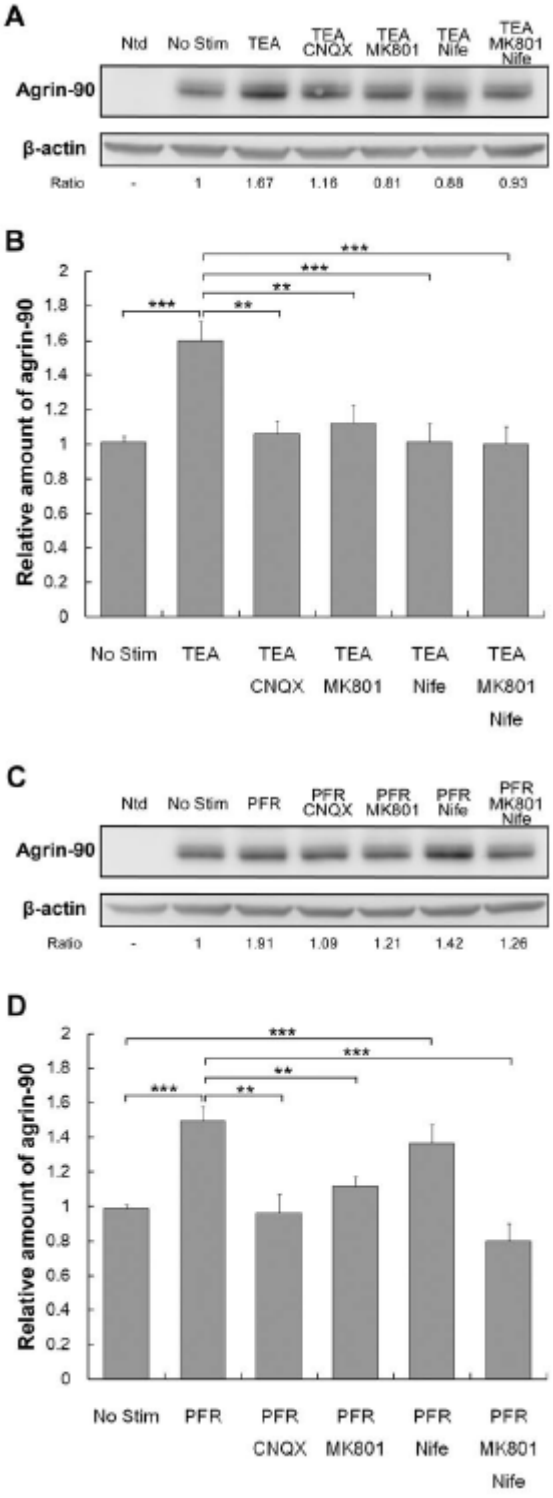

Fig. 3.1. Neurotrypsin –dependent agrin cleavage in P10 mice

The chemical LTP inducers TEA and PFR were used to stimulate neurotrypsin dependent agrin cleavage in whole hippocampi from P10 mice. Response to postsynaptic inhibition was studied by Western blotting of agrin-90.

(**A-B**) Stimulation with TEA. (**A**) Representative Western blots for agrin-90. The β-actin loading control is shown below. No Stim; wild-type hippocampi without stimulation. AMPA and NMDA receptors were blocked with CNQX and MK-801, respectively. L-type VDCCs were blocked with nifedipine (Nife).

(**B**) Quantification of agrin-90 levels under the conditions specified in (**A**). Levels of agrin-90 were normalized to β-actin. The average level found without stimulation was set to 1. Error bars indicate SEM; **p < 0.01; ***p < 0.001, ANOVA with Tukey's post hoc test (n = 13-14).

(**C-D**) Stimulation with PFR. (C) Representative western blot for agrin-90 with β-actin loading control below. Ntd: neurotrypsin-deficient hippocampi.

(**D**) Quantification of agrin-90 levels under the conditions specified in (C). **p < 0.01; ***p < 0.001 by ANOVA with Tukey's post hoc test (n = 10-12).

3.1.2 LTP is intact, but LTP-associated formation of dendritic filopodia is abolished in neurotrypsin-deficient mice

Activation of NMDA-Rs and postsynaptic Ca^{2+} influx is essential for LTP induction (Malenka & Nicoll 1999). Therefore, the recognition of neurotrypsin activation as an NMDA-R-dependent process prompted the question whether neurotrypsin plays a role in LTP expression. To test this possibility, we compared LTP in acute hippocampal slices from 4-6 week-old wild-type and neurotrypsin-deficient mice (Fig. 3.3A, B). LTP was evoked in the CA1 region with 4 1-s trains of 100Hz stimuli. Significant LTP was observed in slices from both wild-type littermates and neurotrypsin-deficient mice (150.5 ± 8.8%, n = 10, $p < 0.001$ and 169.1 ± 38%, n = 7, $p = 0.05$, respectively). There was no difference in the extent of LTP between wild-type and neurotrypsin-deficient mice ($p = 0.66$) (Fig. 3.3B), indicating that neurotrypsin was not essential for LTP expression.

Among the LTP-associated cellular phenomena, the formation of dendritic filopodia is particularly intriguing, because filopodia have been characterized as early forms of spines and, thus, precursors of synapses (Engert & Bonhoeffer 1999; Maletic-Savatic et al 1999; Ziv & Smith 1996). Therefore, we studied whether agrin cleavage is involved in activity-dependent generation of filopodia in the mature hippocampus. To visualize dendritic filopodia in hippocampal slices, we used the transgenic mouse line L15 expressing membrane-targeted GFP (mGFP) in sparse neurons (De Paola et al 2003). Filopodia were counted in reconstructed 3-dimensional images of secondary apical dendrites by inspection over a length of 30-40 µm (Fig. 3.3C-E). Dendritic filopodia (arrows in Fig. 3.3E) were identified according to the following morphological criteria: 1) a protrusion with a length of at least twice the average length of the spines on the same dendrite, 2) a ratio of head to neck diameter smaller than 1.2:1, and 3) a ratio of length to neck diameter larger than 3:1 (Grutzendler et al 2002).

First, we investigated the effect of chemical LTP on filopodia number, again using TEA- or PFR-induced global bursting as a means to mimic tetanus-induced LTP. Our electrophysiological recordings after TEA and PFR stimulation confirmed that both protocols induce robust LTP and corroborated our results obtained with electrical LTP induction that LTP was intact in slices from neurotrypsin-deficient mice (Fig. 3.4.). In addition, tests with propidium iodide indicated that neither TEA nor PFR stimulation induced significant apoptosis in hippocampal slices. Quantification of filopodia in non-stimulated control samples indicated that the average number of filopodia was 0.114-0.118/µm (Fig. 3.3F, H). Following TEA or PFR stimulation, filopodial density was significantly increased to 0.156 or 0.152/µm, respectively ($p < 0.001$ vs No Stim by ANOVA with Tukey's post hoc test).

Administration of the glutamate receptor blockers CNQX or MK-801, or nifedipine, abolished the filopodial response to TEA (Fig. 3.3F). The dependence of the filopodial response on both NMDA-Rs and L-type VDCCs is consistent with previous studies indicating that TEA-induced LTP consists of two mechanistically distinct forms of LTP, one depending on NMDA-Rs and the other on L-type VDCCs (Hanse & Gustafsson 1994; Huang & Malenka 1993; Huber et al 1995). The blockade by MK-801 and nifedipine indicates that the LTP-associated filopodial response to TEA exhibits the same inhibitor profile as TEA-induced LTP and TEA-induced neurotrypsin-dependent agrin cleavage. Likewise, the filopodial response to PFR stimulation was also blocked by the glutamate receptor blockers CNQX and MK-801, but no significant inhibition was found after blockade of L-type VDCCs with nifedipine (Fig. 3.3H). Again, this is consistent with the inhibitor profile of PFR-induced chemical LTP (Okamoto et al 2004).

To examine the role of neurotrypsin in LTP-induced generation of filopodia (Fig. 3.3G, I), we crossed neurotrypsin-deficient with transgenic L15 mice expressing mGFP in sparse neurons. The number of filopodia along secondary apical dendrites of CA1 pyramidal neurons was counted in mGFP-positive, neurotrypsin-deficient mice and in littermate (neurotrypsin-wild-type) controls. CA1 neurons of wild-type mice had 0.107-0.120 filopodia per µm (Fig. 3.3G, I). Filopodia number was significantly increased by both TEA and PFR- stimulation, reaching 0.172/µm and 0.166/µm, respectively (Fig. 3.3G, I). In contrast, neither TEA nor PFR-stimulation induced a significant increase in filopodial density (0.117/µm and 0.119/µm, respectively) in hippocampal slices of neurotrypsin-deficient mice (Fig. 3.3G, I). Representative dendrite pictures with filopodia indicated by the black arrows (Fig. 3.2.). Together, these results indicate that neurotrypsin is not required for induction and expression of LTP, but rather for the LTP-associated generation of filopodia.

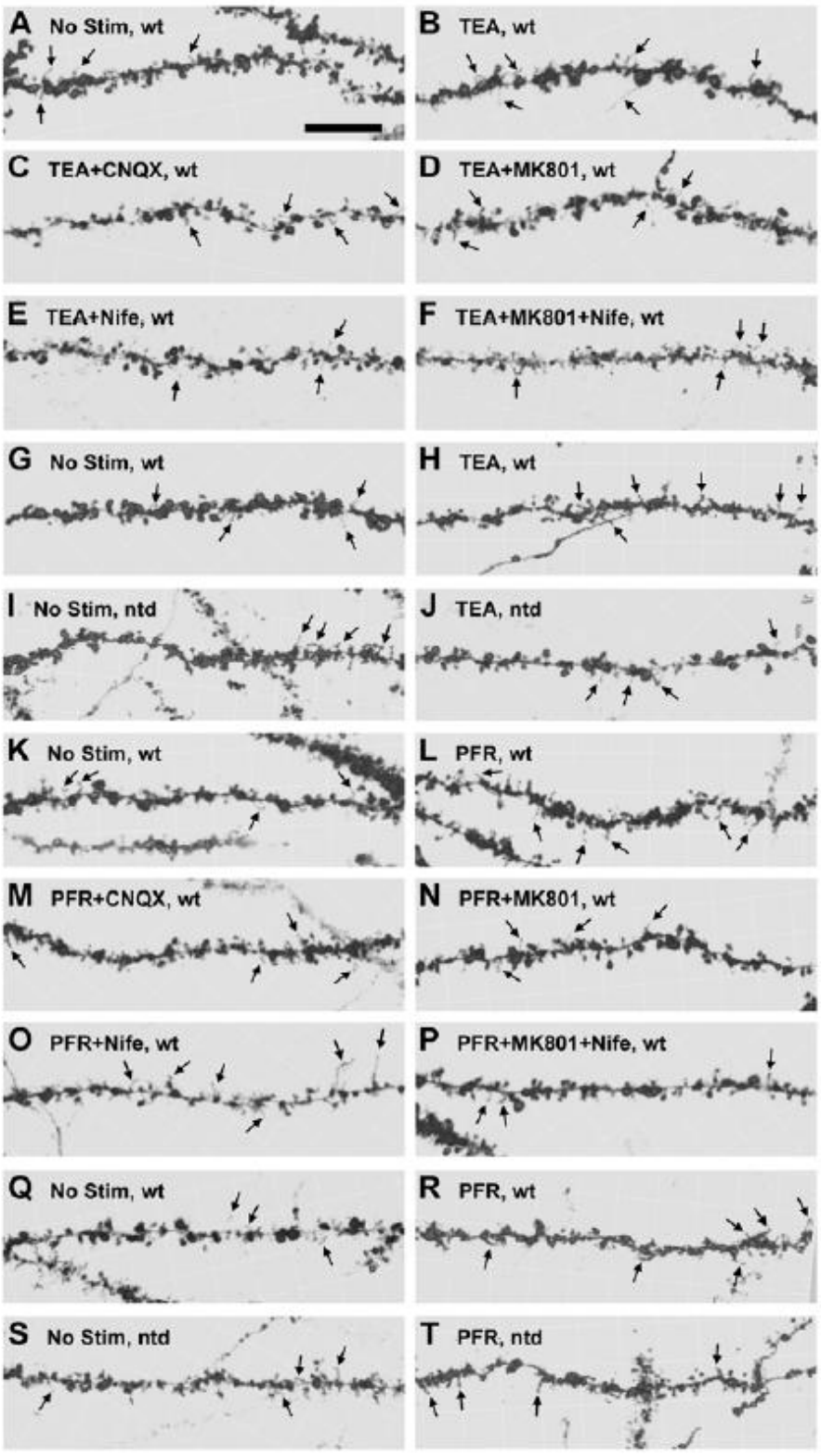

Fig. 3.2 LTP-associated formation of filopodia is abolished in neurotrypsin-deficient mice

Images of dendritic filopodia were obtain with confocal microscope and analyzed using Imaris software. Filopodia were identified according to criteria established by (Grutzendler et al 2002) Scale bar: 10 μm. Black arrows indicate filopodia structures. **ntd**; neurotrypsin-deficient, **wt**; wild-type littermate control.

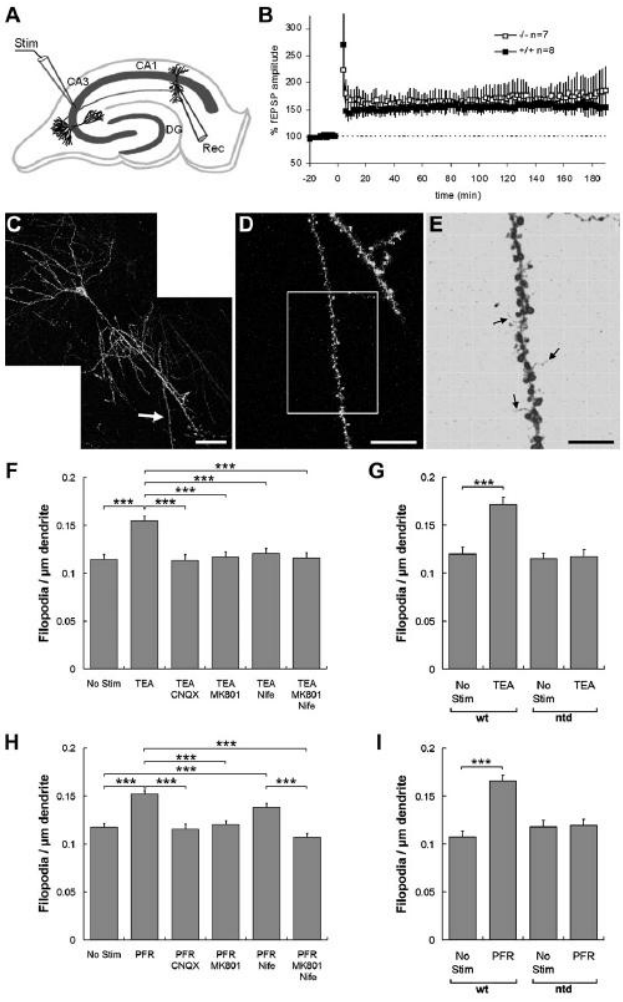

Fig. 3.3 LTP is intact, but LTP-associated formation of filopodia is abolished in neurotrypsin-deficient mice

LTP and LTP-associated promotion of dendritic filopodia were assessed in hippocampal slices of 4-6 week-old neurotrypsin-deficient mice. (**A**, **B**) LTP was studied by stimulation of the Schaffer collaterals and electrophysiological recordings of Schaffer collateral-CA1 synaptic responses (**A**). Test stimuli were delivered at 30s intervals and LTP was induced by delivering four 1-s 100 Hz trains at 30s intervals. (**B**) Comparison of long-term potentiation (LTP) in the hippocampal CA1 area of neurotrypsin-deficient (white squares) and wild-type (black squares) mice. Data are shown as mean ± S.E.M. The results indicate that neurotrypsin-deficient mice have normal LTP. (**C**-**I**) Analysis of filopodia on dendrites of CA1 pyramidal neurons in wild-type and neurotrypsin-deficient mice expressing membrane-targeted GFP in sparse neurons. (**C**) Representative image of a GFP-expressing CA1 pyramidal neuron in a hippocampal slice. (**D**) Higher magnification of the secondary apical dendrite indicated by the arrow in **C**. (**E**) Reconstructed 3D image of the secondary apical dendrite boxed in **D**. Arrows show filopodia identified according to the criteria of (Grutzendler et al 2002). Bars: 50 µm in **C**; 20 µm in **D**; 10 µm in **E**. (**F**-**I**) Filopodia numbers on secondary apical dendrites of hippocampal CA1 pyramidal neurons. (**F**) Number of filopodia per 1 µm of dendrite after TEA stimulation and effect of AMPA and NMDA receptor blockade by CNQX and MK-801, respectively, and blockade of L-type Ca^{2+}-channels by nifedipine (Nife) in L15 mice (wild-type for neurotrypsin). (**G**) Comparison of filopodia formation after TEA stimulation in wild-type and neurotrypsin-deficient mice. (**H**) Filopodia numbers after PFR and effect of CNQX, MK-801, and nifedipine. (**I**) Comparison of filopodia formation after PFR stimulation in wild-type and neurotrypsin-deficient mice. Error bars indicate S.E.M.; ***, $p < 0.001$, ANOVA with Tukey's post hoc test. **wt**.: wild type littermate control. **ntd**: neurotrypsin-deficient mice.

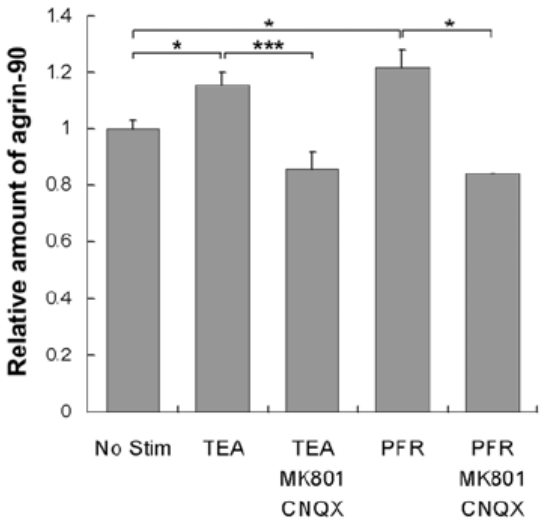

Fig. 3.4 Neurotrypsin dependent agrin cleavage in 4 to 6 week old (juvenal) mice

TEA was used as chemical LTP inducer to stimulate neurotrypsin-dependent agrin cleavage in hippocampal slices from 4-6 week old mice. Response to blockade of postsynaptic glutamate receptors was studied by Western blotting of agrin-90. Error bars indicate S.E.M; *, $p< 0.05$; ***, $p< 0.001$ using ANOVA with Newman-Keuls post hoc test (n = 3-8).

3.1.3 The C-terminal fragment of agrin restores the LTP-induced increase of filopodia in neurotrypsin-deficient mice

Because agrin is the only proteolytic target of neurotrypsin and because LTP-dependent induction of dendritic filopodia was abolished in neurotrypsin-deficient mice, we wondered whether the released agrin fragments (agrin-22, agrin-90, and agrin-110) might function as filopodial inducers. To test this hypothesis, we produced these fragments in HEK293T cells, purified them, and added 50 nM of each to neurotrypsin-deficient hippocampal slices (Fig. 3.5.). We found that administration of agrin-22 (z0) with PFR induced a significant increase of filopodia, reaching levels observed in PFR-stimulated wild-type hippocampi (0.182/µm; Fig. 3.5A-E). Almost the same effect was found when agrin-22 was applied without PFR (0.167/µm). These results identify agrin-22 as the mediator of the filopodia-generating response associated with LTP.

Agrin-90 was unable to rescue PFR-induced filopodia stimulation in neurotrypsin-deficient mice when administered alone or in combination with PFR (0.128/µm or 0.120/µm, respectively; Fig. 3.5F). We also tested agrin-110 that was generated by partial proteolytic cleavage at the α cleavage site and comprised both agrin-90 and agrin-22. Agrin-110 (y0z0) showed only a weak, statistically non-significant rescue (0.136/µm; Fig. 3.5G) even though it contains the C-terminal part of agrin. Therefore, we concluded that the C-terminal domain of agrin was only active when isolated in the form of agrin-22, and thus that β cleavage was important to exert a maximal filopodia-inducing effect.

In summary, we have shown that the neurotrypsin-dependent generation of agrin-22 is essential for LTP-dependent filopodia induction and that the agrin-22-derived signals resulting in NMJ development and those resulting in the generation of filopodia from dendrites of CNS neurons are distinct.

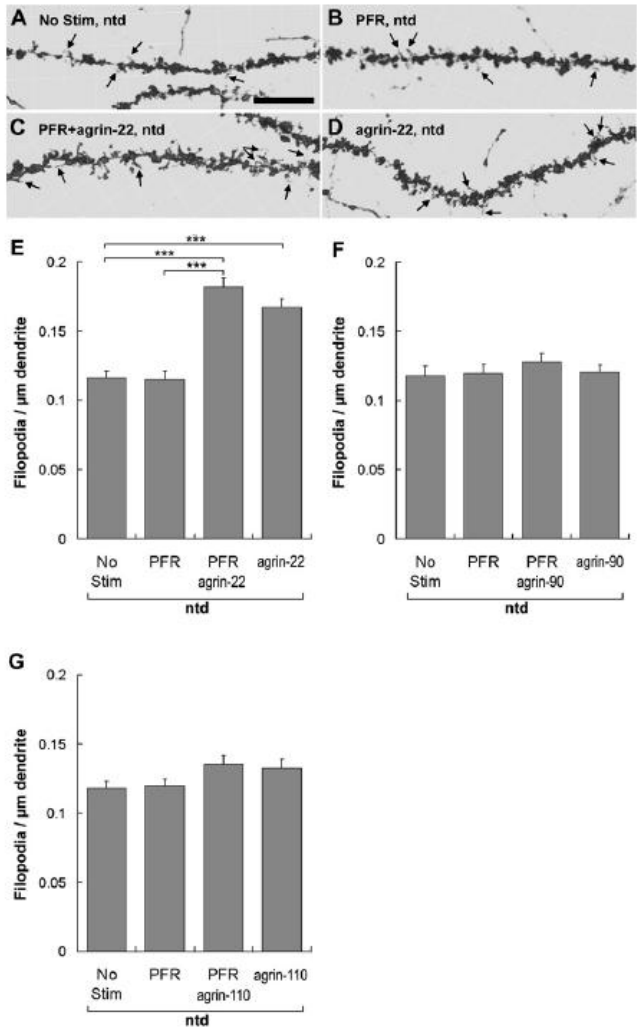

Fig. 3.5 Isolated agrin-22 promotes the formation of dendritic filopodia

The fragments of agrin generated by neurotrypsin-dependent cleavage were tested for their filopodia-promoting activity on secondary apical dendrites of CA1 pyramidal neurons in hippocampal sliced from 4 to 6 week old mice. (**A-E**) Densities of filopodia on dendrites in neurotrypsin-deficient hippocampi with or without agrin-22. (**A-D**) Representative images of dendrites of CA1 pyramidal neurons of neurotrypsin-deficient mice with or without agrin-22. Arrows indicate filopodia. (**E**) Number of filopodia per 1 µm of dendrite. (**F-G**) Filopodia density on dendrites after application of agrin-90 (**F**) and agrin-110 (**G**). Error bars indicate SEM; ***p < 0.001 by ANOVA with Tukey's post hoc test. **ntd**; neurotrypsin-deficient.

3.2 Behavioral phenotype of neurotrypsin-deficient mice

3.2.1 High variability between consecutive series of rotarod tests precluded conclusions about motor skills learning

3.2.1.1 The 1st series of the rotarod tests showed elevated motor performance in neurotrypsin-deficient mice

The rotarod task is a commonly used paradigm for the assesement of motor skill learning (Buitrago et al 2004b; Mizoguchi et al 2002). In my studies mice were trained for 7 consecutive days/sessions, to maintain balance on an accelerating rotating rod. Each session consisted of 10 trials with a 5-6 minutes break in between. A break of 7 days was introduced after the training phase to observe possible changes concerning memory consolidation. After the break mice were tested for additional 2 days. This experimental setup allowed intrasession (within session) and intersession (between session) learning in NT-deficient and wild-type mice to be analyzed precisely.

The results of the 1st series of rotarod tests (Tab. 1) indicated that NT-deficient mice are capable of rapid acquisition of the task. NT-deficient mice perform on the rotarod significantly better during the training phase ($p < 0.0001$) as well as during the two additional days after the break ($p < 0.01$) (Fig. 3.6A). Further, detailed analysis revealed a statistically significant improvement, equal for both genotypes, within one session/ 10 trials ($p < 0.0001$). Mice as well showed significant improvement between sessions/days ($p < 0.0001$) during the training phase and during the additional two days ($p < 0.001$, $p < 0.05$), respectively. This means that after the overnight break the mice started their performances on the rotating rod from a slightly lower level, if compared to the last trial of the previous day, but on a much higher level, if compared to the first trial of the previous day.

To check for possible differences in memory consolidation between genotypes we analyzed the level of performance during the last trial of each day and compared it with the level of performance during the first trial of the next day and we realized that NT-deficient mice showed a significantly greater overnight drop ($p < 0.005$) in comparison to the wild-type mice. This suggested that NT-deficient mice may have a problem with memory consolidation.

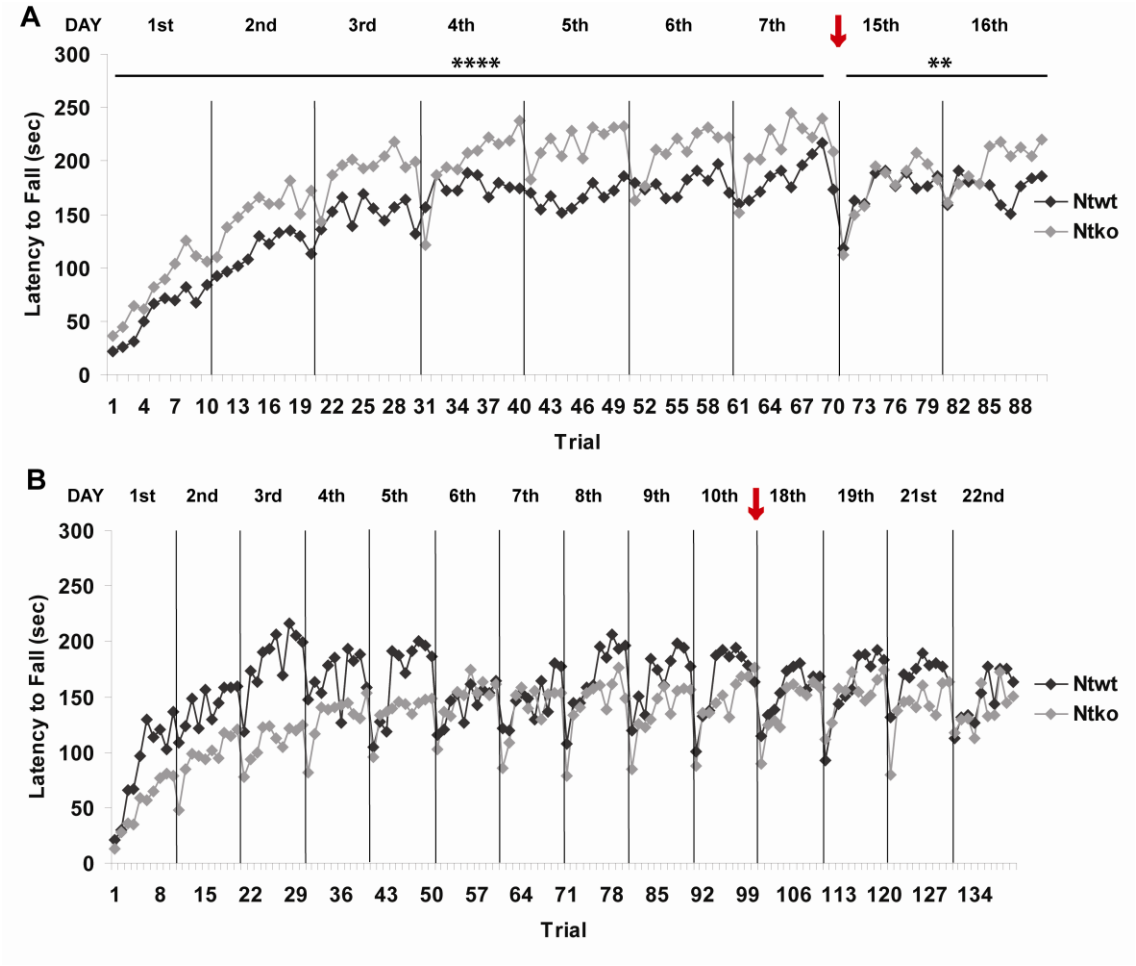

Fig. 3.6. Neurotrypsin-deficient mice show enhanced rotarod performance during the 1st, but not the 2nd, series of the rotarod test.

(**A**) The 1st series consisted of 7 consecutive training days and an additional 2 days after 7 days of a break. In total 25 mice (12 Ntwt/13 Ntko) participated in this series. Sex was equally distributed amongst genotypes. NT-deficient mice show significantly enhanced rotarod performance ($p < 0.0001$), before the break, and after the break ($p < 0.01$). The last trial of a day and the first trial of the following day indicate an overnight drop in the performance. NT-deficient mice show a significantly greater overnight drop in comparison to the wild-type mice ($p < 0.005$). (**B**) The 2nd series consisted of 10 consecutive training days and 4 additional days after a 7 day break. In total 17 mice (6 Ntwt/11 Ntko) took part in this test. Most of the mice taking part in this series of the experiment were females (2 males/15 females). Due to the greater percentage of females, a different performance pattern was observed. The red arrow represents location of 7 day break. ** $p < 0.01$, **** $p < 0.0001$ by Univariate ANOVA, **Ntwt**: wild-type littermate control, **Ntko**: neurotrypsin-deficient mice.

3.2.1.2 The 2nd series of the rotarod tests showed changed motor behavior in female mice

Because the results of the 1st rotarod series indicated enhanced performance of NT-deficient mice we hypothesized that NT-deficient mice may be more vulnerable to over-training, what would result in facilitated transit to habit. Due to our hypothesis we decided to prolong training phase from 7 to 10 consecutive days and testing stage from 2 to 4 days. The latency to fall analysis indicated no significant difference between genotypes during training and testing (Fig 3.6B). During the 2nd series of the test, which was supposed to confirm the previous results, we examined a cohort consisting almost entirely of females (2 males/15 females). The outcome of this round suggested that females acquired motor skills much faster than males (Tab. 2). On average, female mice reached the maximum of their performance already on the 3rd day of training. The above results were consistent with previous studies indicating that males needed more time to reach the same level of motor performance (Buitrago et al 2004a). Based on these results we continued research only on males to avoid unnecessary variability.

3.2.1.3 The 3rd and 4th series of the rotarod tests showed high variability between successive series, which did not allowed to draw conclusions

The two next series of rotarod tests were based on the same protocol, as that of the 2nd series, and were sought to confirm previous results. During the 3rd series similar results as in the first experiment were registered (Tab. 3). Both genotypes were able to improve their performance (Fig. 3.7A). Inter- and intrasession learning was highly significant for both genotypes ($p < 0.0001$). On about the fourth day of testing, both groups of mice reached the plateau. NT-deficient mice showed on average, a significantly higher latency to fall ($p < 0.0001$) during the training as well as during the four additional testing days. Tukey's post hoc test indicated a significant difference ($p < 0.001$) between the three first days and the remaining test days. However, the overnight drop level on the 3rd series of the rotarod test differed from that of the previous tests. A detailed comparison of the last trial on one day to the first one of the next day revealed a significantly higher overnight drop ($p < 0.05$) in the case of wild-type mice, an opposite result compared with the previous one.

During the last 4th series of the rotarod test we encountered unexpected technical problems with the apparatus. The test had to be terminated prematurely, after four testing

days. Mice involved in this experiment could not be use anymore for the rotarod test. Further testing consisted only of 10 mice (5 Ntwt/5 Ntko). Most of the mice have reached the maximum time on the rod already by the second day of training (Fig. 3.7B). Above result differs form the previous one, it is not reliable due to the small animal number and abnormally rapid achievement of the maximal performance.

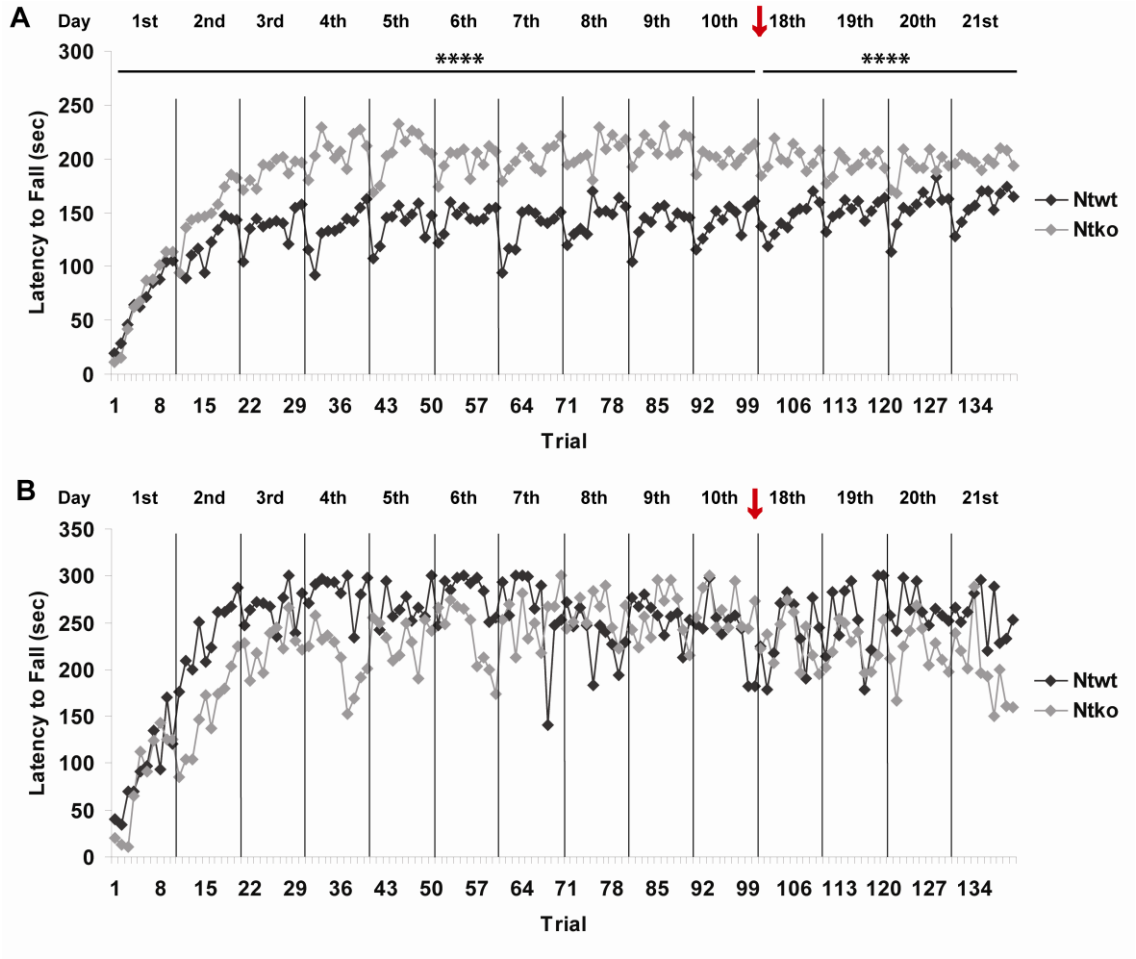

Fig. 3.7 The 3rd and 4th series of the rotarod test reveals high variability amongst both genotypes.

Due to the different female group's performance, further rotarod tests involved only males. Both series consisted of 10 consecutive training days and 4 additional days after a 7 day break. (**A**) The 3rd series of the test involved 27 mice (12 Ntwt/15 Ntko). Significantly better performance of the NT-deficient mice can already be observed during the second day of training, across the training period, and after the break ($p < 0.0001$, by ANOVA). During this series, wild-type mice showed a significantly higher overnight drop ($p < 0.05$) in comparison to the NT-deficient mice. (**B**) The 4th series (10 mice (5 Ntwt/5 Ntko)) of the rotarod test revealed a completely different pattern of behavior. There was no difference between genotypes. Both genotypes had reached maximum performance time (300sec) already during the second day of training. The red arrow represents the location of the 7 day break. **** $p< 0.0001$, by Univariate ANOVA, **Ntwt**: wild-type littermate control, **Ntko**: neurotrypsin-deficient mice.

3.2.1.4 Neurotrypsin-deficient middle-aged mice display increased overnight drop in rotarod performance

The inconsistent results of the rotarod tests forced us to seek the cause of such high variability between series. To this end I performed a detailed analysis across all age intervals including all males that took part in the 1st and 3rd series of the rotarod tests. Mice were divided into five age groups: 3 months old, 6-7 months old, 9 months old, 10-11 months old, and 12-13 months old were analyzed. Unfortunately, we were not able to draw any conclusions since each of the age groups behaved differently and inconsistently (data not show). In general, the rotarod results indicate that NT-deficient mice are able to acquire motor performance on the rotarod. None of the genotypes achieved maximum performance, except during the 3rd series of the test, characterized by a low number of mice.

We also looked closely at the overnight drop across different ages (Fig. 3.8). Results indicated that older NT-deficient (10-13 months old) mice show a significantly higher overnight drop in comparison to the wild-type animals. If we assume that the overnight change reflects the consolidation process, then these results are consistent with previous studies showing consolidation deficits in middle-aged and aged animals (Bach et al 1999; Ward et al 1999). The high level of the overnight drop may stand for consolidation problems in NT-deficient mice.

Due to highly variable results we decided to conduct the grip strength test; to check for difference in muscle strength, the locomotor activity test; to assess differences in general activity, and fear conditioning; to confirm or exclude disturbance in memory consolidation.

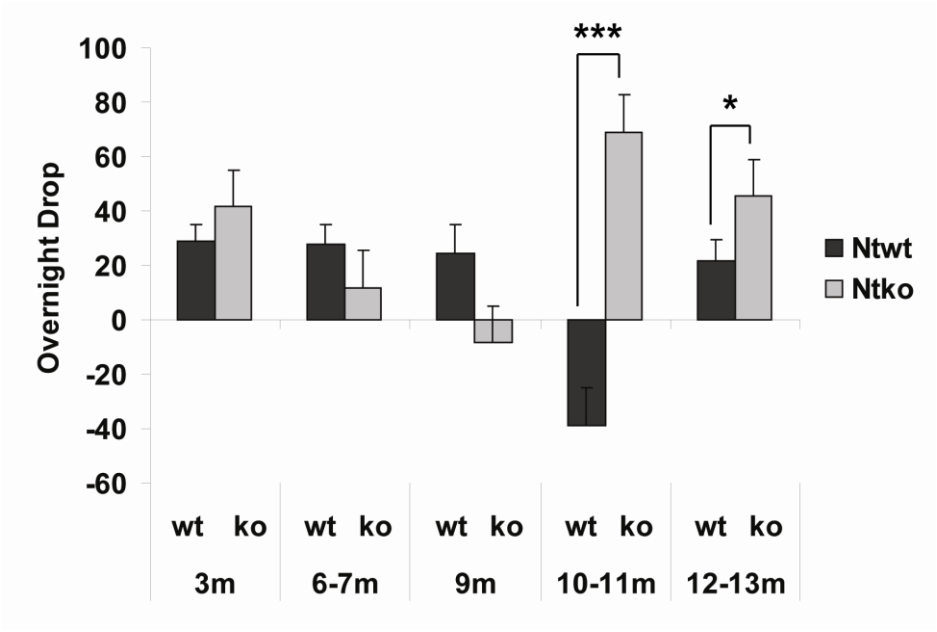

Fig. 3.8 Overnight drop across different ages.

The analysis was performed on 52 mice (24 Ntwt/28 Ntko) performing the rotarod test during the 1st and 3rd series. Only male mice were included in the statistics. Mice were divided into the five age groups: 3 months old (3m), 6-7 months old (6-7m), 9 months old (9m), 10-11 months old (10-11m), and 12-13 months old (12-13m). The two last groups show a significant difference in the overnight drop. NT-deficient mice at the age of 10-11 months; ***$p < 0.001$, and 12-13 months; *$p < 0.05$, by Univariate ANOVA, show a significantly higher overnight drop in comparison to the wild-type mice. Error bars indicate SEM. **Ntwt**: wild-type littermate control, **Ntko**: neurotrypsin-deficient mice.

3.2.2 Front limb strength does not affect rotarod performance

The grip strength test was conducted to determine the influence of front limb strength on the rotarod performance. Due to that, the same mice that participated in the rotarod test were subjects of the grip strength test. The mice study indicate that increased muscle fiber size leads to elevated muscle strength, which can result in enhanced rotarod performance (Bogdanovich et al 2008).

Mice were divided into three age groups: 5-7 months old, 9-11 months old and 12-14 months old. The results confirmed that there is no difference in the strength of the front limbs between genotypes (Tab. 4). We were able to observe that both groups of mice became weaker with time, which is a normal consequence of ageing (Fig. 3.9). No correlation between weight and front limb strength was found.

Therefore, we can definitely confirm that strength of front limb did not affect rotarod performance.

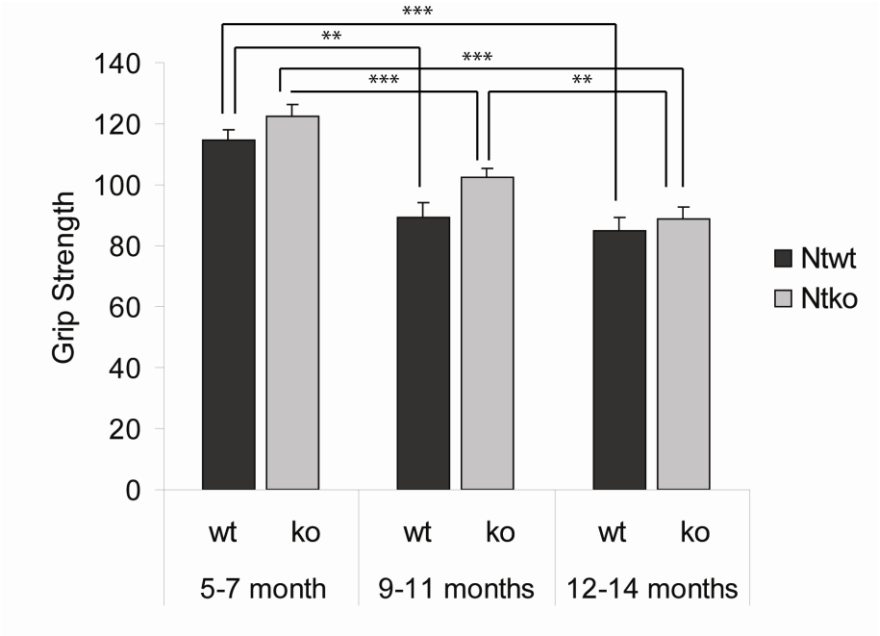

Fig. 3.9 Front limb strength decreases with increasing age of mice.

The analysis was performed on 104 male mice (50 Ntwt/54 Ntko). Mice were divided into three age groups (5-7, 9-11, and 12-14 months old). Grip strength analysis revealed no difference between genotypes. Error bar indicates SEM. Asterisks indicates significant difference between groups, *p < 0.05; **p < 0.01; ***p < 0.001 by Student T-test. **Ntwt**: wild-type littermate control, **Ntko**: neurotrypsin-deficient mice.

Detailed analysis of front limb strength in three age groups revealed no significant difference between genotypes (Fig. 3.10). It is clearly visible that the performance of wild-type and NT-deficient mice remains at the same level across the first and second day of testing. This suggests that repetition of the same action does not affect the grip force. In this part of the grip strength analysis, a decrease in the front limb strength across age is also visible.

In summary, NT-deficient mice do not show elevated muscle strength. Both genotypes show declining muscle strength, characteristic for aged mice.

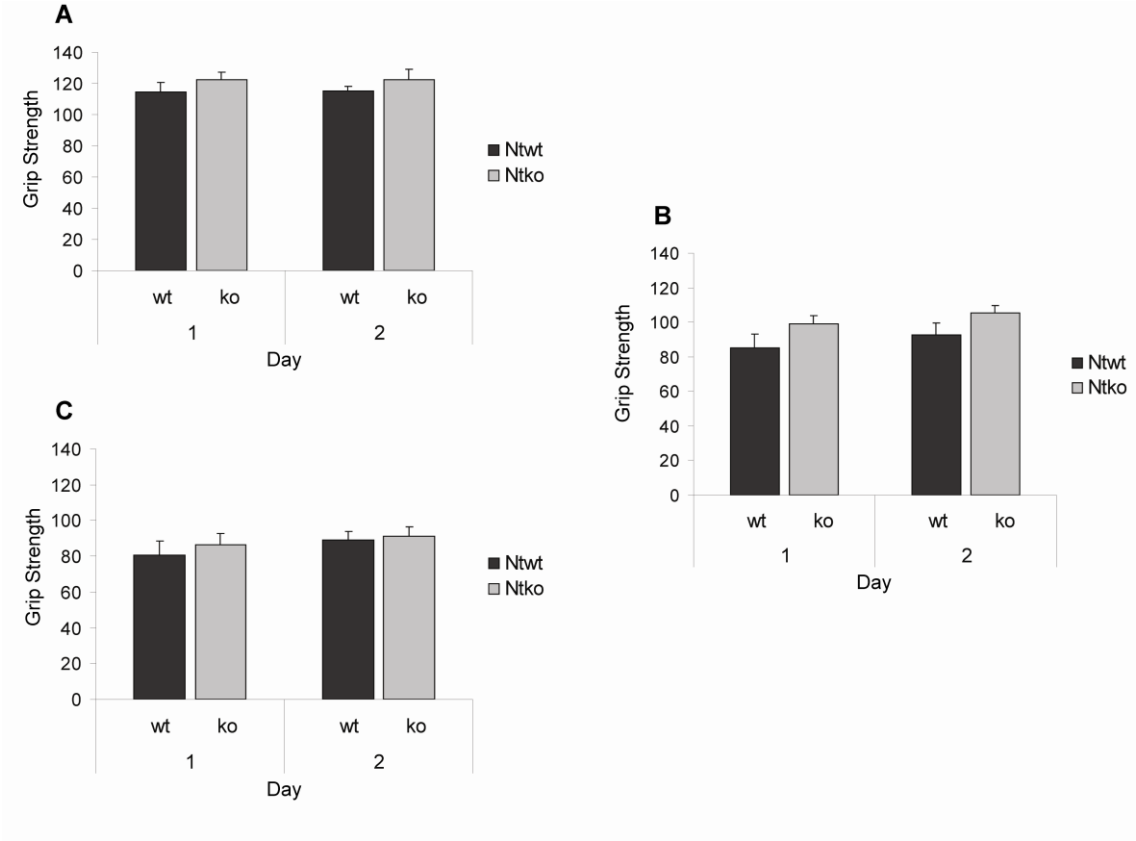

Fig. 3.10 Detailed analysis of the mice grip strength across age.

The total number of mice was analyzed depending on age, difference between genotype and day of test. (**A**) Mice at 5-7 months. (**B**) Mice at 9-11 months. (**C**) Mice at 12-14 months. Error bars indicates SEM. **Ntwt**: wild-type littermate control, **Ntko**: neurotrypsin-deficient mice.

3.2.3 Neurotrypsin-deficient mice show enhanced locomotor activity during the dark -phase

Locomotor activity is a multidimensional behavior where amount and level of activity, as well as degree of spatial and dynamic organization can be assessed. Unconditioned locomotor behavior can be affected by genetic manipulation (Lanuza et al 2004) and pharmacological applications (Crawley & Goodwin 1980). It differs across mice strains (Paulus et al 1999) and decreases with age (Weinert & Waterhouse 1999). To asses the level of general locomotor activity we have conducted a locomotor activity test. Activity of mice was registered for two consecutive weeks with a weekend break of two days in between. The first day of each week was treated as the habituation period and was not included into the statistical analysis.

The locomotor activity measurements indicated significantly higher activity of NT-deficient mice during the dark/active phase of the day (Tab. 5). The experiment was performed twice with an interval of two months to observe changes over age. During the 1st series of testing, NT-deficient mice showed a highly significant difference in activity ($p < 0.0001$) in comparison to the wild-type mice (Fig. 3.11A). Detailed analysis of mice (Fig. 3.12) at all ages (6, 7, 8, 9, and 10 months old), revealed a significant difference between genotypes only in the case of younger mice (Fig. 3.12A-B); 6 months old ($p < 0.0001$), 7 months old ($p < 0.05$), and 8 months old ($p < 0.05$), which declined with age. The older mice (Fig. 3.12C), 9 and 10 months old, showed no difference in the locomotor activity between genotypes (Tab. 7). During the 2nd series of the ACTIVISCOPE test (Fig. 3.11B), the difference between NT-deficient and wild-type mice decreased (Tab. 6), but still stayed significant ($p < 0.05$).

These results confirmed the generally accepted hypothesis that locomotor activity decreases with age. In addition, the greater activity of young NT-deficient mice may affect other motor learning experiments. Due to this, further tests that were performed with a particular emphasis on the influence of activity on the motor or spatial learning.

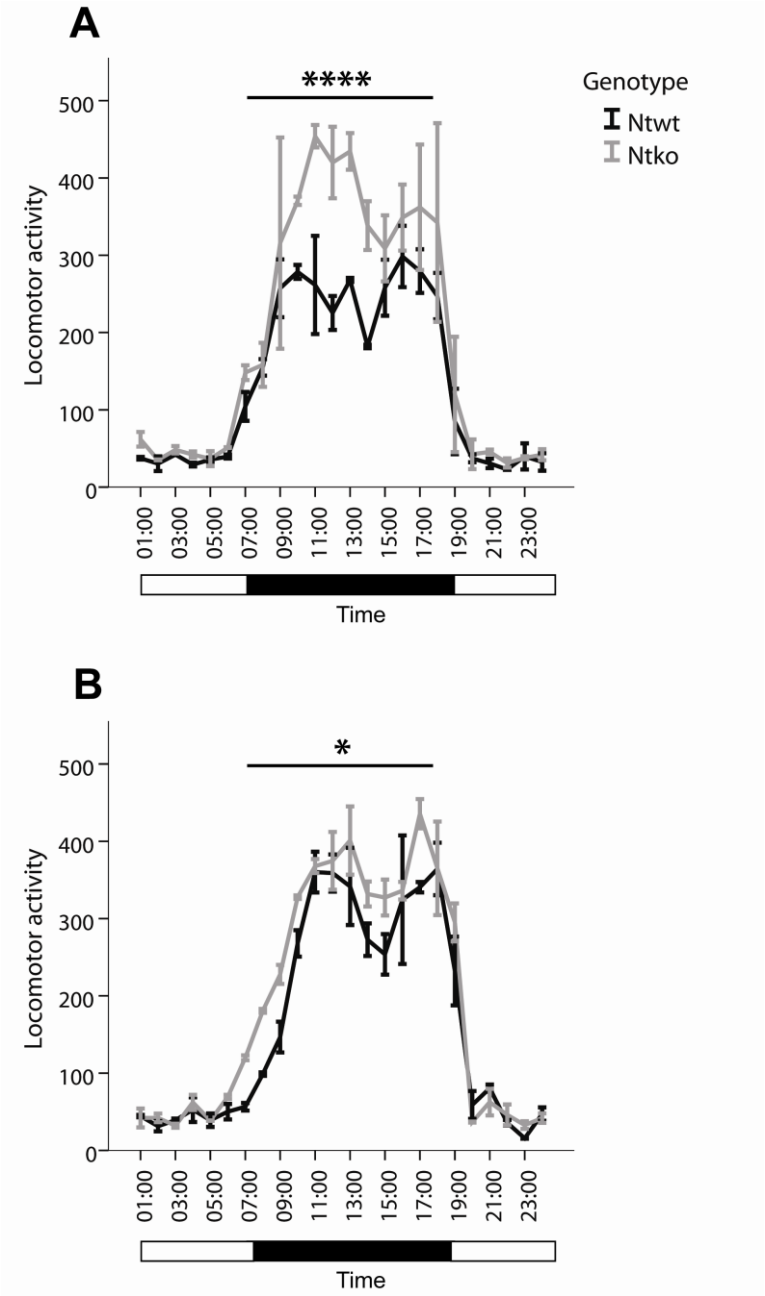

Fig. 3.11 Neurotrypsin-deficient mice show significantly higher locomotor activity during the dark phase.

Locomotor activity test was performed twice with the same cohort of mice with an interval of two months. In total 24 mice (13 Ntwt/11 Ntko) participated in activity measurements. The black time line represents dark/active phase (7am-7pm), whereas, the white one stands for the light/non active phase. (**A**) The 1st series of the locomotor activity test included mice at the age of 6-10 months. NT-deficient mice showed significant higher activity during dark/active phase ($p < 0.0001$), in comparison to the wild-type animals. (**B**) During the 2nd series of locomotor activity tests mice were 2 months older. NT-deficient mice still showed significantly higher activity ($p < 0.05$), but difference between genotypes decreased with age. * $p< 0.05$, **** $p < 0.0001$ by Univariate ANOVA. Error bars indicate SEM. **Ntwt**: wild-type littermate control, **Ntko**: neurotrypsin-deficient mice.

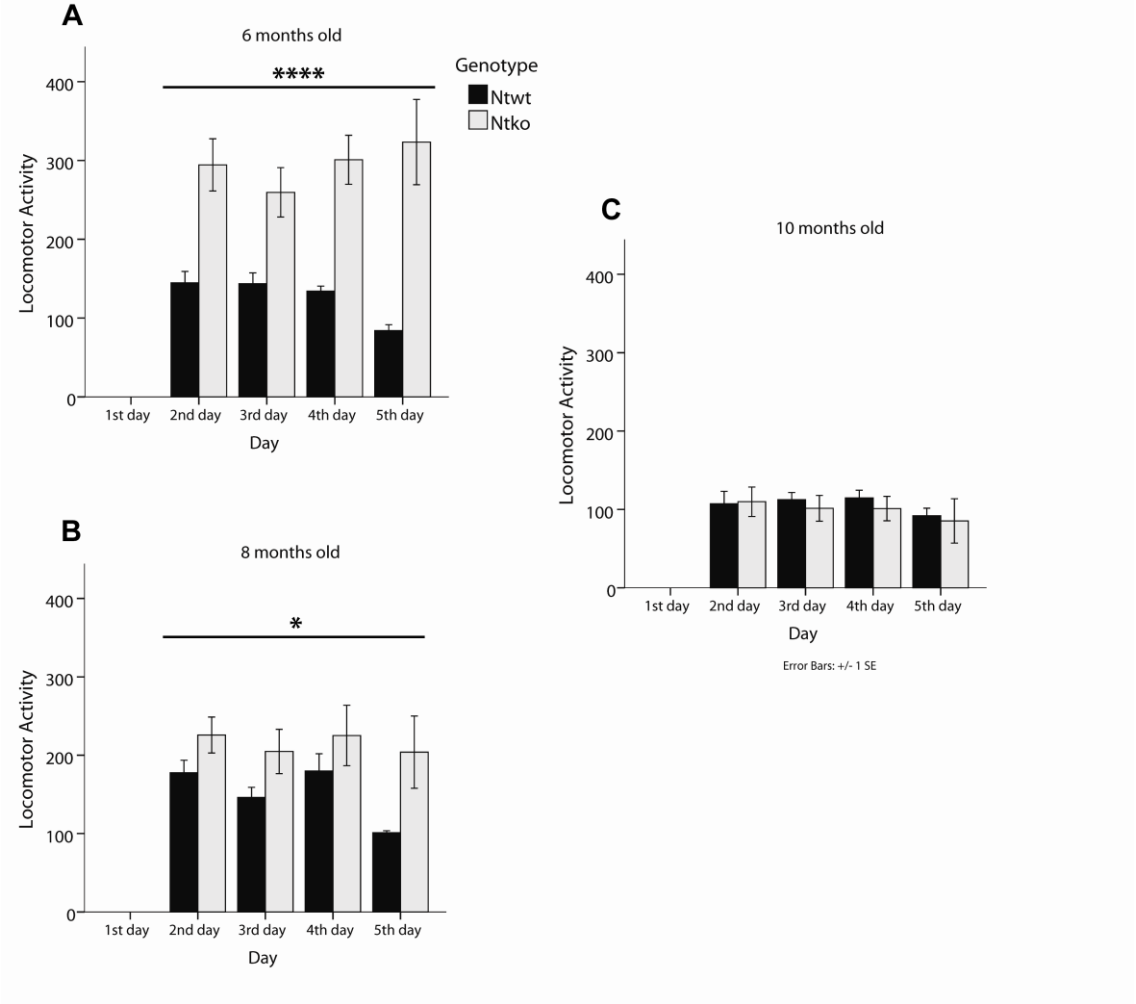

Fig. 3.12 Enhanced locomotor activity of the neurotrypsin-deficient mice decreases with age.

The total number of mice 20 (10 Ntwt/10 Ntko) were divided into five age groups: 6, 7, 8, 9, and 10 months old. (**A-B**) The younger, 6 ($p < 0.0001$) and 8 ($p < 0.05$) months old NT-deficient mice showed a significantly higher activity level, which decreased with age. (**C**) There was no difference in activity between genotypes at the age of 10 months. Error bars indicate SEM. * $p < 0.05$, **** $p < 0.0001$, by Univariate ANOVA. **Ntwt**: wild-type littermate control, **Ntko**: neurotrypsin-deficient mice.

3.2.4 Memory consolidation of fear conditioning is not affected in neurotrypsin-deficient mice

To asses memory consolidation in a different system, we performed a fear conditioning test with a six day break in between training and testing. The presented results include two separate cohorts (1st and 2nd) of wild-type and NT-deficient mice.

The analysis of the response to the training indicated a highly significant acquisition ($p < 0.0001$) in both series of experiment (Tab. 8). There was a non-significant tendency toward a lesser fear response in the NT-deficient mice (Fig. 3.13A). However, statistical analysis indicated that there was no difference in the response between genotypes. During the 2nd series mice generally showed a tendency to freeze more than the one in 1st series, but their freezing level was also higher during the baseline recording. Based on the training response results, one mouse was excluded from further statistics due to excessive freezing during the baseline.

Reponses to the context and response to the cue are two distinct reactions that depend on different brain regions. Rats with lesion of the dorsal striatum showed significantly lower freezing to the presented tone in comparison to controls, however, lesion did not disturb contextual fear response (Ferreira et al 2003). This suggests that dorsal striatum is responsible for response to the cue and dorsal hippocampus is required for proper expression of fear (Maren et al 1997). Our results showed highly significant retention during contextual response ($p < 0.0001$) (Tab. 9), which was not affected by the genotype or a cohort (Fig. 3.13B). Observation of the context response during the 1st series revealed the significance of the sex ($p < 0.024$) and *sex* x *response* ($p < 0.015$) correlation. Successive cohorts consisted only of males to avoid unwanted correlation and variability.

The analysis of the response to the cue clearly showed highly significant ($p < 0.0001$) freezing to the tone (Fig. 3.13C). No significant difference between genotypes was noted, even though NT-deficient mice on average freeze less in response to the tone (Tab. 10).

Fear conditioning is one of the fastest acquired experiences and thus is easily consolidated into long-term memory. Our protocol consisted of one training day separated by a six day break from two testing settings (context/cue). NT-deficient mice showed no significant difference from wild-type mice across acquisition and during cued and contextual response. This indicates that neurotrypsin-deficient mice show no disturbance in the amygdala function and present a normal pattern of memory consolidation after fear conditioning.

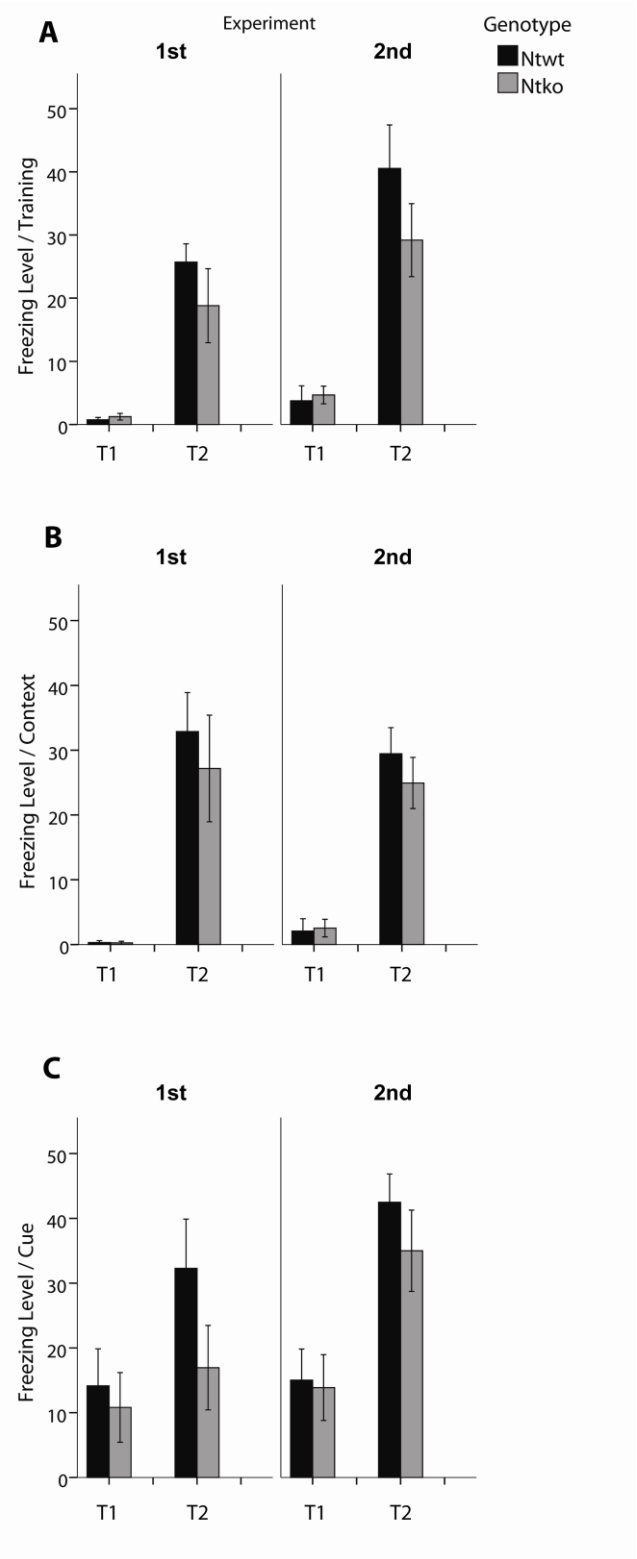

Fig. 3.13 Fear conditioning results across two cohorts.

The 1st series of fear conditioning tests was represented by 21 mice (12 Ntwt/9 Ntko); cohort consisted of males and females. The 2nd series was represented by 26 mice (11 Ntwt/15 Ntko), only males. All graphs show the degree of mice freezing in response to training, context and cue.

(**A**) Training response; where T1 represents baseline and T2 stands for the last training cycle. NT-deficient mice showed a non-significant tendency toward elevated fear response, with a high variability between cohorts.

(**B**) Response to the context; T1; baseline and T2; context exposure after six days. There was no difference between genotypes.

(**C**) Tone response; T1; freezing level before tone and T2; freezing level with the tone. There was no difference between genotypes in response to the tone. Error bars indicate SEM. **Ntwt**: wild-type littermate control, **Ntko**: neurotrypsin-deficient mice.

3.2.5 Reaching and grasping abilities of neurotrypsin-deficient mice

The staircase test was introduced by Montoya in 1990 as a test for assessing rat's reaching and grasping ability (Montoya et al 1990). Later, the test was adjusted for mice. This type of test is sensitive to the unilateral lesions in the striatum (Fricker et al 1996), the subthalamic nucleus (Henderson et al 1999), and the motor cortex (Montoya et al 1991). If our hypothesis concerning facilitated transit to habit formation in NT-deficient mice is correct we should be able to observe elevated reaching and grasping abilities in those animals.

One week before the test, mice were food deprived and their weight was consistently maintained throughout the entire experimental. Both genotypes lost weight at the same rate and maintained the same weight until the last day of testing (Fig. 3.14B). During the experiment, a significant effect of the days across genotypes ($p < 0.001$) was observed. No difference between genotype in number of collected pellets was noted (Fig. 3.14A) (Tab. 11). Three of the twenty one mice were excluded due to their high weight. To enter the staircase chamber and perform the test properly, mice cannot be heavier than 25 g (Manual Instruction for Rodent Staircase Test, Lafayette Instrument Company, USA).

Our results indicate that NT-deficient mice were able to acquire the ability to reach and grasp sugar pellets from the different levels of the steps as efficiently as wild-type mice. We were not able to observe any difference between genotypes.

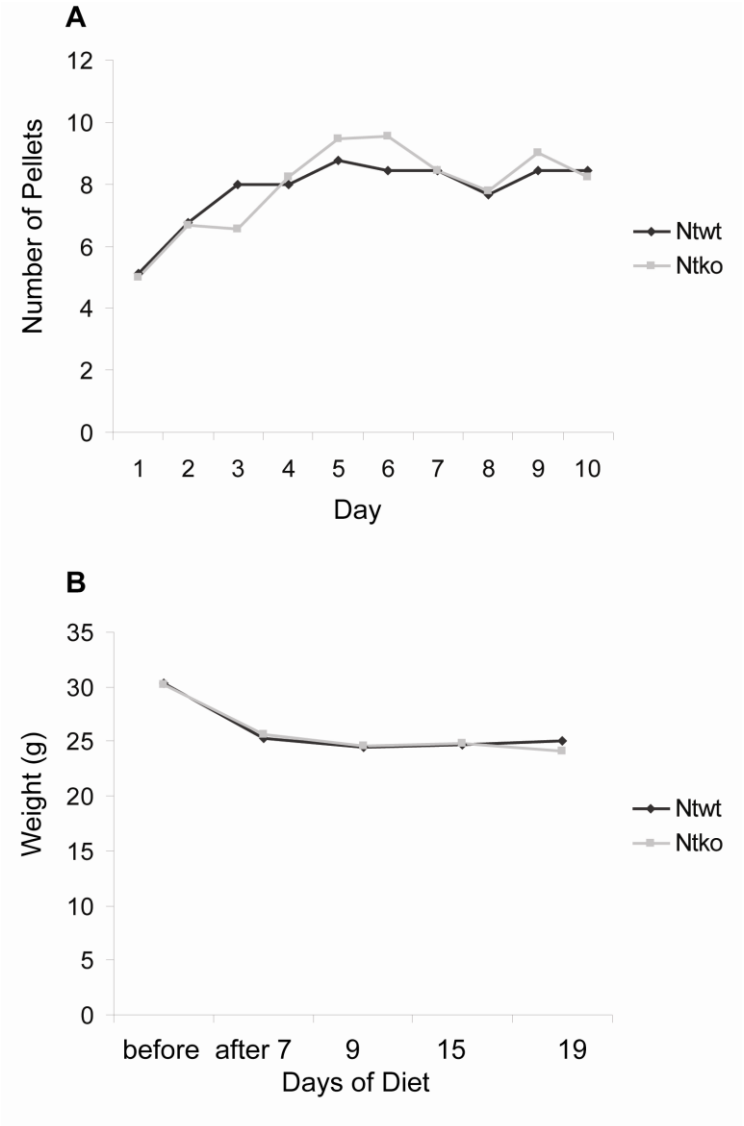

Fig. 3.14 Neurotrypsin deficiency does not affect reaching and grasping ability.

In total 18 male mice (9 Ntwt/19 Ntko) were tested. (**A**) Number of collected pellets does not differ between genotypes. Both groups showed significant improvement within the days ($p < 0.001$). (**B**) Mice were food deprived until they reached 80-85% of their starting body weight. The quantity of received food was monitored to maintain a constant weight until the end of the experiment. **Ntwt**: wild-type littermate control, **Ntko**: neurotrypsin-deficient mice.

3.2.6 Neurotrypsin-deficient mice exhibit enhanced reversal learning capacity during the first days after re-location of the hidden platform

3.2.6.1 The 1st and 2nd series of the water-maze tests showed that wild-type and neurotrypsin-deficient mice exhibit equal capacity to find the hidden platform during the acquisition stage

3.2.6.1.1 The 1st series of water-maze experiments (performed by Florence Molinari)

The Morris water-maze is a commonly used navigation task, which was developed by Richard G. Morris in 1981 (Morris 1981). The first water-maze tests with NT-deficient mice were performed in our laboratory by Florence Molinari. According to her protocol mice were trained for three consecutive days, six trials per day, and tested during the two days of reversal learning. During the reversal learning stage the hidden platform is place on the opposite quadrant of the maze. During the first trials of the reversal learning the mice must learn that the escape platform is not localized in the previous quadrant of the maze and that from now the hidden platform can be fond on the opposite quadrant. All data was analyzed using Univariate ANOVA. Data were split according to the phase of the experiment in acquisition and reversal learning.

The results indicated rapid learning of the first platform position during the acquisition phase and fast adaptation to a new platform position during reversal learning for both genotypes (Fig. 3.15A). However, the amount of time spent in the old goal quadrant dropped rapidly in wild-type mice and remained near chance levels during both days of reversal learning. NT-deficient mice, in contrast, showed a persistent preference for the old goal quadrant during the first day of reversal stage and developed a clear avoidance of this quadrant during the second day (Fig. 3.15B).

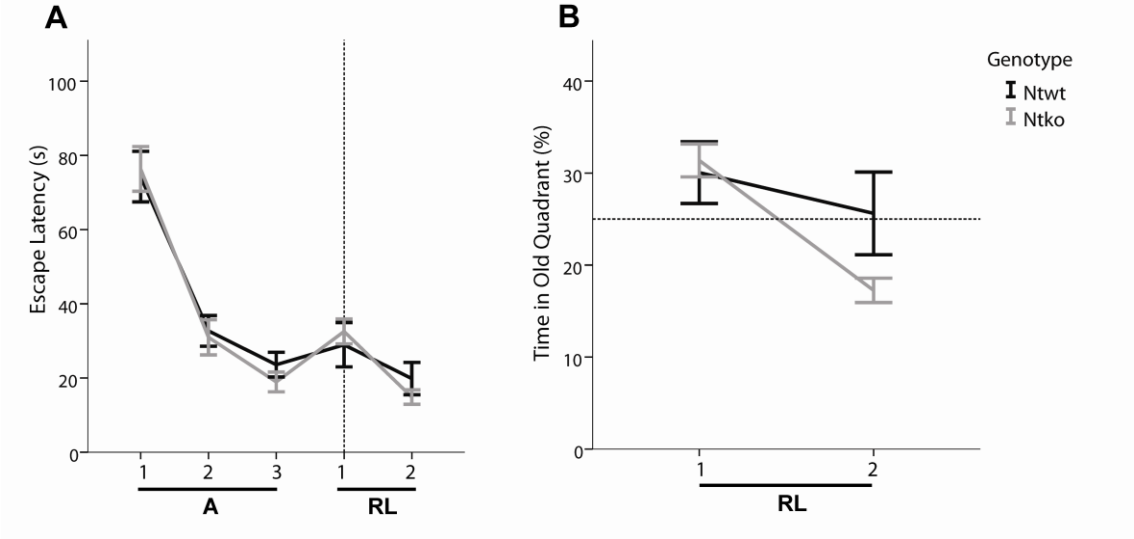

Fig. 3.15 Spatial learning of the neurotrypsin-deficient mice during the 1st series of Morris water-maze test (Florence Molinari).

In total, 33 mice (16 Ntwt/17 Ntko; 17 males/16 females) were tested. Mice were trained for 3 consecutive days, after which a hidden platform was placed on the opposite site of the maze and mice performed reversal learning. Each point represents average of 6 trials. (**A**) Escape latency during acquisition (days 1-3) and reversal learning (days 4-5). (**B**) Time spent in the old goal quadrant during the reversal learning stage. NT-deficient mice showed more persistent preference for the old quadrant during the first day of reversal learning and developed clear non-significant avoidance during the second day. Error bars indicate SEM. **A**; acquisition, **RL**; reversal learning, **Ntwt**: wild-type littermate control, **Ntko**: neurotrypsin-deficient mice.

3.2.6.1.2 The 2nd series of water-maze experiments

The results of the 1st series of water-maze tests prompted us to repeat this experiment with particular emphasis on the reversal learning phase. The previous protocol was extended from three to six training days, to over-train mice, and reversal learning was tested for four instead of two days. The escape latency (Fig. 3.16A) and the path efficiency (Fig. 3.16B) during the acquisition stage revealed undisturbed improvement over the acquisition phase ($p < 0.0001$), equal for both genotypes. Mice showed rapid learning of a first platform position. Detailed analysis of the escape latency and the path efficiency during the first two days of the reversal phase showed no significant difference between genotypes. However, NT-deficient mice presented non-significant tendency toward faster recognition of the new platform position during the first, but not the second day, of reversal learning (Fig. 3.16A-B).

Analysis of escape latency /trials within day (except for the first day of acquisition and the first day of reversal) indicated no difference between genotypes. The path efficiency during the first day of the reversal phase suggested that NT-deficient mice choose the correct path on their way to the platform more often. These results were confirmed by time in the quadrant assay, which suggested that NT-deficient mice, during the first trial of reversal learning, showed a reduced preference to the old quadrant. Furthermore, NT-deficient mice presented a non-significant tendency toward a more efficient path during the third and fourth day of the reversal learning. These promising conclusions raised the question: what will happen if we extend reversal learning?

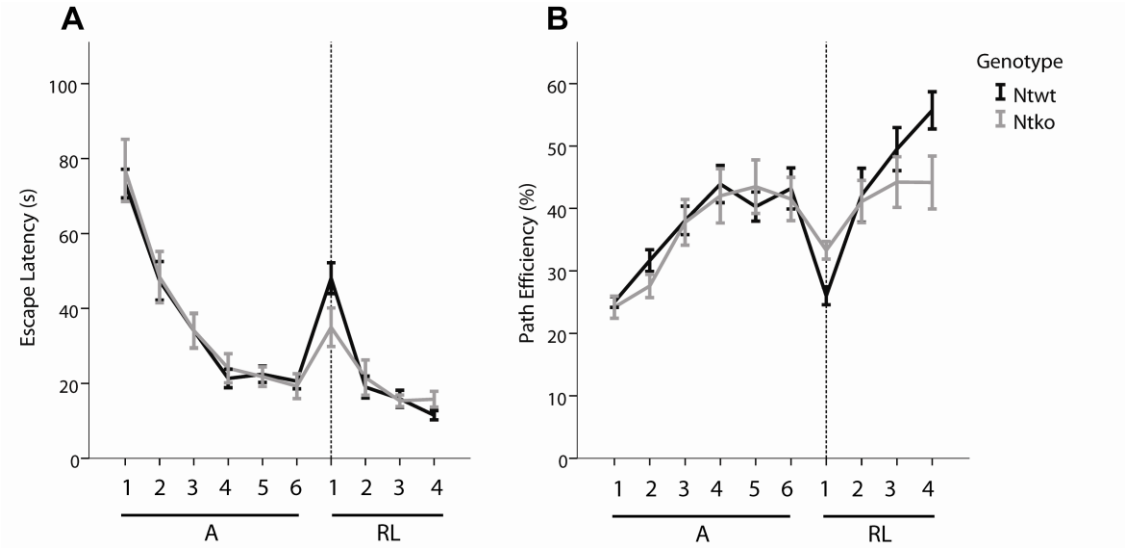

Fig. 3.16 Spatial learning of the neurotrypsin-deficient mice during the 2nd series of Morris water-maze test.

In total, 21 mice (12 Ntwt/9 Ntko; 13 males/8 females) were tested. Mice were trained for 6 consecutive days, on the seventh day reversal learning started. Each point represents average of 6 trials. (**A**) Escape latency analysis was not affected by genotype but indicated a non-significant tendency toward a faster recognition of a new platform position during the first day of the reversal learning. (**B**) Path efficiency measurement was not affected by genotype, but again we observed a non-significant tendency in NT-deficient mice toward faster location of the hidden platform during the reversal learning. Error bars indicate SEM. **A**; acquisition, **RL**; reversal learning, **Ntwt**: wild-type littermate control, **Ntko**: neurotrypsin-deficient mice.

3.2.6.2 The 3rd and 4th series of the water-maze tests revealed enhanced reversal learning capacity of neurotrypsin-deficient mice during the first days after platform relocation

3.2.6.2.1 The 3rd series of water-maze experiments

The results from the 2nd series of the water-maze showed a non-significant tendency toward faster localization of the hidden platform by the NT-deficient mice during the first day of the reversal learning. To obtain further insight, our protocol was further extended from four to seven days of reversal learning days.

The results of the 3rd series of water-maze tests confirmed that there was no difference between genotypes during the acquisition phase. Both genotypes were able to localize the hidden platform at its initial position, showing significant improvement over training days ($p < 0.0001$). In contrast, detailed analysis revealed significant differences in the performance during the reversal learning stage. NT-deficient mice showed enhanced performance during the reversal test phase. The performance of the NT-deficient mice indicated the significantly more efficient selection of the swimming path ($p < 0.05$) (Fig. 3.17A) and a significantly lower absolute direction error ($p < 0.005$) (Fig. 3.17B). Further analysis revealed a significantly shorter distance to current goal ($p < 0.05$) and an increased time in current goal quadrant ($p < 0.05$) characteristic for NT-deficient mice. A full factorial ANOVA indicated a significant difference ($p < 0.0001$) in the performance of mice with the lowest weight (weight < 30 g). Due to this, three mice were excluded from further statistics.

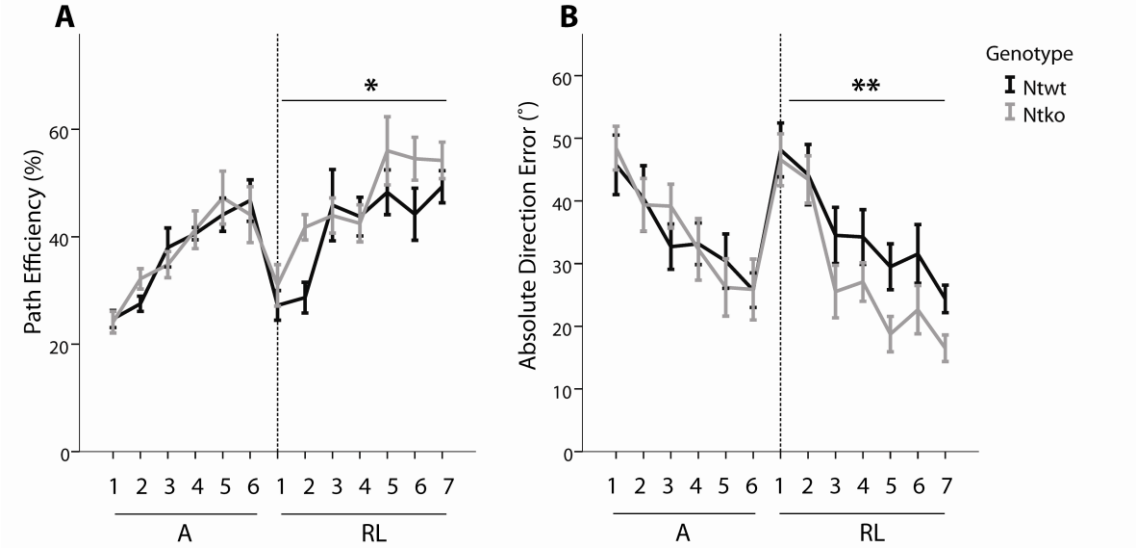

Fig. 3.17 Spatial learning of the neurotrypsin-deficient mice during the 3rd series of Morris water-maze test.

In total, 20 mice (10 Ntwt/10 Ntko; only males) were tested. Mice were trained for 6 consecutive days, on the seventh day reversal learning started and continued for next seven days. Each point represents average of 6 trials. (**A**) Path efficiency analysis revealed significantly more efficient selection of the swimming path by NT-deficient mice ($p < 0.05$). It seems that NT-deficient mice react faster to the new platform position. (**B**) Absolute direction error as well was affected by genotype; we observed significantly lower level of the direction error in NT-deficient mice ($p < 0.005$). Error bars indicate SEM. **A**; acquisition, **RL**; reversal learning, **Ntwt**: wild-type littermate control, **Ntko**: neurotrypsin-deficient mice. * $p < 0.05$, ** $p < 0.01$ by Univariate ANOVA.

3.2.6.2.2 The 4th series of water-maze experiments

To corroborate these promising data, the 4th series of the water-maze test was conducted. The data presented below come from the combination of two independent experiments (3rd and 4th). Each experiment was introduced as one of the variable in the ANOVA calculation and presented minor effects; it may suggest that the baselines in the two experiments were different. We decided to combine two experiments and leave the experiment as one of the factors in a statistical model.

The detailed analysis confirmed the previous results, indicating that NT-deficient mice show undisturbed and rapid acquisition of a first platform position (Tab. 16). The escape latency examination defines a significantly shorter swimming time ($p < 0.05$) during the reversal learning phase in NT-deficient mice (Fig. 3.18A). A closer analysis of single day showed no *genotype* x *trial* or *genotype* x *day* interactions. This means that statistically all trials and days contributed similarly to the genotype effect. It seems that, over time, the wild-type mice are able to reach the same high level performance as the NT-deficient mice. Both genotypes reached a performance plateau starting from the fourth day of the reversal phase. The accurate analysis of the direction towards the goal; absolute direction error (Fig. 3.18B) (Tab. 17) and path efficiency (Fig. 3.18C) (Tab. 18) suggests that NT-deficient mice probably used a different strategy to get to the goal. They were significantly better at finding the platform during the reversal learning. NT-deficient mice were significantly more accurate in choosing the right direction to the goal ($p < 0.0001$), and their path towards the platform position was significantly more efficient ($p < 0.05$).

Additional analysis of the time in the current goal quadrant (Fig. 3.18D) and the distance to the current goal (Fig. 3.18E) revealed further meaningful differences in spatial-oriented behavior of the NT-deficient mice. On average they spent significantly more time in the quadrant with the platform ($p < 0.05$) (Tab. 19) and showed a significantly shorter distance to the goal ($p < 0.05$) (Tab. 20) already during the acquisition phase. Those differences increase with time, during the reversal learning phase, in regard to distance to the current goal ($p < 0.001$), and stay at a comparable level in the case of time in the current goal quadrant ($p< 0.05$). Again, a full factorial ANOVA assay revealed no *genotype* x *trial* or *genotype* x *day* interaction. Similar to the escape latency analysis, both genotypes seemed to reach a performance plateau after the fourth day of the reversal learning and at the end of the experiment wild-type mice reached the same performance level as the NT-deficient mice.

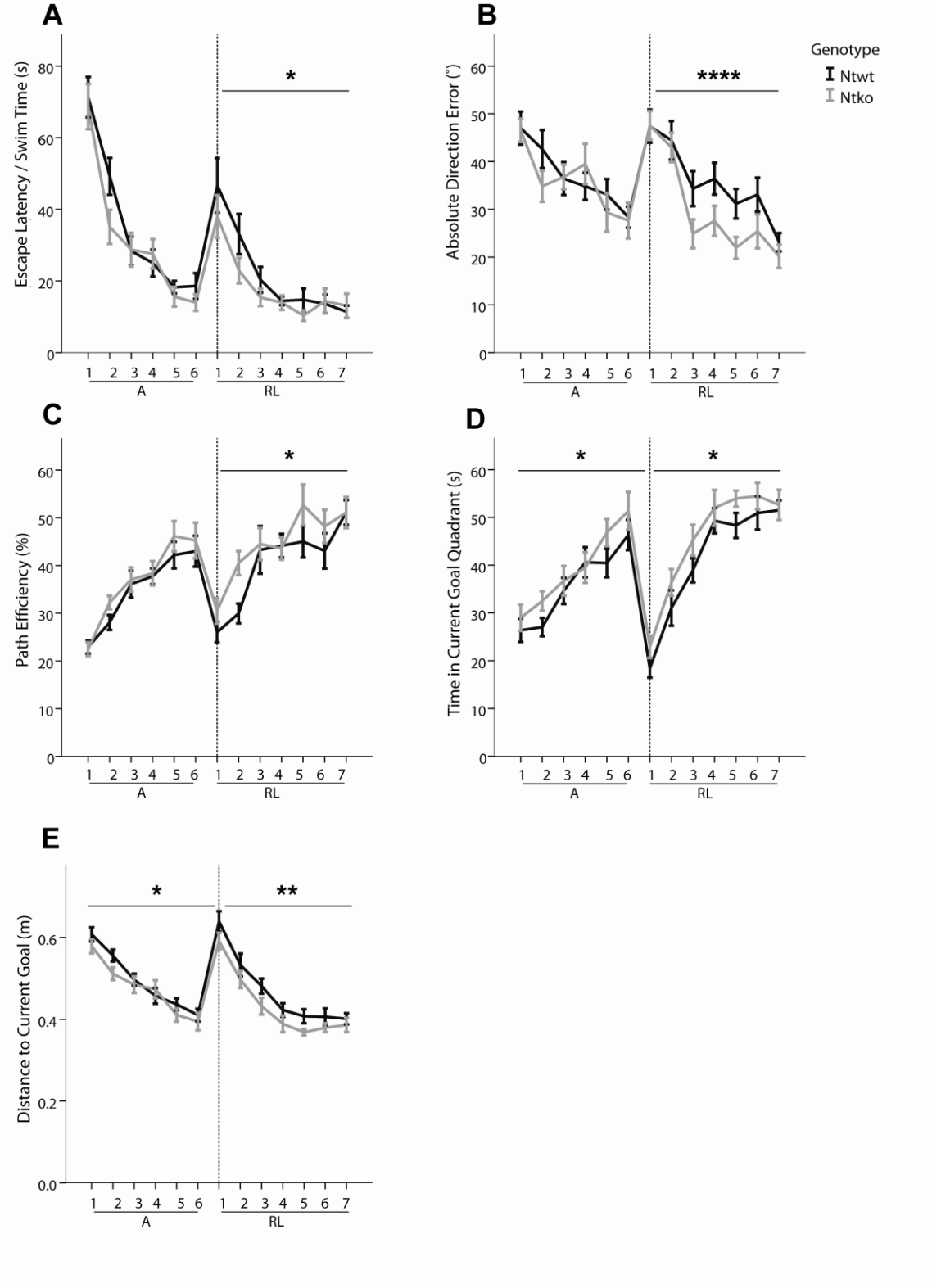

Fig. 3.18 Neurotrypsin-deficient mice show enhanced ability to find the hidden platform during reversal learning stage

In total, 26 mice (13 Ntwt/13 Ntko; only males) were tested. Both genotypes show improvement within days across the acquisition and reversal learning phases ($p < 0.0001$). (**A**) NT-deficient mice showed a significant shorter swimming time during the reversal learning phase ($p < 0.05$). They were able to find the hidden platform faster than wild-type mice. (**B**) During the reversal learning, NT-deficient mice showed a significantly lower direction error ($p < .0.0001$) in comparison to the wild-type mice. This suggests that they chose the right

direction to the goal more precisely, and this ability seemed to improve over time. (**C**) The swimming path of the NT-deficient mice was significantly more efficient ($p < 0.05$) than the one chosen by the wild-type mice. (**D**) NT-deficient mice on average spent more time in the current goal quadrant during the acquisition ($p < 0.05$) and reversal learning ($p < 0.05$). (**E**) During the acquisition phase NT-deficient mice showed a significantly shorter distance to the current goal ($p < 0.05$). This difference increased during the reversal learning this ($p < 0.001$). **A**; acquisition, **RL**; reversal learning, Error bars indicate SEM. **Ntwt**: wild-type littermate control, **Ntko**: neurotrypsin-deficient mice. * $p < 0.05$, ** $p < 0.01$, **** $p < 0.0001$ by Univariate ANOVA.

Further detailed time in quadrant analysis revealed no significant difference between genotypes during the first 30 seconds of the first and the second trial of the reversal learning phase (Fig. 3.19A-B). During the first 30 seconds of the first reversal learning both groups of mice preferred old goal quadrant (Fig. 3.19A). Further analysis of the first 30 seconds of the second trial again revealed no significant difference between genotypes concerning quadrant preference (Fig. 3.19B).

In conclusion, quadrant analysis of the first 30 seconds of the first and the second trial of the reversal learning revealed preference to the old goal quadrant. We did not *observe genotype x trial* correlation. On average NT-deficient mice had the capacity to significantly better localization of the platform already during the acquisition phase (time in current goal quadrant/distance to the current goal). Furthermore, NT-deficient mice were significantly more successful in localizing a new platform position during the reversal stage.

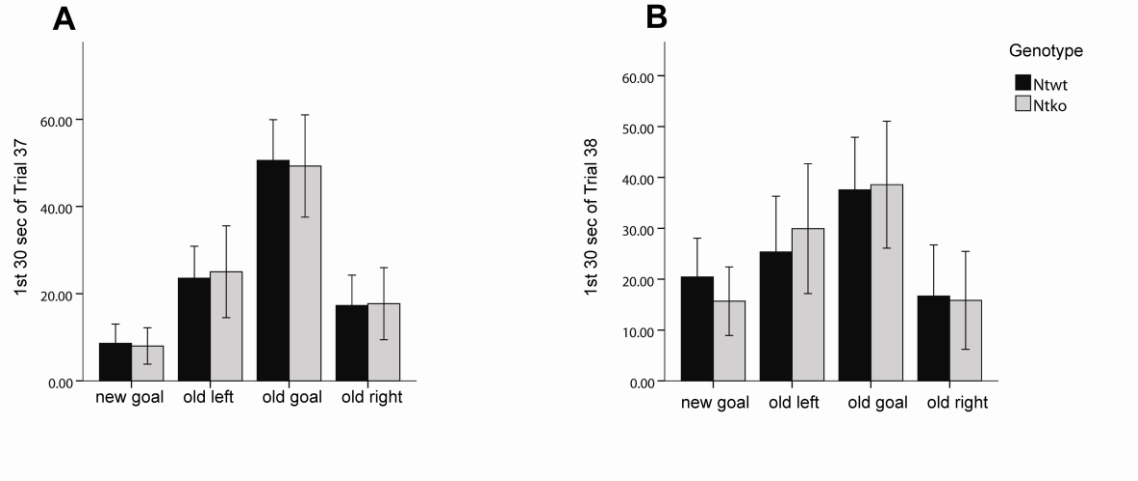

Fig. 3.19 Quadrant analysis. Time in quadrant (%).

Quadrant analysis shows % of time spent in each quadrant of the maze during the first two days of reversal learning. (**A**) The first 30 sec of the first reversal learning trial (37th trial). On average mice spent most of the time in the old goal quadrant. Genotype does not affect quadrant preference. (**B**) The first 30 sec of the second reversal learning trial (38th trial). Mice continued to spend a greater % of time in the old goal quadrant, but tendency towards new goal and old left quadrant can be observed. Genotype does not affect quadrant preference. Error bars indicate SEM. **Ntwt**: wild-type littermate control, **Ntko**: neurotrypsin-deficient mice.

3.2.6.3 Enhanced locomotor activity does not influence performance in water-maze

Our previous studies showed that NT-deficient mice present elevated locomotor activity which may influence tests such like Morris water-maze.

The primary analysis of the data from 3rd and 4th series indicated that there was no difference across days in the distance traveled to the goal (Fig. 3.20A), confirming that both genotypes travelled an equal distance during the whole experiment (acquisition and reversal learning stage) (Tab. 21). The swim path analysis assured that, despite the increased activity of NT-deficient mice (general activity results), they did not show an extended travel distance (Fig. 3.20B). Both groups of mice presented significant improvement within days ($p < 0.0001$) during the acquisition and reversal phases of the test (Tab. 22). This outcome confirms that water-maze test results are independent of mice locomotor activity. None of the genotypes showed a tendency towards swimming next to the wall of the maze confirming no anxiety-like inclination (Fig. 3.11C) (Tab. 23).

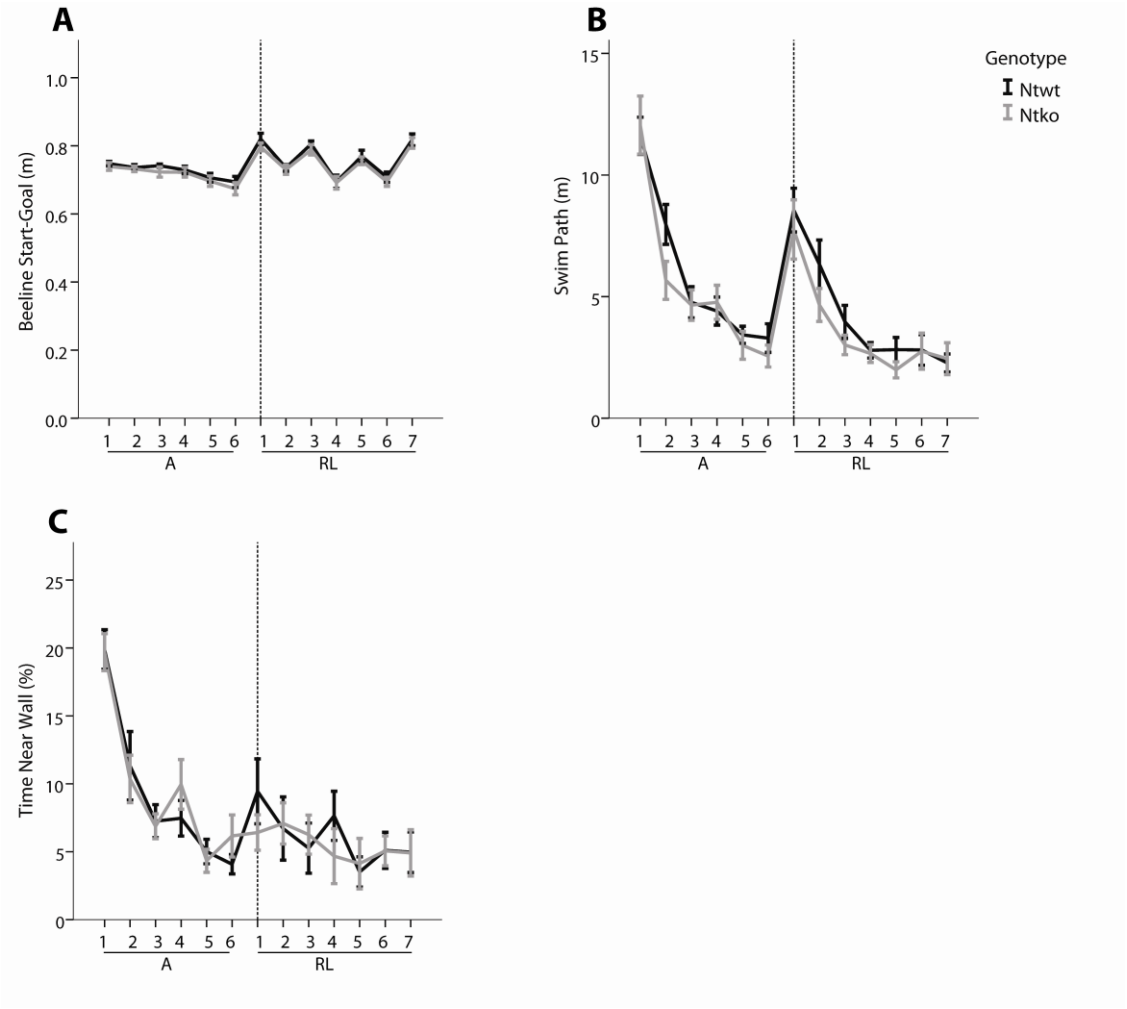

Fig. 3.20 There is no difference in distance traveled to the goal between neurotrypsin-deficient and wild type mice. None of the genotypes showed an elevated anxiety level.

In total, 26 mice (13 Ntwt/13 Ntko) were included in the statistics. Each graph was divided into two parts, with a black line, representing a 6 day acquisition period and a 7 day reversal learning phase. (**A**) A beeline start-goal is a control measurement indicating that, during both phases and across all days of the experiment both genotypes had exactly the same distance to travel. (**B**) The swim path analysis represents distance traveled to get to the goal. Genotype does not affect swim path. (**C**) Both genotypes spent similar amount of time next to the wall, thus there are no tendencies toward anxiety-like behavior. **A**; acquisition, **RL**; reversal learning. Data were analyzed using Univariate ANOVA. Error bars indicate SEM. **Ntwt**: wild-type littermate control, **Ntko**: neurotrypsin-deficient mice.

3.2.7 Neurotrypsin-deficient mice show undisturbed pattern of the fear extinction

The water-maze results suggested that the better performance of NT-deficient mice during reversal learning could be the result of a weaker memory trace that was generated by the previously learned task. According to this hypothesis the NT-deficient mice would not need to extinguish previously acquired information to perform better in changed spatial task. Therefore, we were interested in observing results of the fear extinction test in NT-deficient mice. Will NT-deficient mice show facilitation in memory extinction? The purpose of a fear extinction test is to decrease the previously acquired response to the CS with a noxious US pairing. Continued presentation of the non-reinforced CS (tone) should result in a progressive decrease of the conditioned fear response (Herry et al 2010).

Our results indicated highly significant acquisition of a fear response ($p < 0.0001$) equal for both genotypes (Fig 3.21A-C). The above outcome is similar to the previous results shown in fear conditioning paradigm (Tab. 24-26). To analyze extinction of previously acquired response mice were placed in the same apparatus, but with changed inside, so that mice would consider it a new environment. Extinction analysis revealed rapid and unaffected by genotype extinction of the fear response (Fig. 3.21D) (Tab. 27). Recovery of fear-related response was represented by the difference between E5 block of the first day and E1 block of the next day (Fig. 3.21E). The analysis of recovery revealed no significant difference in freezing level between genotypes. The re-extinction process (E2-E5) (Fig. 3.21E) was unaffected by genotype (Tab. 28).

Concluding, the fear extinction test did not present the hypothesized effect. NT-deficient mice showed an undisturbed patter of extinction.

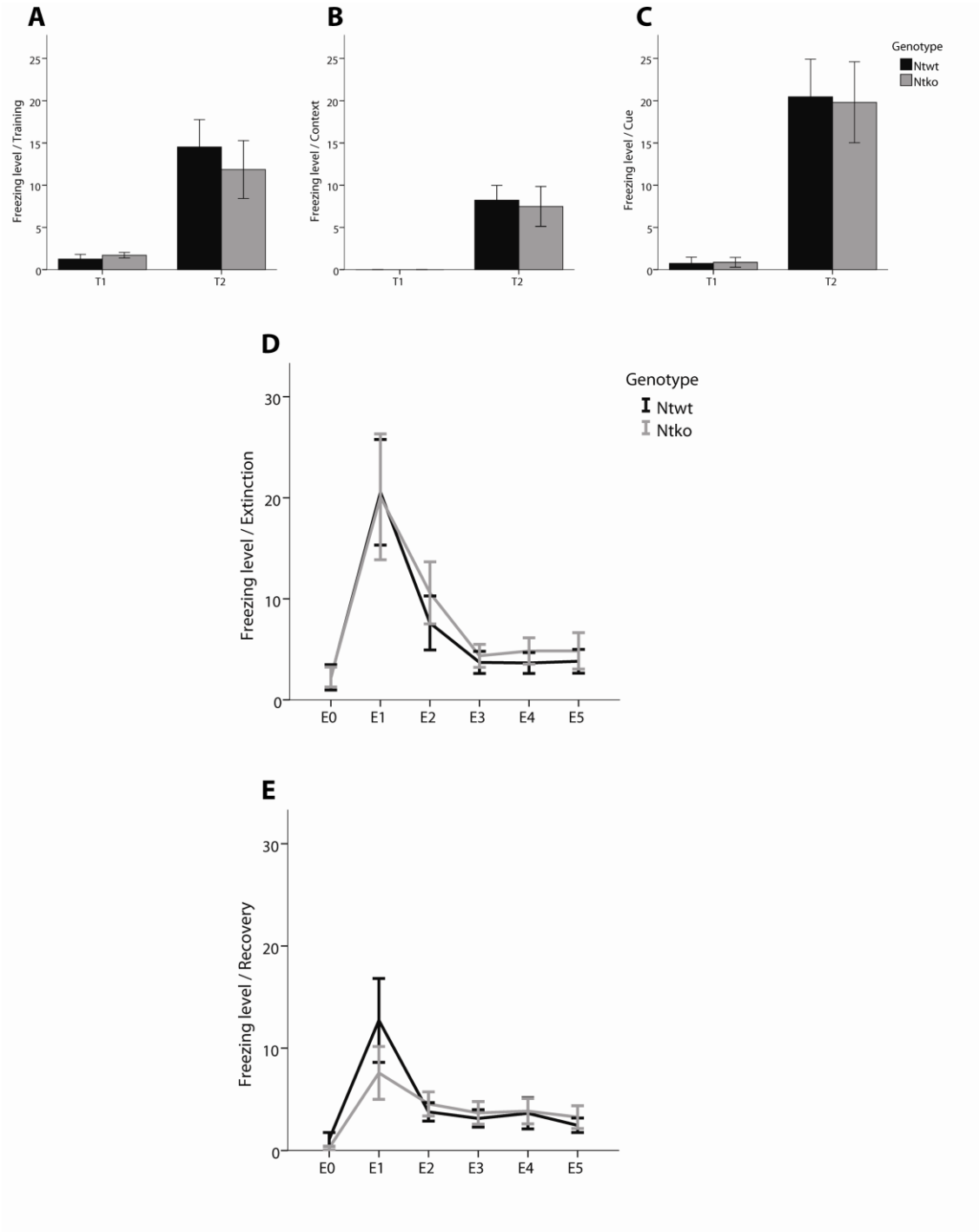

Fig. 3.21 Neurotrypsin-deficient mice show normal fear extinction pattern

After the fear conditioning paradigm (**A-C**) mice underwent two days of the extinction protocol. Results were grouped into the session blocks (**E1, E2, E3, E4**, and **E5**), each block included four tone presentations with a 2 sec break in between. **E0** represents freezing level (baseline) during the first 70 sec without tone presentation. (**D**) The first day of fear extinction protocol. Extinction was rapid and unaffected by genotype. (**E**) The second day of extinction protocol. The difference between **E5** of the first day and **E1** of the next day represents recovery, in this case not affected by genotype. The next four blocks represent re-extinction; no difference between genotypes was noted. Error bars indicate SEM. **Ntwt**: wild-type littermate control, **Ntko**: neurotrypsin-deficient mice.

3.2.8 Hippocampus/striatum cooperation during double dissociation water-maze experiment

It has been demonstrated that learning and memory is cooperatively performed by multiple memory systems residing in distinct brain areas (Packard et al 1989). Learning associated with cue recognition depend on the striatum, whereas acquisition of spatial information relies on the hippocampus(Yin & Knowlton 2006). When, during the water-maze, an animal has two possible strategies that lead to the goal, then the hippocampus-dependent strategy is used first whereas striatum-dependent automatic skills overcome the previous strategy and start to dominate after extensive training (Lee et al 2008). Based on our initial hypothesis, NT-deficient mice exhibit an impairment of their hippocampal function, which facilitates a faster conversion to habit. Therefore, we were interested in observing the learning pattern of NT-deficient mice after exposing them to a water-maze task that can be resolved using both systems. We hoped that because of the impairment in their hippocampal function, NT-deficient mice will preferably choose the cue learning strategy and thus present a faster switch to habit.

The two cue water-maze test was conducted according to the protocol of Lee. Lee was able to demonstrate that lesions of the dorsal striatum impair cue learning and enhance spatial learning. In contrast, lesions of dorsal hippocampus impair spatial learning and potentiate cue acquisition (Lee et al 2008). However, our results revealed no significant difference between genotypes. Analysis of the escape latency during the first phase of the one cue presentation indicated that escape latency decreased ($p < 0.0001$) equally for both genotypes (Tab. 13), indicating that learning occurred and was not affected by genotype (Fig. 3.22A). Further swim time analysis during cue discrimination (only training trials) (Tab. 14) indicated that there was no significant decrease across days; meaning that there was no further learning across days (Fig. 3.22B). Repeated analysis of escape latency, this time during the cue discrimination phase, showed no effect of the genotype. The analysis of the distance to the cue was performed across all three probe trials (Tab. 12). On average, independent of genotype mice were closer to the distractor cue (Fig. 3.22C). This tendency did not change across all three probe trials. Similar results were found by the analysis of the time in quadrant (data not show).

NT-deficient mice were able to learn the task as efficiently as wild-type mice, and they did not present any difference during the presentation of the cue. For unknown reasons, both groups of mice preferred the distractor cue more than the correct cue, even though mice were divided into two groups, with either a vertical or a horizontal striped cylinder as the correct cue. This was done to avoid a greater preference of one of the cues by the

animals. In conclusion, I was not able to support my hypothesis by applying this experiment.

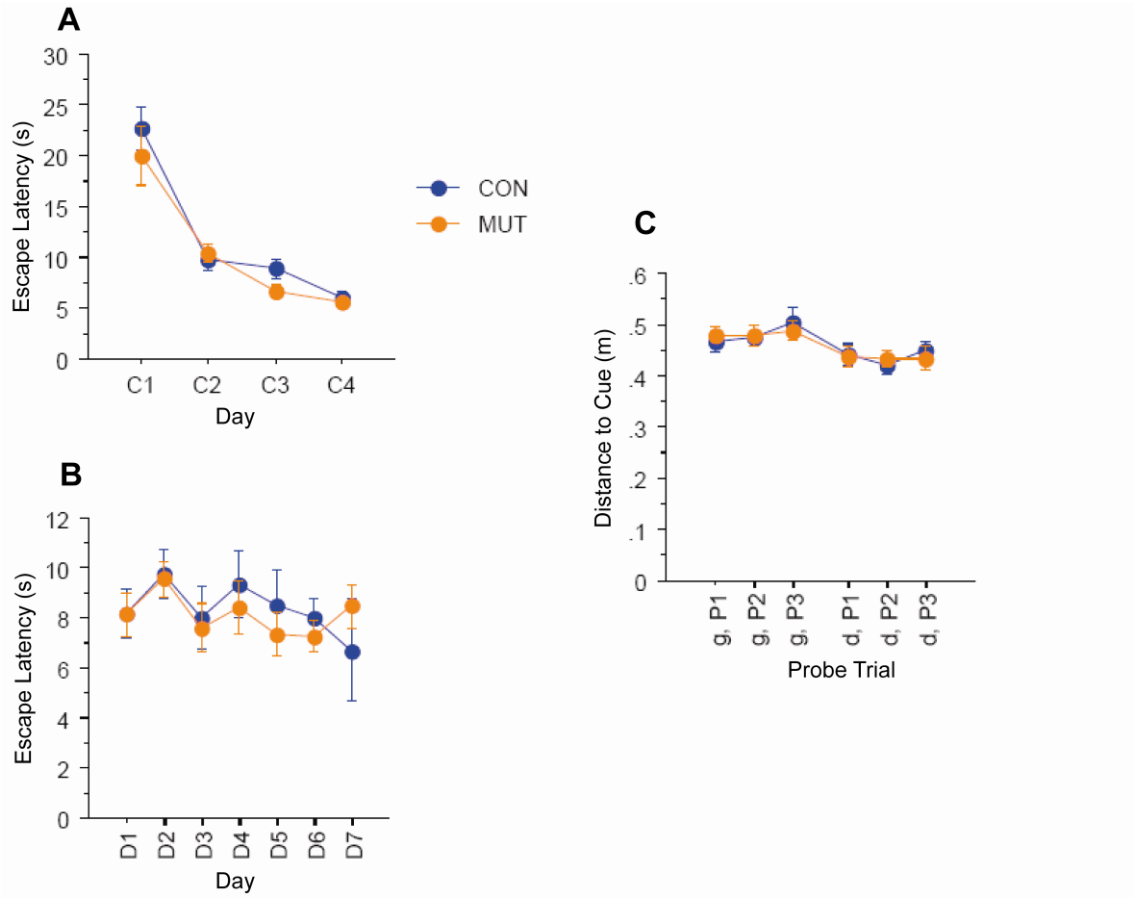

Fig. 3.22 A double dissociation water-maze showed no changes in the neurotrypsin-deficient mice in regard to hippocampus/striatum cooperation

A double dissociation experiment includes 5 consecutive days of shaping; mice acquire the ability to find a platform hidden under water and marked with a grey cylinder. Each mouse was exposed to the platform once in each quadrant in pseudo-random order. During the next 7 days, mice were exposed to two different cues. An escape platform was placed in the centre of a quadrant and was marked with stripes (the goal cue). The other striped cylinder (the lure cue) was placed in adjacent a quadrant. The lure cue did not allow the animal to escape from the water. In total 30 mice (11 males/19 females; 13 Ntwt/17 Ntko) took part in this experiment. (**A-B**) Escape latency (sec) (**A**) Escape latency during the shaping decreased independently of genotype indicating that learning occurred and was not affected by genotype ($p < 0.0001$, by ANOVA). (**B**) Escape latencies during cue discrimination phase were not affected by genotype. There was no significant decrease across days, indicating that there was also no learning across days. (**C**) The distance to the cue was analyzed over 3 probe trials (no platform for escape was provided) that were equally spread throughout the training phase (10th, 12th, and 14th day). The distance to the cue across all trials was equal in both genotypes. Both genotypes were on average closer to the distractor cue ($p < 0.05$, by ANOVA) **g**; goal, **d**; distractor. Error bars indicate SEM. **Ntwt, CON**: wild-type littermate control, **Ntko, MUT:** neurotrypsin-deficient mice.

3.2.9 Neurotrypsin deficiency does not facilitate a faster switch to habit

The T-maze test in our laboratory was designed to observe the transition from hippocampus-dependent place learning to caudate-dependent response learning. This transition occurs due to extended training of mice to approach a consistently baited arm in a cross-maze, starting from the same start box. During a single probe the test mouse is placed in the start box on the opposite site to the one used during training. Mice which entered the correct arm during the probe trial are place learners and mice which entered unbaited arm are response learners. Mice subjected to prolonged over-training showed the tendency towards caudate-related response learning.

We conducted two series of the T-maze test, which differed in the number of possible terminations of the trial. The 1st series, due to the system settings, allowed us to observe only three possible outcomes of the: the trial was rated as *terminated successfully*, when the mouse poked its nose into the correct arm and as a result was rewarded with a sugar pellet. The trial was rated as *time out*, when the mouse did not manage to reached the goal in the specified time. The rating *moving error* indicated that the mouse did not move. During the 2nd series of the T-maze test, changes that were made to the SOF-700RA-9 testing software in order to allow us to observe the fourth type of trial termination namely, *decision error*. The rating decision error indicated that the mouse chose the wrong arm and poked its nose into the head detector, an action that was terminated without any reward (Fig. 3.25A). The introduced changes allowed us to observe which arm the mouse visited first. Both rounds presented similar tendencies but in some cases differed in the activity level.

3.2.9.1 The 1st series of the T-maze test showed a reduced number of successfully reached goals in NT-deficient mice

The T-maze test was conducted in our laboratory to definitively confirm or rule out the hypothesis that NT-deficient mice exhibit a facilitated switch to habit formation.

Results from the 1st series of the T-maze test revealed wild-type mice to be significantly more successful in goal reaching (Fig. 3.23A) than NT-deficient mice, but only during training phases ($p < 0.01$; 1st training phase, $p < 0.05$; 2nd training phase). No difference between genotypes was observed during probe trials (Tab. 30). The detailed analysis of single day performance revealed a lack of improvement over test days. Over time, mice across

both genotypes showed a tendency to be less interested in the reward, consequently their performance decreased and they tended to commit more errors (data not show).

In addition, results from the 1st series revealed no significant difference between genotypes in latency to reach the goal (Fig. 3.23B) (Tab. 29).

In conclusion, both genotypes showed tendency towards lesser interest in the reward. What more, NT-deficient mice show reduced number of successfully reached goals during training phases.

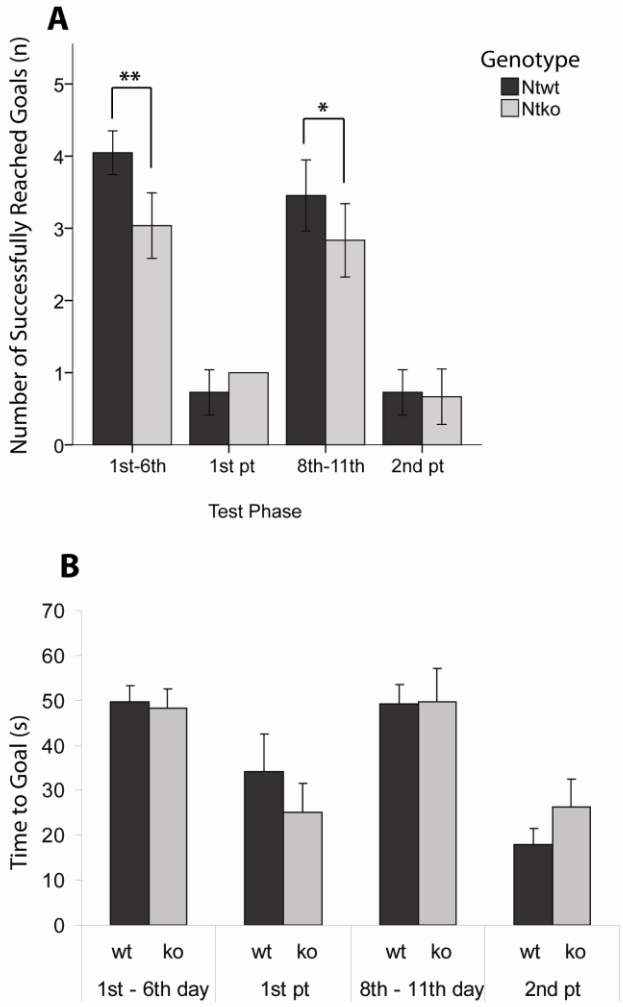

Fig. 3.23 The 1st series of T-maze test

The 1st series of the T-maze test. T-maze test was divided into four phases: two training phases: from 1st to 6th day and from 8th to 11th day, and two probe trials (**pt**) in between the first and second training phase and at the end of the second training phase. In total 20 male mice (11 Ntwt/9 Ntko) participated in the 1st series of the T-maze test.

(**A**) NT-deficient mice showed significantly reduced ability to reach a goal during both training sessions. No difference between genotypes was observed during probe trial.

(**B**) Independent of genotype, mice show equal time to reach a goal and no improvement across training sessions.

Error bars indicate SEM. Asterisks indicate significant difference between genotypes, *p < 0.05, ** p < 0.01; by Univariate ANOVA. **Ntwt**: wild-type littermate control, **Ntko**: neurotrypsin-deficient mice.

3.2.9.2 The 2nd series of experiment suggested locomotor activity influence on the T-maze test

In contrast to the 1st series results, the 2nd series of T-maze test revealed no significant difference between genotypes in number of successfully reach goals (Fig. 3.24A). The number of times the goal was successfully reached during the training phases was much lower than during the 1st series, whereas in the case of the probe trials, it stayed at a similar level (Tab. 32). Similar differences in level of behavior across both cohorts have been previously observed in our lab. A high variability means that these kinds of tests are highly sensitive to any changes. Although we were meticulous in our design to create an equal environment, we are not able to avoid differences between cohorts.

Further analysis revealed differences between successive sessions as well in case of time to goal. During the first training phase and the second probe trial of the 2nd series NT-deficient mice needed significantly less time to get to the baited arm ($p < 0.05$) than wild-type mice (Fig. 3.24B). There was no significant difference observed during the second stage of training (Tab. 31). The above results, especially the one concerning the second probe trial, may suggest that after extensive training NT-deficient mice had already reached the habit formation phase. Automatization of the skill results in faster and more efficient performance. Another, more likely explanation may be that NT-deficient mice show elevated locomotor activity, which may result in a shorter time to get to the goal. Unfortunately, the setup of the apparatus did not allow us to analyze animal speed.

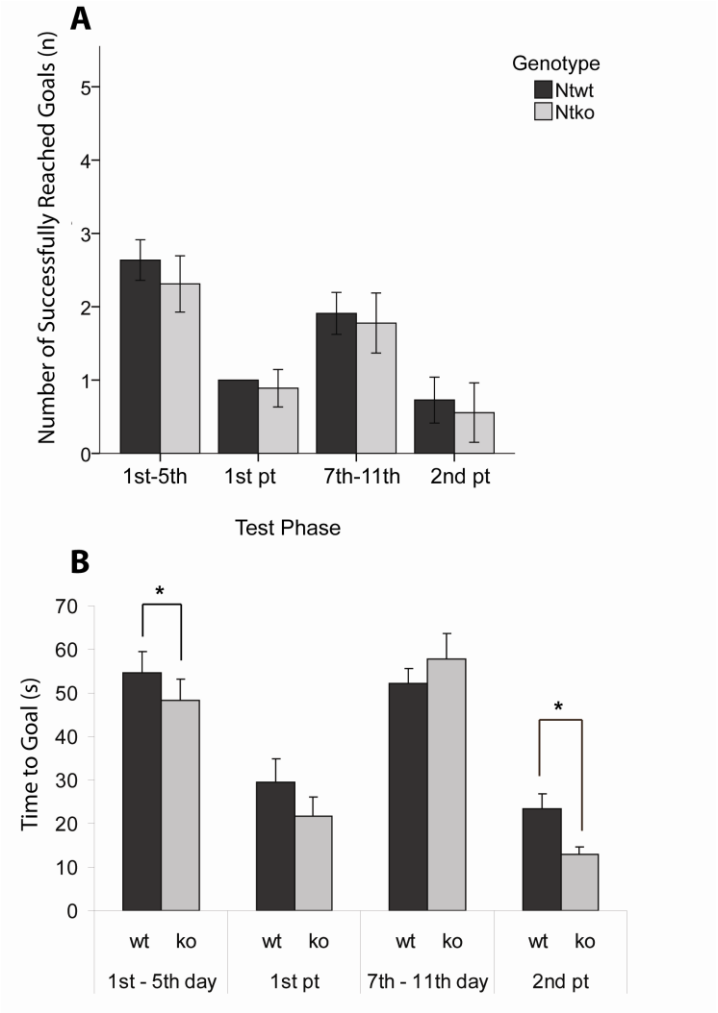

Fig. 3.24 Te 2nd series of T-maze test

The 2nd series of the T-maze test. T-maze test was divided into four phases: two training phases: from 1st to 5th day and from 7th to 11th day, and two probe trials (**pt**) in between the first and second training phase and at the end of the second training phase. In total 20 male mice (10 Ntwt/10 Ntko) participated in the 2nd series of the T-maze test.

(**A**) No difference between genotypes in number of successfully reached goal was observed. Independent of genotype, mice show decreasing interest in reaching the goal.

(**B**) NT-deficient mice presented significant increased latency to goal during the first training phase and the second probe trial.

Error bars indicate SEM. Asterisks indicate significant difference between genotypes, *p < 0.05, by Univariate ANOVA. **Ntwt**: wild-type littermate control, **Ntko**: neurotrypsin-deficient mice.

3.2.9.2.1 The 2nd series of the T-maze test indicated that neurotrypsin-deficient mice do not display facilitated response learning

According to our hypothesis NT-deficient mice would show a facilitated switch to habit, their place learning preference would be overcome by the response learning. It is very important to mention that habit induction in mice is an extremely long process, requiring much more training time than in rats (Yerkes & Dodson 1908).

The analysis of the first arm entry revealed that during the training phase, the choice of arm was identical for both genotypes (Fig. 3.25B). The number of correct arm entries in the case of the NT-deficient mice, remained constant across all three experimental phases, indicating that the training provided was not quite sufficient for habit induction in these mice.

In conclusion, the above results indicate that, probably due to their elevated locomotor activity, NT-deficient mice showed a significantly shorter time to reach the goal. However, their ability to reach the goal successfully is reduced in comparison to the wild-type mice. This result suggests that NT-deficient mice were not able to acquire the ability to choose the correct arm, in order to be rewarded, as efficiently as the wild-type mice did. Both analyses were conducted twice and presented high variability between rounds. The first arm entry assay revealed no genotype effect.

We were not able to observe clear difference between spatial and response learning. The T-maze results definitively refuted our hypothesis of the facilitated transient from the A-O model into S-R behavior.

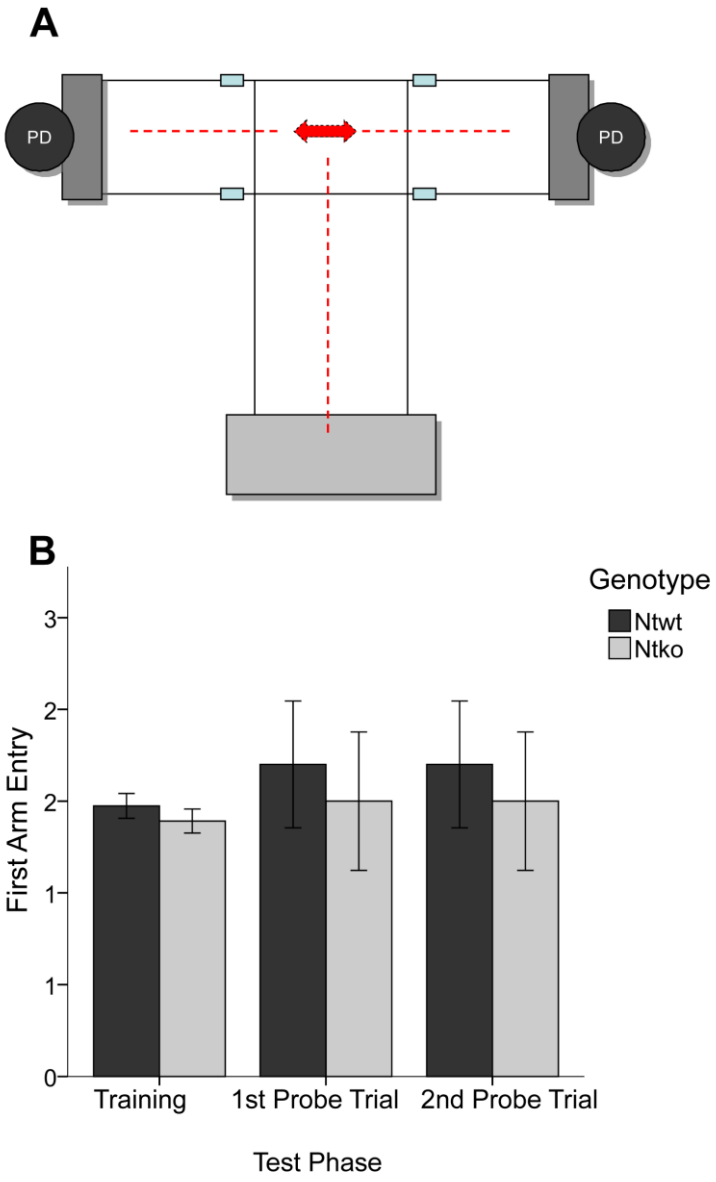

Fig. 3.25 First arm entry during training and both probe trials.

(**A**) Schematic representation of the T-maze apparatus. The light grey rectangle represents the start box from which the mouse starts the trial. Red arrow represents two possible directions to turn. Four blue rectangles represent I/R photobeams sensors detecting right or left turn. Both arms of the maze end with nose poke detectors (dark grey rectangles) and pellet dispensers (black circles). (**B**) The first arm entry analysis shows which arm the mouse decided to turn at first. Analysis was divided into three phases: training, as an average of first and second training phase, and first and second probe trials. No difference between genotypes was noted. Error bars indicate SEM. Data was analyzed using Univariate ANOVA, data was divided according to the test phase: training, first and second probe trial. **Ntwt**: wild-type littermate control, **Ntko**: neurotrypsin-deficient mice

4 DISCUSSION

4.1 Neurotrypsin-dependent agrin cleavage and its contribution to the formation of dendritic filopodia

4.1.1 Neurotrypsin-dependent cleavage of agrin requires postsynaptic activation

Our findings suggest that NT-dependent agrin cleavage requires postsynaptic activity. Studies using neurotrypsin-pHluorin show that depolarization drives synaptic exocytosis of NT and induces the refilling of the intracellular NT store (Frischknecht et al 2008). Further analysis of agrin-90 as a reporter of NT activity revealed that blockage of the presynaptic P/Q- and N-type calcium channels with ATX and CTX, respectively, results in the inhibition of NT externalization (Matsumoto-Miyai et al 2009). NT is released from the presynaptic terminal as inactive precursor, which has a typical zymogens activation site at which the protease is cleaved and activated. The protease domain remains connected to the N-terminus by the disulfide bridge. Our results revealed that full functionality of NT requires postsynaptic activation. The mechanism underlying NMDA-dependent NT activation remains unexplained.

During our experiments we applied two types of chemical stimulation: TEA and PFR. Previous studies showed that chemically induced LTP is sufficient to stimulate molecular mechanisms, which underlie synaptic plasticity (Luzhkov & Aqvist 2001; Otmakhov et al 2004). Application of above stimulations to the hippocampal CA1 region induces LTP without additional electrical stimulation (Otmakhov et al 2004; Ramakers et al 2000). TEA stimulation was successfully used in studies concerning dual mechanism of LTP (Huang & Malenka 1993). Results of these stimulations indicate that blockage of the AMPA and NMDA receptors, during TEA and PFR stimulation, with CNQX and MK801 inhibitors, respectively, prevented agrin cleavage. Furthermore, selective inhibition of L-type VDCC in the case of TEA stimulation resulted in a significant decrease of agrin cleavage. In contrast, only non-significant reduction of the PFR-induced agrin cleavage was observed. Therefore, TEA-induced generation of agrin-90 revealed a contribution by NMDA and L-type VDCC receptors, whereas PFR-induced LTP depended only on the NMDA receptor activity. These results are consistent with previous studies showing existence of compound LTP, characterized by two distinct induction mechanisms and different signal transduction cascades,

one relying on both NMDA and L-type VDCC receptors, whereas the other relies only on NMDA receptors (Cavus & Teyler 1996; Hanse & Gustafsson 1994; Morgan & Teyler 1999). The activity-dependent formation of filopodia presented a similar pattern, which suggested a close correlation between NT-dependent agrin cleavage and activity-dependent filopodia formation.

Our findings strongly suggest that the NT/agrin system may be considered as a coincidence detector for pre- and postsynaptic activation. Previous studies on LTP mechanisms have implicated the role of coincident pre- and postsynaptic activity in the LTP induction process (Bourne & Nicoll 1993). In 1949, Donald Hebb proposed that correlated activity of pre- and postsynaptic neurons can result in the strengthening or weakening of existing synapses (Hebb 1994). Based on these findings, NMDA receptors can be viewed as a molecular coincidence detector of glutamate release and postsynaptic depolarization.

Our studies confirm the role of the NMDA receptors as a detector of coincidence pre- and postsynaptic activity. In the case of PFR-induced LTP, NMDA-dependent LTP (Otmakhov et al 2004), the depolarization-dependent removal of the Mg^{2+} block was inhibited by selective AMPA receptor antagonist CNQX. Additionally, application of NMDA receptor antagonist MK801 does not allow the channel to serve as a detector for the coincidence of presynaptic activation. In contrast, in TEA-induced LTP, which depends on the NMDA and L-type VDCC receptors, NT-dependent agrin cleavage was inhibited by both MK801 and nifedipine. Thus, together these results confirm that the NT/agrin system fulfilled the conditions, which underlies the coincidence requirement for LTP.

4.1.2 The neurotrypsin-dependent 22 kDa fragment of agrin is essential for the formation of filopodia

Our detailed studies on the functional role of the NT-dependent agrin fragments characterized agrin-22 as a mediator of the filopodia-generating response associated with LTP. In NT-deficient mice cleavage of agrin by NT was completely abolished, therefore no activity-dependent filopodia formation was found. However, we were able to restore filopodia formation by exogenous administration of agrin-22. Therefore, we postulate that agrin-22 may be one of the regulatory factors generated via proteolysis of extracellular matrix proteins. Our results are in accordance with previous studies that reported about a

regulatory role of extracellular proteolysis for synaptic plasticity (Shiosaka & Yoshida 2000).

The most prominent representatives among serine proteases in the hippocampus are neuropsin and the plasminogen activators. Neuropsin is a member of the large kallikrein-like multigene family. Its extracellular proteolytic activity is modulated by an NMDA-dependent signaling system (Matsumoto-Miyai et al 2003). Neuropsin cleaves L1cam (immunoglobulin superfamily adhesion molecule) during the early phase of LTP.

Human tPA is a serine protease originally know as a fibrinolytic protease converting plasminogen into the active protease plasmin (Collen et al 1993). The function of tPA depends on the brain-derived neurotrophic factor (BDNF), which stimulates its expression and release (Fiumelli et al 1999). Behavioral studies of tPA-deficient mice revealed a significant impairment in inhibitory avoidance and context conditioning learning (Calabresi et al 2000; Pawlak et al 2002).

Our findings imply that agrin-22 is a molecule responsible for activity-dependent generation of dendritic filopodia. None of the other NT-dependent agrin fragments (agrin-90 and agrin-110) were able to restore abolished filopodia formation in NT-deficient mice. The receptor mediating the downstream signaling of agrin-22 remains unclear. Studies on NMJ indicated that agrin is a nerve-derived factor that induces reorganization at the motor endplate. At the NMJ, the agrin signal is mediated via the low density lipoprotein receptor-related protein 4 (Lrp4) (Kim et al 2008). Lrp4 forms complex with tyrosine kinase MuSK and myotube-specific accessory component (DeChiara et al 1996; Glass et al 1996), resulting in synapse formation, reorganization of the postsynaptic membrane, and presynaptic differentiation. Mice lacking either agrin or MuSK exhibit severe defects in their NMJ (DeChiara et al 1996; Gingras et al 2007; Ksiazek et al 2007).

In contrast, in the CNS the α3 subunit of the Na^+/K^+-ATPase (α3NKA) was identified as a neuronal receptor for agrin. As a result of agrin binding to the α3NKA, inhibition of its pump function was observed, thus suggesting a depolarizing agrin function on CNS neurons (Hilgenberg et al 2006). Further research concerning the agrin receptor and its downstream signaling in the CNS are required.

In summary, we demonstrated that NT is crucial for agrin cleavage and, as a result of agrin-22, we observed LTP-dependent formation of dendritic filopodia in the CA1 hippocampal region. Referring to previous *in vitro* research indicating agrin as a modulator of filopodia formation in the CNS (Annies et al 2006; McCroskery et al 2006) we propose the NT/agrin system as a mediator of LTP associated synapse formation. Numerous *in vitro* studies on hippocampal and cortical neurons have demonstrated that reduction of agrin

expression strongly affects synaptic differentiation (Bose et al 2000; Serpinskaya et al 1999).

According to the widely accepted hypothesis, dendritic filopodia are considered as an immature form of synapse (Holtmaat et al 2008; Knott et al 2006). Formation of new filopodia is strongly correlated with expression of NMDA-dependent LTP. Observation of cultured neurons *in vivo* showed that dendritic spines, which were formed by motile newly formed filopodia, become stable over time (Vaughn et al 1974; Ziv & Smith 1996). Further examination of axo-dendritic synaptogenesis indicated that newly formed filopodia tended to initiate physical contact with nearby axons and, thus became direct precursors of dendritic spines (Ziv & Smith 1996). The above findings suggest that activity-dependent formation of filopodia may by crucial for the rearrangement of neural circuits, thus affecting memory and learning. Recent imaging studies revealed that extensive motor learning (accelerating rotating rod (Yang et al 2009) and single seed reaching (Xu et al 2009)) promotes remodeling of pre-existing neuronal connections. Motor training promotes rapid formation of postsynaptic dendritic spines within an hour. The newly formed spines are stabilized during subsequent training and contribute to lifelong memories. These findings indicate the role of synaptic structural plasticity in memory formation and triggered our interest in the behavioral phenotype of NT-deficient mice.

4.2 The role of the neurotrypsin/agrin system in learning processes in the adult CNS

4.2.1 Undisturbed multiple memory systems cooperation in neurotrypsin-deficient mice

In the previous chapter we presented arguments supporting why NT-dependent agrin cleavage and formation of agrin-22 may be considered as a detector for coincident pre- and postsynaptic activity. Now we will discuss the role of the NT/agrin interaction as a regulatory system in learning and memory processes.

The preliminary rotarod results suggested faster facilitation of habit formation in NT-deficient mice as a result of an impairment in the hippocampus function. Unfortunately, high variability in the subsequent series of rotarod tests precluded conclusions about the capacity of motor skill learning of NT-deficient mice. This kind of high variability between our subsequent rotarod tests was in accordance with previous study showing that high variability even of individual animals is characteristic for motor learning paradigms (Buitrago et al 2004a). In addition, the rotarod test is characterized by high sensitivity to the task parameters, such as the difference in acceleration and fixed-speed parameters, as well as differences in the laboratory environment (Bohlen et al 2009; Rustay et al 2003).

Our results concerning front limb grip strength indicated no difference between genotypes but significant age-related weakening of the front limb. Earlier studies shed light on the importance of muscle strength in the case of motor tests. Study on myostatin clearly demonstrated that increased muscle mass, and thus elevated muscle strength, significantly improved rotarod performance (Bogdanovich et al 2008). Our grip strength results excluded any muscle effect on the rotarod test.

Further motor learning studies using the staircase test showed no difference in reaching and grasping abilities between wild-type and NT-deficient mice. The staircase test is sensitive to lesions of the striatum (Fricker et al 1996) and the motor cortex (Montoya et al 1990; Montoya et al 1991) rather than malfunction of the hippocampus. In case of facilitated transit to habit formation we expected to observe an increased number of successfully collected sugar pellets by NT-deficient mice. A previous rat study showed evidence of goal-oriented and habit learning in reaching and grasping tests (Gholamrezaei & Whishaw

2009). Our initial hypothesis that NT-deficient mice exhibit an increased vulnerability to over-training and, therefore, show a facilitated transit from goal-oriented (A-O model) to habit (S-R) behavior was eventually ruled out by the results of our T-maze tests.

4.2.2 Age-related effects on memory consolidation in neurotrypsin-deficient mice

The rotarod test allows to assess intrasession and intersession learning. The protocol allowed us to keep track of the differences between the training trials of the previous day in order to compare them with the first trials of the next day, and as a result we could follow any overnight drop in the performance level. The collected data revealed that NT-deficient middle-aged mice present a significantly greater overnight drop in comparison to wild-type mice. Our further studies confirmed that NT-deficient mice showed no disturbance in memory consolidation after fear conditioning, although we suspected the presence of neurological changes to appear with advancing age. Numerous studies have documented a broad range of age-related motor performance deficits in laboratory animals (Carlsson 1978; Ingram et al 1981; Joseph et al 1978). The causes of age-related changes are not fully understood but there are a few widely accepted theories. One of the crucial elements in motor-dependent tasks is the cerebellum. The age-associated decrease of cerebellar Purkinje cells (Larsen et al 2000) combined with reduced functional efficiency of the hippocampus (Barnes 1999) are responsible for reduced motor learning at advanced age. Another potential mechanism correlated with age-dependent changes in motor behavior is reduced angiogenesis in the hippocampus (Black et al 1989). Behavioral studies indicated the role of angiogenesis in new motor tasks acquisition (Kerr et al 2010). Numerous postmortem and computed tomographic studies indicate a reduced weight and size of the brain in elderly human and an increase in ventricular size, especially after 60 years (Cutler et al 1984; Dekaban 1978). In addition, research on familial Alzheimer disease (FAD) revealed the role of presenilin 1 (PS1) in age-dependent impairment of spine morphology and synaptic plasticity in the CA1 hippocampal region (Auffret et al 2009). PS1 is a family member of the multi-pass transmembrane proteins. The result of PS1 cleavage is a large N-terminal and small C-terminal fragment, which together form a functional protein (De Strooper et al 1998). The overexpression of PS1 results in synaptic dysfunction in aging mice (Auffret et al 2009).

Previous behavioral studies using NT-deficient mice demonstrated decreased activation of CREB in hippocampal neurons 90 min after Morris water-maze training (Mitsui et al 2009). The cAMP responsive element binding protein (CREB) is a nuclear protein,

which modulates transcription of genes (Brindle & Montminy 1992; Sassone-Corsi 1995). Increased concentration of cAMP or calcium starts the phosphorylation and activation of CREB (Gonzalez & Montminy 1989). Rat studies using social transmission of food preferences revealed that lower activation of CREB after training may cause a rapid forgetting in aged animals (Countryman & Gold 2007). Furthermore, mice lacking CRAB protein exhibited abnormal long-term, but not short-term memory (Kogan et al 1997). Previous studies suggested that CREB is crucial for the conversion of short-term potentiation to long-lasting memories (Dash et al 1990; Silva et al 1998). The reported effect of CRAB activation could explain the higher overnight drop observed during the rotarod test in the middle-age and aged NT-deficient mice.

4.2.3 Neurotrypsin-deficiency enhances spatial learning ability

Many previous studies demonstrated that LTP underlies activity-dependent plasticity in the hippocampal system linking structural changes with processes of learning and memory formation (Bliss & Gardner-Medwin 1973; Grant et al 1992; Morris et al 1986). Our studies, applying electrophysiological stimulation to the Schaffer collaterals and recording of the elicited synaptic responses in the CA1 region revealed intact LTP in NT-deficient mice (Matsumoto-Miyai et al 2009). Nonetheless, NT-deficient mice showed enhanced spatial learning and elevated locomotor activity compared to wild-type mice.

Previous studies revealed that elevated coincidence of pre- and postsynaptic activation in the synapses can be correlated with enhanced learning. Overexpression of the NMDA receptor 2B (NR2B) resulted in increased activation of NMDA receptors and, thus, transgenic mice exhibited elevated long-term memory, faster extinction of previously acquired paired events, and better learning during the water-maze hidden-platform test (Tang et al 1999). Similar improvement in finding the platform was exhibited by mutant mice lacking the DNA fragmentation factor 45 (DFF45). Transgenic mice showed a shorter mean path length and shorter distance from the platform than wild-type mice (Slane et al 2000). DFF45 is one of the factors forming the heterodimeric protein complex responsible for DNA fragmentation during the apoptosis process (Enari et al 1998). In conclusion, both NR2B and DFF45 are considered important for plasticity and memory formation, respectively. Their overexpression or deficiency affects the ability to learn during various behavioral tests. The only published study concerning behavioral aspects of NT in the adult CNS revealed prolonged interest in a familiar mouse and longer social interaction with an intruder mouse in social-related tests. Furthermore, Golgi-Cox staining in NT-deficient

mice indicated decreased spine density on apical dendrites of the hippocampal CA1 region (Mitsui et al 2009). The above observation in changed spine number is consistent with our studies on filopodia formation in secondary apical dendrites. Our studies showed that NT-dependent formation of agrin-22 is crucial for the formation of the dendritic filopodia (Matsumoto-Miyai et al 2009) and filopodia are considered precursors of nascent spines.

Numerous developmental studies showed that immature dendrites tend to form a large amount of highly motile dendritic protrusions, called filopodia. These immature structures intensively extend and retract exploring neuropil looking for possible presynaptic partner to create synaptic connection (Dunaevsky & Mason 2003; Jontes & Smith 2000; Yuste & Bonhoeffer 2004; Ziv & Smith 1996). Further studies indicated that adult brain is not so inflexible as considered at the beginning. Similar behavior of motile dendritic filopodia was observed during the adult synaptic plasticity (Engert & Bonhoeffer 1999; Maletic-Savatic et al 1999). The number of filopodia decreases with time, as they are slowly replaced by stubby and mushroom spines (Fiala et al 1998). The process of development consists of delivery, via transport vesicles, of molecular complexes into presynaptic membrane. In contrast, molecules necessary for the postsynaptic reorganization are recruited from postsynaptic cytoplasm. After initialization of a contact the full maturation process requires further accumulation of synaptic vesicles in the presynaptic terminal and neurotransmitters recruitment to the postsynaptic membrane (Matus 2005). In adult brain only ~0.2% of filopodia will be transformed into mushroom spines (Majewska et al 2006), and even less, because only ~3% of new population of spines will survive the first month (Holtmaat et al 2005). Two-photon time-lapse microscopy confirmed that different types of spines originate from filopodia (Parnass et al 2000). What more, experience-dependent structural changes observed in the barrel cortex indicated that a novel sensory experience enhanced filopodia transition into stable synaptic connection (Holtmaat et al 2006). According to our hypothesis activity-induced filopodia will search for presynaptic contact, possibly creating connection with an axon to make a synapse with a *de novo* generated bouton. Newly formed filopodia may as well grow towards already existing spine, developing postsynaptic specialization (Knott et al 2006). This way multiple spine boutons are created resulting at some point in spine elimination. In this manner newly formed filopodia contribute to neuronal plasticity by establishment of novel neuronal circuits. Therefore, NT/agrin system plays a role in reorganization and stabilization of new connections between neurons.

Recent motor learning-oriented studies revealed a correlation between spine remodeling and behavioral improvement after learning. Two-photon imaging of spines in the motor cortex before and after rotarod training indicated experience-dependent rapid forma-

tion of spines (Yang et al 2009). A similar effect can be observed after a forelimb reaching task (Xu et al 2009). Our behavioral tests, such as the rotarod, water-maze and ACTIVISCOPE, indicated elevated locomotor activity and increased learning ability in NT-deficient mice. NT-deficient animals demonstrated an increase in time in the current goal quadrant and a decrease in the distance to the current goal already during the acquisition phase. In addition, NT-deficient mice showed significantly faster recognition of the hidden platform after its relocation, i.e. during the reversal learning. We noted that during the first testing day, the level of performance in both groups was identical, revealing that the NT-deficient mice did not have an advantage over wild-type mice from the beginning of the test. Results of the studies concerning dendritic filopodia formation and reversal learning in the spatial-oriented paradigms suggested that abolished formation of new filopodia in NT-deficient mice may cause the composition of a weaker memory trace or lack of its stabilization during the initial stage of the acquisition. The weaker memory trace may serve as an advantage during the reversal phase, because it is easier to overcome in the situation when a new solution is necessary.

In conclusion, NT-deficient mice showed an undisturbed LTP and exhibited an elevated level of spatial learning in the water-maze during the acquisition phase. However, the lack of NT results in enhanced reversal learning, indicating the importance of NT in experience-depending formation of memory. In connection to our filopodia studies we propose that the NT/agrin system play a homeostatic role during the creation of a strong and long lasting memory trace. The mechanisms of action of the NT/agrin system in the adult CNS remains unclear and requires future research.

4.2.4 Elevated locomotor activity is characteristic for neurotrypsin-deficient mice

Our locomotor activity analysis, using the ACTIVISCOPE system, revealed an elevated general activity of NT-deficient mice during the dark/active phase. Further analysis demonstrated age-dependent decrease of activity. Previous studies indicated that elevated locomotor activity can influence behavioral tests. During the open field and water-maze tests hyperactive rats showed an increased number of ambulation, increase number of errors. The radial arm maze test revealed increase amount of required training (Akaike et al 1991).

The results of an activity monitoring differ from those of a previously published, study of the behavior of NT-deficient mice. According to Mitsui et al, an open field test indicated similar activity levels between motopsin/NT-deficient and wild-type mice (Mitsui et al 2009). They base their statement on the standard open field test, which consisted of 10 min sessions for three days, which in reality was a habituation period for the exploratory test. Our 24 hour approach, using the ACTIVISCOPE system, allowed us to register mouse activity every 10 min for five consecutive days. Only four days are included in our statistic, the first day was considered as a habituation period, but if we analyze the first day of the locomotor activity test (data not show), then we do not observe any difference between genotypes (1^{st} and 2^{nd} round $p > 0.5$). Therefore, it is justified to claim that only an exact and extended method allows for the full analysis of the general activity of NT-deficient mice.

One of the most common causes of elevated activity is a decreased level of anxiety-like behavior. Anxiety can be defined as a response to real or potential threats (Belzung & Griebel 2001). Previous research revealed the effect of anxiety levels on posture and balance during the rotarod test. The rotating beam might be considered by mice as a potentially dangerous situation, and the choice of posture and balance strategies may be due to contrasting levels of anxiety. According to these study anxious mice were more prone to fall off the rotating beam and showed more imbalance then non-anxious mice (Lepicard et al 2003). These results demonstrated that less anxious mice may be predisposed to stay longer on the rotating rod, raising the question whether our NT-deficient mice are less anxious? A previously published study, using plus maze and light/dark box revealed no difference in anxiety-like behavior in motopsin/NT-deficient mice (Mitsui et al 2009). However our fear conditioning tests revealed a non-significant tendency towards a decreased fear response to the cue. The light-dark transition test performed in our laboratory by F. Molinari indicated that NT-deficient mice spend significantly more time in the light compartment ($p < 0.05$) then wild-type mice (unpublished data). In addition, according to literature, C57BL/6J male mice show lower levels of anxiety in comparison to other strains (An et al 2011). Furthermore, a significant difference in the anxiety-like level can be observed within strains (Harro et al 1990).

Earlier, unpublished studies performed in our laboratory suggested a close correlation between NT expression and hyperactivity. They indicated association between NT expression in the CA1 hippocampus region and hypothyroidism. Hypothyroidism is a condition characterized by the deficiency in the production of thyroid hormone. The most common reason for this state is iodine deficiency, but it can also be caused by malfunction of the thyroid or the pituitary gland, or the hypothalamus (Topliss & Eastman 2004). Fetal and

neonatal development is sensitive to the level of thyroid hormone (Gilbert 2004; Iannacone et al 2002). Several rodent studies show a link between hypothyroidism and attention-deficit/hyperactivity disorder (ADHD)-like behavior (Akaike et al 1991; Dugbartey 1998; Negishi et al 2005). In our laboratory we induced prenatal hypothyroidism by application of methimazole with drinking water starting from E9. The methimazole effect on the hippocampus was analyzed on P15, *in situ* hybridization clearly indicated a significantly decreased level of NT expression in the CA1 hippocampal region. Unfortunately, we did not check for general activity in these mice. Taking into account the proven correlation between hypothyroidism and hyperactivity we can speculate that these mice would show an elevated activity level. Elucidating further, NT-deficient mice can not be considered as an animal model for ADHD due to a lack of deficits in learning and memory processes characteristic for ADHD-like animal models. Overall, our results indicated close association of the elevated general locomotor activity with NT expression in the CNS.

4.2.5 Head-vector searching strategy in neurotrypsin-deficient mice

Our water-maze results, including the time taken to reach the goal, the efficiency of the chosen path, and the direction error revealed that NT-deficient mice showed a significantly elevated ability to find the relocated hidden platform during the reversal learning phase. One possible cause of this type of behavior may be a change in their searching strategy. During the hidden-platform test mice are allowed to freely explore the environment in order to acquire and memorize geometric aspects of their surrounding environment. During the course of the test mice should rely on the previously memorized information in order to perform place navigation towards the goal. The place navigation system is based on the place cells supported by the hippocampus (O'Keefe & Dostrovsky 1971; O'Keefe 1978). Place cells fire at maximum rate when the animal is at a correct place and experiencing the particular panorama characteristic for that place. The created spatial map consists of place fields formed during new environment exploration and lasts for months (O'Keefe 1976; O'Keefe & Conway 1978). Proper functioning of place cells during spatial learning requires induction of long term synaptic plasticity. It has been shown that the formation of the place cells memory trace is NMDA receptors dependent (Nakazawa et al 2004).

Cognitive maps based on the activity of the place cells are the most common system for place navigation, however, not the only one. In 1984, James B. Ranck, Jr. was the first to

notice a non-hippocampal, heading-based navigation system. Head-vector (HD) cells are considered to be a more primitive system that was eventually overtaken by place cells. HD cells fire as a function of an animal's current heading, irrespective of the location (Taube et al 1990a; b). Spatial learning tests confirmed that hippocampal lesions disturb the system based on the cognitive maps but not HD searching strategy. Rats with hippocampal lesions found the platform more efficiently than control animals in the first trial of a session (Pearce et al 1998).

Intriguingly, the localization pattern of place cells correlates with NT expression, whereas there is no correlation between the localization of HD cells and NT expression. HD cells can be found in the presubiculum (Ranck 1984), the striatum (Mizumori et al 2000; Wiener 1993), the anterior dorsal thalamic nuclei (Mizumori & Williams 1993), and the lateral mammillary nucleus (Stackman & Taube 1998). We speculate that NT-deficient mice tend to use the HD cells system, because their place cells-based navigation system is disturbed.

Studies of rats with a hippocampus lesion are in accordance with our hypothesis that NT-deficient mice apply a searching strategy that is based on the HD cells instead of the place cells.

Their change of the navigation strategy resulted in an elevated searching ability visible during the reversal learning phase of the water-maze test. Further studies focused on navigation strategies in NT-deficient mice are required.

5 Conclusions

The use of animal models in research on neurological disorders is justified by the similarity between the nervous systems. However, although mice share similar basic brain functions such as motor control activity and response to stress etc., with humans, we can not use mice models to study complex human behavior. We can only observe changes in behavior as a result of our manipulation.

Our chemical stimulation results indicate the role of NT-dependent agrin cleavage in the processes of dendritic filopodia formation. In addition, previous studies revealed a strong correlation between filopodia formation and LTP induction in the NMDA-dependent manner responsible for learning and memory processes. This stimulated our interest in the behavioral phenotype of NT-deficient mice. The set of behavioral tests used during our studies allowed us to discover the possible role of the NT/agrin interaction in adult the CNS. Deficiency of the NT and thus, absence of agrin-22, results in elevated locomotor activity and enhanced acquisition of spatial learning. In addition, disturbance in the NT/agrin learning system may cause change from place cells navigation system into HD cells searching strategy.

Further, accurate analysis of NT-dependent enhanced new skills acquisition in relation to human MR is required.

6 MATERIALS AND METHODS

6.1 Biochemical analysis

6.1.1 Generation of transgenic mice

Neurotrypsin-deficient mice

NT-deficient mice were generated in order to demonstrate dependence of agrin cleavage on the presence of NT. The genomic DNA containing exon 10 and 11 of murine NT, responsible for encoding the proteolytic domain, was obtained from a C57BL/6 genomic DNA library. The targeting vector included a loxP site upstream of exon 10 and a floxed neomycin resistance sequence downstream of exon 11. Vectors were linearized and electroporated into C57BL/6-derived embryonic cells, which were subsequently injected into blastocysts. Germ-line male chimeras were crossed with C57BL/6 females to yield heterozygous offspring. Mice obtained this way were crossed with CMV-Cre mice to remove the floxed region. As a result, mice lacking the region encoding the proteolytic domain were generated. Animals were tested for NT deficiency by PCR.

Mice expressing membrane-targeted GFP

The mouse line L15 expressing membrane-targeted green fluorescent protein (GFP) in sparse neurons was generated in the laboratory of P. Caroni at Friedrich Mischer Institute for Biomedical Research, Basel, Switzerland. A construct containing cDNA for enhanced GFP was fused to the membrane-anchoring domain (first 41 aa) of a palmitoylated mutant of MARCKS29 under the Thy1 promoter. The L15 line was chosen. It was characterized by a low number of mGFP-labeled cells within the CA1 area of the hippocampus. The transgenic mice had no detectable phenotype, and the expression of these transgens did not affect the physiology and anatomy of the hippocampus.

6.1.2 Mouse genotyping

Tail biopsies were collected from all mice before weaning. They were digested in 300µl alkaline lysis reagent (0.25 M NaOH, 0.2 mM Na_2EDTA, pH 12.0) in 95°C for 45 min on a rocking platform. Samples were neutralized with 300 µl neutralizing reagent (40 mM Tris-base, pH 5.0) and stored at -20°C. For each PCR reaction two sets of reaction mix were prepared (10x buffer with $MgCl_2$, dNTP's [2.5 mM each], 25 mM $MgCl_2$, 5 u/µl Taq-

Polymerase) taking into account different primers for the two genotypes (NT-wild-type: 0.5 µM mNTendF and 0.5 µM mNT2R; NT-deficient: 0.5 µM mNT3F and 0.5 µM mNT2R).

Primer sequence:

mNT3F: 5'-GCT GAC ATA GCT TGC TTG CAT TTG-3'

mNTendF: 5'-CTC CTG GAG TTT ATA CCA GAG TCC-3'

mNT2R: 5'-GTC AGG TTA GTC TCA GGA GAT CTG-3'

PCR program: 1x (3' 94°C), 40x (45'' 94°C, 45'' 62°C, 60'' 72°C), 1x (5' 72°C).

Expected product size: mNT3F/mNT2R~650bp; mNTendF/mNT2R~490bp; Samples were analyzed in two rows on 2% agarose gel.

6.1.3 Antibodies

Rabbit antiserum R132 was raised against the C-terminal 90 kDa agrin fragment, where R139 rabbit antiserum was raised against the C-22 kDa fragment of agrin (Reif et al 2007). The C-90-kDa and C-22-kDa anti-agrin sera were purified by affinity chromatography. Both antibodies were able to detect the full-length agrin signal. The peroxidase conjugated secondary antibodies for Western blot analysis were purchased from sigma Aldrich Co. (USA).

Table 1. Antibodies

Name / antigen	Antibody species	type	Dilution for Western blotting
R132 (C-90-1)	rabbit	affinity purified	1 µg / ml
R132 (C-90-1)	rabbit	serum	1 : 1000
R139 (C-22-2)	rabbit	affinity purified	1 : 250
beta-actin	mouse	IgG	1 : 10,000
Peroxidase-conjugated secondary anti-mouse	goat	IgG	1 : 20,000
Peroxidase-conjugated secondary anti-rabbit	goat	IgG	1 : 30,000
Peroxidase-conjugated secondary anti-goat	rabbit	IgG	1 ; 10,000

6.1.4 Western blot sample preparation

Animal spinal cord was interrupted prior to any procedure. This was followed by decapitation then removal of the skin and opening of the skull. Whole brains of C57BL/6 wild-type and NT-deficient P10 mice were carefully removed from the skull. Whole brains were cut along the brain middle line into two hippocampi. Each of them (with the adjacent cerebral cortex) was homogenized separately in 50 µl of sucrose buffer (0.32 M sucrose, 5 mM HEPES pH 7.4, 0.5 mM EDTA) with protease inhibitors cocktail (1:100, Sigma-Aldrich, USA). Samples were centrifuged at 10 000 rpm for 15 min in 4°C. Supernatant was collected and stored at -20°C.

Protein concentration was measured based on bicinchoninic acid method using BCA Protein Assay Kit (Pierce, USA). Procedure used to measure the concentration was based on the original protocol; however volumes were customized to our needs.

6.1.5 SDS-PAGE and immunoblotting

6.1.5.1 SDS-PAGE

75 µg of protein samples, positive and negative controls were solubilized in reducing SDS-PAGE loading buffer LDS 4 x (Invitrogen, USA), boiled for 10 min at 75°C and loaded on self-casted 10% polyacrylamide gels. Each gel consisted of two parts: running part, lower gel stock (1.5 M Tris, 0.4% SDS, H_2O, pH adjusted with 6 M HCl to pH 8.8), acrylamide, TEMED, 10% APS and stocking part, upper gel stock (0.5 M Tris, 0.4% SDS, H_2O, pH adjusted with 6 M HCl to 6.8), acrylamid, TEMED, 10% APS. Proteins were electrophoretically separated under constant current of 25 mA per gel (Laemmli 1970) in gel running buffer (10x running buffer: 248 mM Tris, 1.918 M glycine, 1% SDS, H_2O).

6.1.5.2 Immunoblotting

After electrophoresis proteins were blotted to Immobilon-P polyvinyline fluoride membranes (Milipore AG, Switzerland). For the optimal detection of the full-length agrin, proteins were transferred at 20 V overnight at 4°C in a Criterion Blotter wet transfer chamber (BioRad, Switzerland) using 0.5 x blotting buffer (12.5 mM Tris, 91 mM glycine, 10% methanol). Afterward, the transfer membranes were soaked in methanol and air-dried for 10-15 min. For further procedures, membranes were cut below the 50 kDa mark. The upper part of the membrane was incubated for 1 h with the primary antibody R132 or R139 diluted in Tris-buffered saline (TBS; 10 mM Tris/HCl, 150 mM NaCl, pH 8.0) containing 0.1% Tween-20 (TBST) and 10% milk. The lower part was incubated with the primary antibody against beta-actin diluted in the same buffer, but with 5% milk. After washing with TBST, the blots were incubated with peroxidase-conjugated secondary antibodies for

45 min, then washed again and subsequently developed with chemiluminescent substrate Chemiglow (Alpha Innotech GmbH, Germany) and LAS-3000 Image Reader (Fujifilm Europe GmbH, Germany). Density of the bands was quantified using Aida Imager Analyzer v. 3.52 (Raytest GmbH, Germany). For all analyses, the agrin signal was first normalized to its corresponding β-actin signal, which was used as the internal loading control. The signal from the unstimulated wild-type sample was used as the positive control and was adjusted to 1; other samples were compared to it.

6.1.6 Chemical stimulation

For acute slice analysis, 4-6 week old mice (young adults) were used. The whole brain was rapidly dissected according to the method described in section 5.1.2 and placed for 3 min in ice-cold artificial cerebrospinal fluid (ACSF). After that time the hippocampi, together with the adjacent cerebral cortex, were cut out and sliced vertically to the long axis of the hippocampus into 400 µm thick slices using a Mcllwain tissue chopper (Mickle Laboratory Engineering Co, UK). The slices were transferred into room-temperature ACSF without calcium (120 mM NaCl, 3 mM KCl, 1.2 mM NaH_2PO_4, 23 mM $NaHCO_3$, 11 mM glucose, 2.4 mM $MgCl_2$) oxygenated with 95% O_2/5% CO_2 and incubated for 1 h. The incubation is required to provide sufficient time for recovery after dissection. The right stimulation slices were incubated in ACSF with calcium (2.4 mM $CaCl_2$) for an additional 20 min with constant oxygenation. If possible, the same number of slices was used for each condition. Each stimulation experiment contained one control condition. Control slices passed through every phase of stimulation but no substances that cause long-term potentiation excitation and no inhibitors were added.

6.1.6.1 Tetraethylammonium stimulation (TEA)

For TEA stimulation slices were incubated in standard ACSF with 30 mM tetraethylammonium (Sigma Aldrich, USA) for 10 min (Albouy et al). Stimulation was performed in room temperature with constant oxygenation.

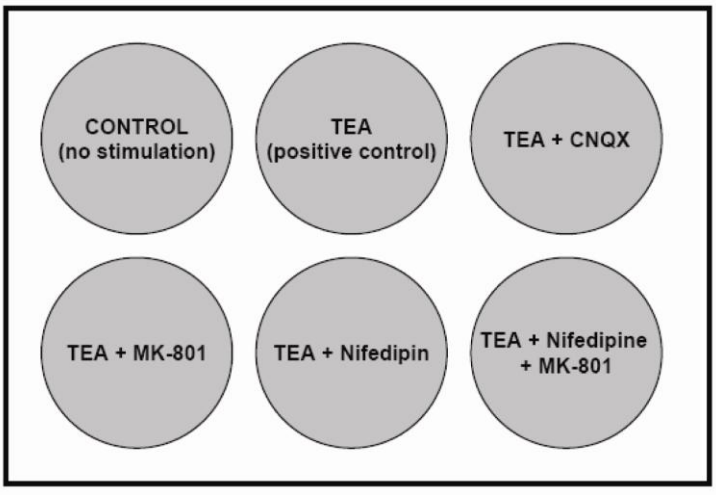

Fig. 5.1 TEA stimulation

All possible stimulation conditions used in the experiment; all conditions were equally oxygenated and stimulated at the same time.

Each circle represents one wall of the 6 wall plate.

6.1.6.2 Picrotoxin-Forskolin- Rolipram stimulation (PFR)

In PFR stimulation, a combination of 50 µM picrotoxin, 50 µM forskolin and 0.1 µM rolipram (Sigma Aldrich, USA) is applied. Slices were stimulated at room temperature in ACSF with high Ca^{2+} (4 mM $CaCl_2$) and without Mg^{2+} with constant oxygenation for 16 min.

All inhibitors were added into the ACSF right before stimulation in the following concentration: CNQX, 20 µM; MK-801, 20 µM; nifedipine, 50 µM (Sigma-Aldrich, USA). The same protocol was applied to whole hippocampi dissected from P10 brains. For histological analyses, tissue after stimulation was fixed by incubation in 4% paraformaldehyde, 4% sucrose in PBS, pH 7.4, overnight at 4°C. Fixed brain slices were placed on the glass slips mounted in Vectashield mounting medium (Vector laboratories, Inc. Burlingame, CA), and stored in 4°C for further fluorescence analysis. Tissue for western blotting was snap frozen in liquid nitrogen and stored at -80°C.

6.1.7 Filopodia quantification

Transgenic mouse line L15 overexpressing membrane-targeted green fluorescent protein (GFP), under the control of Thy 1 promoter, was used to visualize dendritic filopodia. Acute hippocampal slices were prepared as described in section 5.1.4. Using a 100x objective of confocal microscope (Leica SP1) serial images of secondary apical dendrites of hippocampal CA1 pyramidal neurons were taken at z-steps of 0.12 µm. Only healthy looking, complete dendrites that could be tracked back to the cell body were analyzed. All images were reconstructed into 3D using the Surpass Volume mode in the Imaris software (Bitplane AG). Filopodia were counted over a length of 30-40 µm along 27-40 independent secondary apical dendrites (~1 mm in total length) from three independent experiments. Dendritic filopodia were identified according to the morphological criteria established by (Grutzendler et al 2002). A detailed description can be found in section 1.3.1. Counting of filopodia was done blind with respect to conditions and genotype.

6.1.8 Statistics

Data from at least three independent experiments were collected and expressed as mean ± standard error mean (SEM). All data were tested for significance using ANOVA Turkey's post hoc test.

6.2 Behavioral studies

Prior to any behavioral procedures, mice were transported from the mouse housing facility to the separate room (vivarium), where they stayed for the duration of the behavioral experiments. Mice were kept under reverse 12 h light/dark conditions with a constant room temperature in the Mouse IVC Green Line system (Tecniplast, USA) with a single cage air supply. Cages were changed every second week and access to water and food was checked at least twice per week. Before the first test was initiated, the animals were allowed to habituate for at least one week to their new environment. If not specified in particular experiments, food and water were available *ad libidum.* All tests were conducted during the dark phase of the cycle and repeated every day at the same time.

6.2.1 Locomotor activity

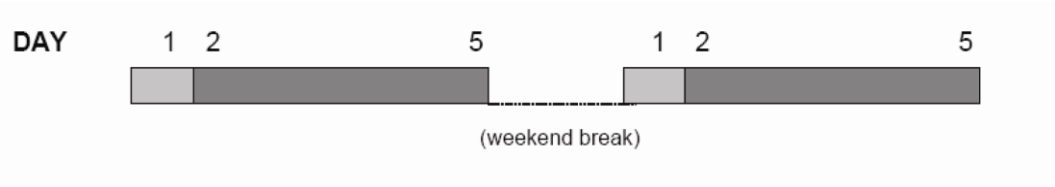

Fig. 5.2 Activiscope protocol

The light gray rectangles represent the first day of experimentation, and were treated as habituation period. The dark gray rectangles stand for the next consecutive four days of the test.

During the experiment, mice were housed in individual cages in a separate room with reverse day/night cycle (vivarium). An infrared sensor was mounted above each cage to register animal movement (ACTIVISCOPE, NewBehavior AG, Zürich, Switzerland). The sensor was able to register activity across the metal cage grid. Paper houses were removed from the cages for the duration of the experiment to avoid signal disturbance. Ambient light changes as well as room temperature were recorded. Activity was registered for 5 consecutive days during the week period and mice went back to their vivarium over the weekend. After the weekend, the recording was repeated for the next 5 days. General locomotor activity was calculated as the average of two runs, starting from day 2 until day 5. Day 1 of the experiment was treated as the habituation period and was not included into statistical analysis. The described protocol was developed and is commonly used in the Anatomy Institute, University of Zurich.

6.2.2 Rotarod task

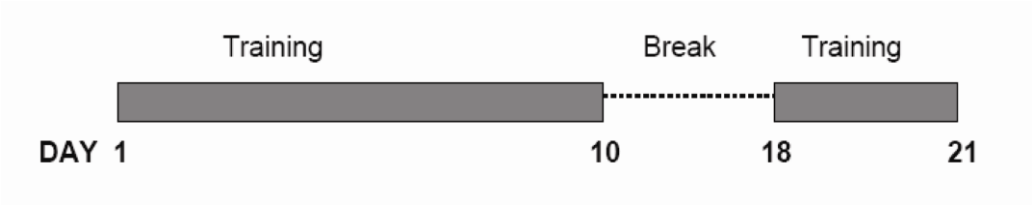

Fig. 5.3 Rotarod protocol

The first larger rectangle represents the early training phase, consisting of ten days. The second smaller rectangle represents subsequent training sessions covering four consecutive days. The dotted line between the two training sessions stands for the one-week break.

A five-line rotarod (TSA System GmbH, Germany) with an acceleration capability was used. The apparatus consisted of a 20 cm raised drum split into five separate compartments. Only three out of five lines were simultaneously occupied. The surface of the rod was covered with rubber matting to prevent slippage and provide enhanced grip for mice. During the first day, before the initial trial, the animals were allowed to stay on the stationary rod for 2min. This habituation trial was repeated if necessary. Mice were gently taken by the tails, transported from their cages and placed on the rod (three animals at a time). When all three mice were stable on the rod, rotation and recording was simultaneously started. One session consisted of 10 trials with a 5-6 min break in between. During the break, animals were placed in their separate waiting cages. Each trial started with a drum velocity of 4 rpm and constant acceleration of 0.1 rpm was applied until a maximum velocity of 30 rpm. A single trial was finished after 300 sec or until the mouse fell off the rod, which activated a photocell beam that stopped rotation. A light-beam sensor located below each compartment recorded the time and velocity of the drum when a mouse fell down. Latency to fall was recorded by TSA Rotarod System V 4.0.9. Changes between trials provided information on within session learning.

To test improvement between sessions, mice were trained for 7 consecutive days/sessions. All mice were retested for an additional 2 days after a 7 day break. This gap between two training phases allowed for observation of possible changes concerning memory consolidation. In the second version of this protocol, training was prolonged to 10 constitutive days and mice were retested for 4 additional days, with a 7 day break in between. Body weight was recorded one day prior to the first trial and rechecked on the last day of the test. Protocol was adapted to the mouse conditions from (Buitrago et al 2004b).

6.2.3 Grip strength test

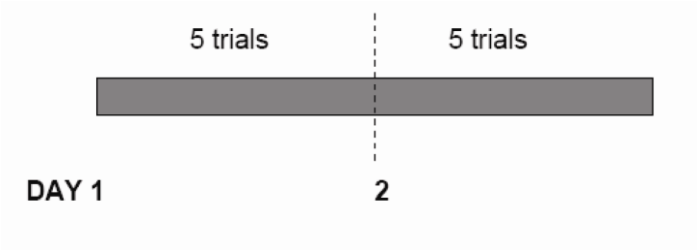

Fig. 5.4 Grip strength test protocol

The dark gray rectangle represents two consecutive days testing. Five trials were performed each day.

Self-made apparatus, composed of a grip strength meter mounted in the horizontal position to a stable foundation was used to rate the strength of the front paws. To facilitate grip, the apparatus was provided with an additional handle. For the test, a mouse was taken by the tail and gently brought closer to the handle. As soon as the animal had grabbed the handle with two front paws, the mouse was slowly and with minimal force pulled away by the tail until it released the grip. The force applied to the handle at the moment of the grasp release was recorded. Only trials with mice holding the handle correctly were taken into account. In the case of incorrect grabbing, the trials were repeated until five correct grasps were registered.

Each animal participated in 5 trials for 2 consecutive days. Body weigh was recorded one day prior to the test. The same mice, which took part in the rotarod test, were tested for the grip strength. Results were presented as means from all trials over two days. No difference between days was noted. Protocol was developed and used in the Anatomy Institute, University of Zurich.

6.2.4 Morris water maze

In all versions of the experiment a 150 cm diameter white polypropylene swim tank was used. The maze was filled with 25°C warm water, until a depth of approximately 15 cm, and made opaque by adding 2 l of milk. The water in the pool was filled and drained daily. A video camera was placed above the center of the pool to register images of swimming animals. Mice were trained to escape from the pool by locating a quadratic goal platform (14 x 14 cm) made of wire mesh hidden 1 cm below the surface. Latency to find the escape platform, swim path length and floating time were measured for all training trials. To interpret spatial aspects of behavior, the time in current goal quadrant, path efficiency

(%), distance to current goal and absolute direction error (°) were analyzed. All data were collected on the computer with running tracking system EthoVision 2.30 (Noldus Information Technology, Wageningen, The Netherlands). For each trial, the system recorded the xy position and object area. Collected raw data were transferred and analyzed using public software Wintrack 2.4 (by D.P. Wolfer).

6.2.4.1 Classical Morris water-maze

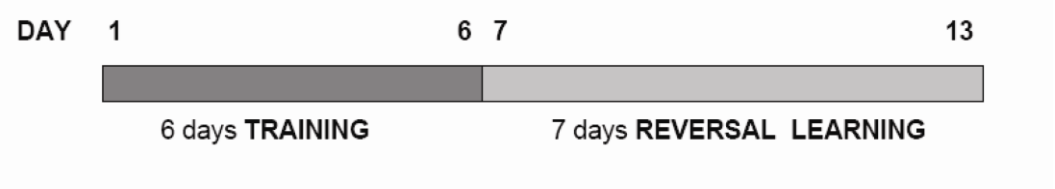

Fig. 5.6 Classical Morris water maze protocol

The dark gray rectangle represents six consecutive days of training and the light gray represents the next seven days of reversal learning.

In the classical Morris water maze experiment, animals swim to find a hidden platform. To locate the platform, mice used distant visual landmarks in the environment. Mice were divided into four groups (SW, SE, NE, NW), and each had to find the platform, which was located in a different position (Fig. 5.7). Four different target positions allowed observation of differences in place preferences resulting in goal placement, if any occurred. Animals were subjected to a series of 6 trials daily for 6 consecutive days using a semi-random start location. At the beginning of every trial, the animal was placed in the pool facing the wall of the tank in a white plastic cup. When the mouse found the platform it was removed from the maze using a wire mesh grid and placed in the cage under the heating lamp to avoid temperature shock. Mice were allowed to look for the platform for a maximum of 2 min. If they failed to find it they were removed from the water and placed in the cage.

Learning abilities were assessed by 6 daily trials for 4 constitutive days of reversal learning. In this experiment, the platform was moved to the opposite site. This revealed whether or not animals can extinguish their initial learning and acquire a direct path to the new goal. In the second version of this protocol, reversal learning was prolonged to 7 consecutive days in order to observe the exact differences during reversal learning. Protocol was

adapted for mice conditions from the rat place navigation study (Morris 1981). Protocol from the Anatomy Institute, University of Zurich was used.

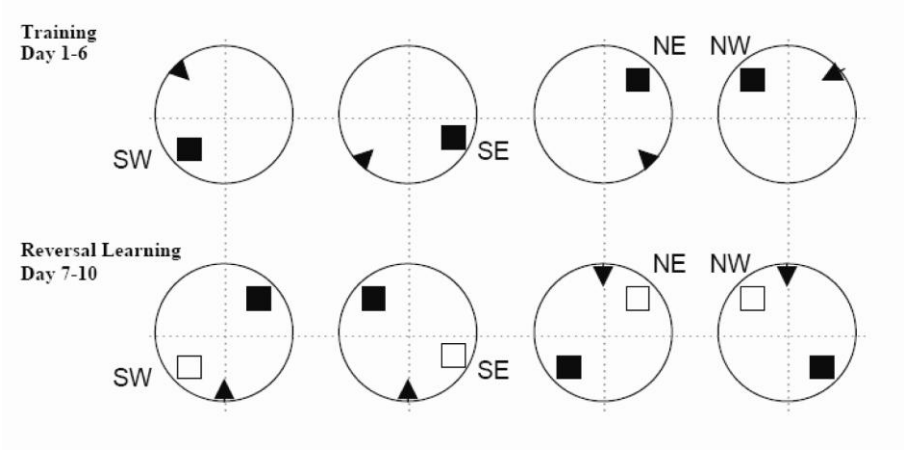

Fig. 5.7 All possible platform positions in the classical Morris water maze protocol

During training the platform (black square) remained in the same position for 6 consecutive days (days 1 - 6) only the start point (arrowhead) changed. During the following days (days 7 – 10), reversal learning took place. The platform was positioned at the opposite quarter of the tank (new position – black square, old position – white square).

6.2.4.2 Two-cue Morris water-maze

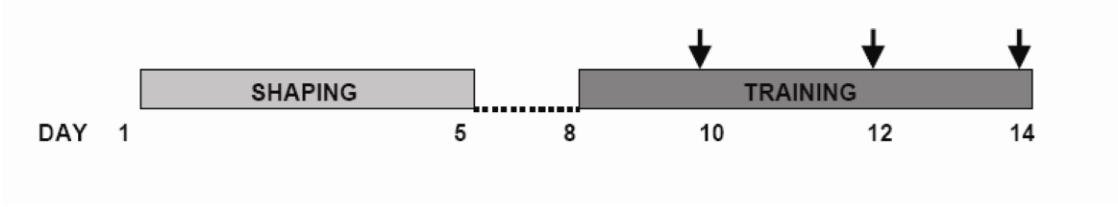

Fig. 5.8 2-cue Morris water maze protocol

The first light gray rectangle represents the shaping phase and the dark gray indicates the training period. Each arrow represents a single probe trial. The dotted line between shaping and training phases represents time without trials.

The 2-cue Morris water maze test was adapted from (Lee et al 2008). In this version of the test, a platform was marked by one of the cues. Cylinders (11 cm high, 2.5 cm in diameter) were painted gray, or with black and white vertical or horizontal stripes (1 cm width). All cylinders were manufactured in the Biochemistry Department workshop according to description by (Lee et al 2008). The first 5 constitutive days consisted of shaping this was necessary for the right performance during the 2-cue phase. On the first day, each mouse

was placed on the platform marked with the gray cylinder for 30 sec and returned to the cage. This procedure was repeated 4 times in every quadrant of the pool. For the next 4 days of shaping, 4 trials per day were performed. Animals were placed in the water opposite to the escape platform and allowed to find the marked platform on their own. Each animal was exposed to the platform once in each quadrant (NE, SE, NW, and SW) in pseudo-random order (Fig. 5.9). After 5 days of shaping, the mice were left in the vivarium for 2 days.

For the experiment, animals were divided into two groups, with either a vertical or a horizontal striped cylinder as the correct cue. This was done to avoid a higher preference by the animals for one of the cues. The escape platform was placed in the center of a quadrant and was marked by the stripes (the goal cue). The other striped cylinder (the lure cue) was placed in the adjacent quadrant. The lure cue didn't allow the animal to escape from the water. Animals were allowed to swim for a maximum of 2 min. They completed 4 trials per day for the next 7 days of the training. To assess acquisition of the task, 3 probe trials were performed on the fourth trial of days 10, 12 and 14. In the probe trial, cue location was determined exactly as in regular training but both cues were placed on the stands to prevent escape from the water. Search for the platform was allowed for 60 sec, after which the mouse was removed from the pool.

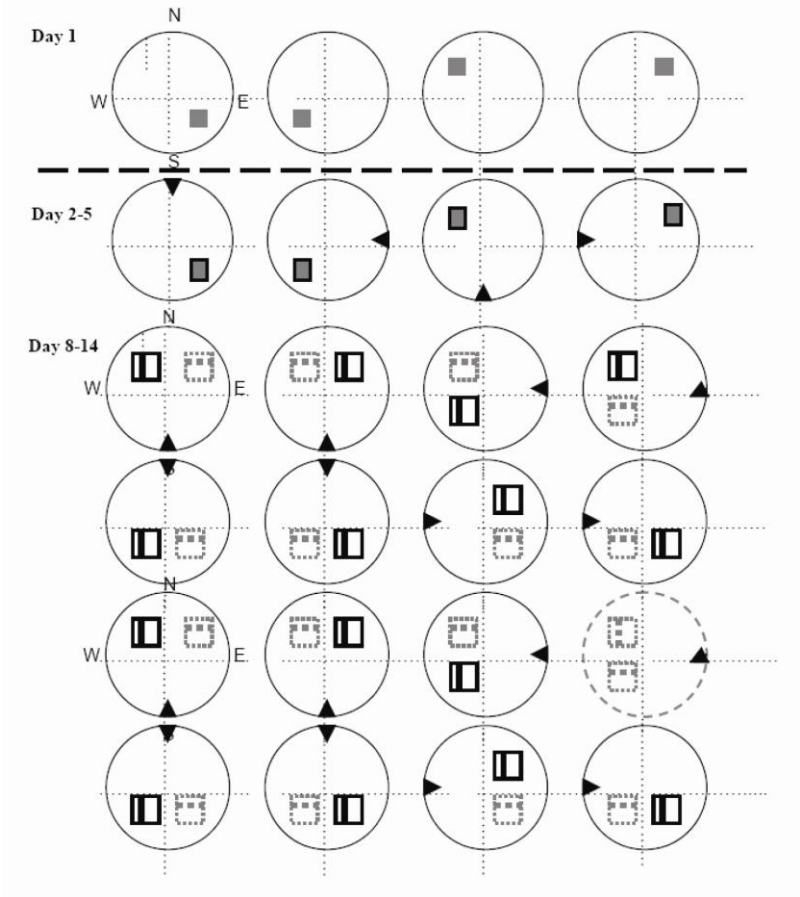

Fig. 5.9 All possible platform positions in the 2-cue Morris Water Maze

Each circle represents the water maze. Gray squares represent cylinders without stripes but with the platform, providing escape from the water. Correct goals are marked with black squares with vertical stripes. Doted squares stand for lure cues, cylinders with horizontal stripes without platforms. Black arrowheads are starting points. Dashed circles are a probe trial, which was repeated on day 10, 12 and 14.

6.2.5 Fear conditioning

The Fear Conditioning System (TSA, Bad Homburg, Germany) consisted of a soundproof test chamber (58 x 30 x 27 cm^3) equipped with a light, fan and a sound source. A small Plexiglas box (35 x 20 x 20 cm^3) with a shock grid was situated in the middle of the chamber. The grid was connected to a shock/scrambler unit providing an electric shock with adjusted intensity and duration. Photo cells automatically recorded mice motor behavior and video cameras monitored each mouse in the single unit. Auditory cue and footshock were delivered automatically, controlled by software. The training and context test were conducted in the same training chamber.

6.2.5.1 Classical fear conditioning

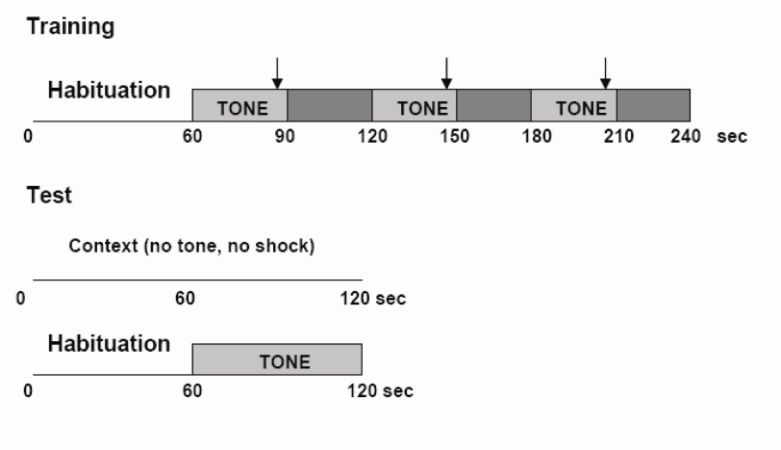

Fig. 5.10 Classical fear conditioning protocol

Each light rectangle represents time when tone was delivered to the mouse. The arrows indicate time point when footshock was received. Dark gray rectangles represent 30 sec break in between each tone/shock pairing.

On day 1 of conditioning training, each mouse was taken from its home cage and placed into the conditioning chamber. Animals were allowed to explore the environment for 60 sec. After that time, the auditory cue (92 Db conditioned stimulus (CS)) was delivered for 30 sec. During the last 2 sec of the tone, the unconditioned aversive stimulus (US), a mild footshock (0.25 mA) was received. This kind of pairing (tone + shock) was applied three times during a single session. Animals were left in the chamber for an additional 30 sec after the last pairing in order to create an association between the aversive stimulus and the properties of the chamber. The time spent freezing during the training

day was considered as a control measure of unconditioned fear. Freezing was defined as no movement other then respiratory.

Testing was performed on day 7, after a 6 days break, in order to observe long-term fear conditioning memory. Each mouse was placed in the same chamber for 2 min. No foot-shock or tone was administered. The number of seconds spent freezing in the same chamber was used as a measure of contextually conditioned fear. The second phase of testing consisted of placing animals in the same chamber but the inside had been changed in such a way that the animals would consider it a completely new environment. A Plexiglas plate was placed on the grid with some wood shavings and a big stone. The mouse was allowed to explore the new environment for 60 sec and then a 60 sec tone was delivered. Cued conditioning was calculated by comparing freezing time in the changed chamber in the presence of the cue with freezing time in the absence of the cue.

6.2.5.2 Fear Extinction

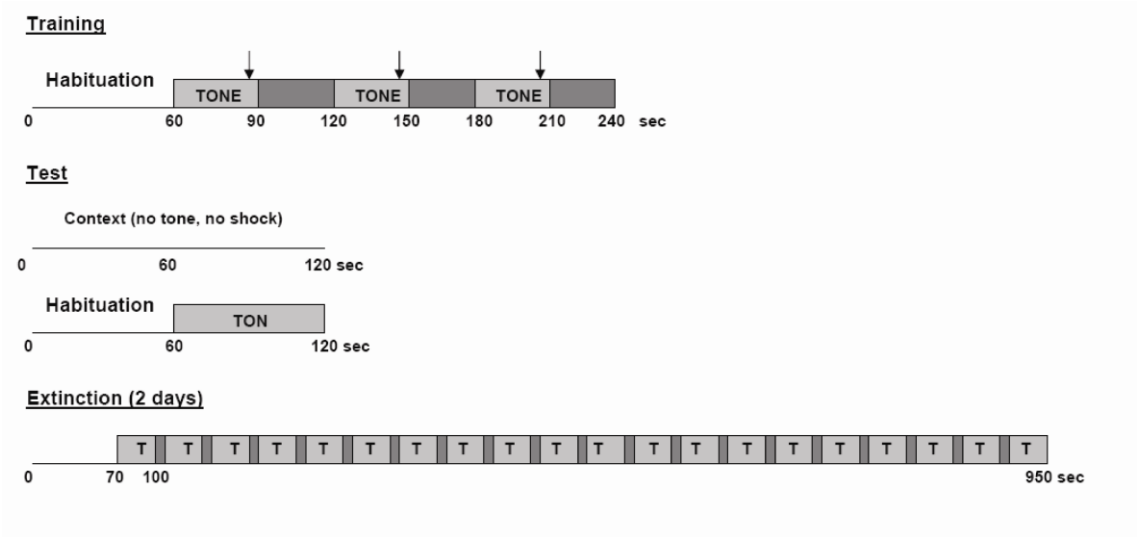

Fig. 5.11 Fear extinction protocol

Each light rectangle represents time when tone was delivered to the mouse. The arrows indicate time point when footshock was received. Dark gray rectangles represent 30 sec break in between each tone/shock pairing in the case of training phase. Small dark gray rectangles between 20 times tone repetitions represent 2 sec break.

The first part of the experiment: training and test were conducted according to the same protocol as *classical fear conditioning*. Fear extinction was performed on day 3 and 4,

without a break. Mice were placed in the same chamber, but with the inside changed so that mice would consider it a new environment. The Plexiglas plate was placed on the grid with some wooden shavings and a big stone. Animals were allowed to explore their new environment for the first 70 sec and then a 30 sec tone was delivered, and repeated 20 times with a 2 sec break in between. The same protocol was conducted on day 4.

6.2.6 Staircase test

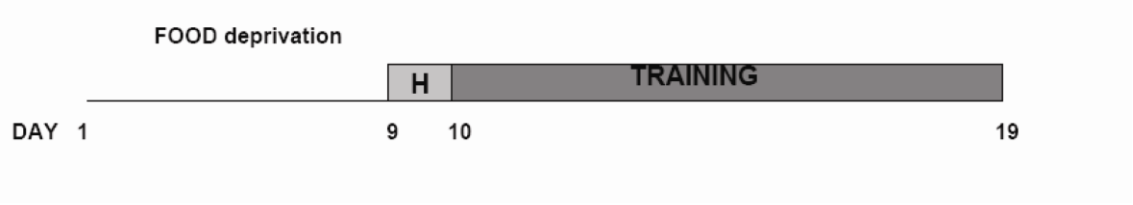

Fig. 5.12 Staircase protocol

The light gray rectangle represents one day of habituation procedure and the long dark one indicates ten days training phase.

The test was performed in 4 chambers (Lafayette Instrument Company Inc, USA) simultaneously. The apparatus is designed so that the central platform runs the full length of the corridor with a narrow space on both sides, into which a removable double staircase with eight steps on each side can be inserted. Each step has a small well were a sugar pellet can be placed. Mice can enter the corridor and reach down from the left side with the left paw and from the right side with the right paw. There was no possibility of the animal to turning around in the corridor and it must exit the corridor backwards. A small open compartment is situated at the beginning of the corridor. Due to the space limitation inside the chamber and to increase motivation, mice were food deprived until they reached 80-85% of their starting body weight. The quantity of received food was monitored to maintain a constant weight until the end of the experiment. During the last two days prior to the test, a maximum of 10 sugar pellets were placed in the home cage of each mouse to habituate them to the bait. On day 9, animals participated in a single habituation session. They were allowed to explore the chamber for 10 min. Sugar pellets were placed along the central platform, but no pellets were inserted in to the staircase well.

For the next 10 consecutive days, every mouse participated in a single 20 min session. The duration of a single session is important due to the typical mice behavior; mouse after grasping the sugar pellet to consume it, the mouse retreats to the small starting compart-

ment at the beginning of the corridor to consume the pellet. Each daily trial began by placing the animal into the starting compartment and inserting the removable baited double staircase (1 pellet per well). At the end of each session, pellets remaining in the well and knocked to the floor were counted. Body weight was monitored during the entire experiment. Mean over the eaten pellets was calculated across all days of the experiment. Number of missing pellets from day 10 was compared with the number on day 19. Protocol was adapted from (Baird et al 2001; Montoya et al 1991).

6.2.7 T-maze test

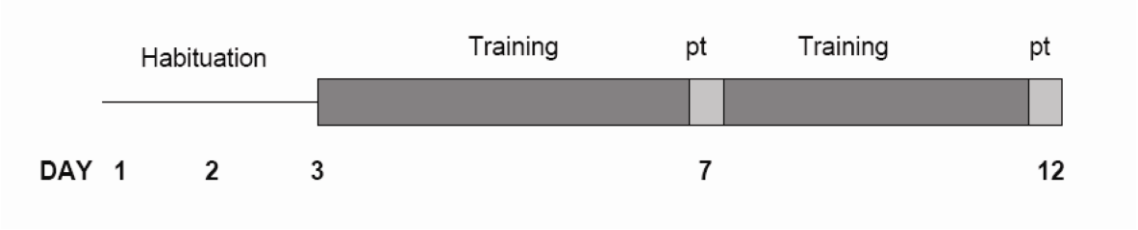

Fig. 5.13 T-maze protocol

The dark gray rectangles represent two training sessions ending with single probe trials (light gray rectangles).

The T-maze test was performed using the T-maze test package for mice (Med Associates Inc., St.Albans, Vermont, USA). Apparatus consisted of four modular mouse runways. Each runway was constructed of an easily cleaned white polypropylene floor with transparent polycarbonate walls and I/R photobeams sensors at both walls situated at the beginning of the arms. Two of the opposite arms ended with transparent start/goal boxes with the auto guillotine door. The two remaining opposite arms ended with head entry detectors and pellet dispensers. In the middle of the maze a modular mouse hub was situated that consisted of four exits/entries. During all trials, three of the doors were always open, the two pellet dispenser arms and one of the start/goal box arms.

Mice were food deprived until their body weight reduced to 80-85 % of their initial weight and were maintained at this level throughout the experiment. During two days of habituation time, animals were introduced into the maze. They were placed into the cross-maze in the start box and allowed to explore the area freely for 5 min. There were no food pellets in the maze during that time. For the next five consecutive days, mice were trained to traverse the maze, turn into the right arm and consume sugar pellets localized at the end of it. The first trial of each day contained a hint how to get to the proper arm of the maze in or-

der to get a reward. Four pellets were placed along the line, from the outside of the starting box until the end of the goal arm. During this first trial, in the case of an incorrect response, the mouse was allowed to trace back to the baited arm. The remaining four trials were carried out without any additional bait. The session was considered successfully terminated when the mouse reached the correct arm, poked its head into the head detector and activated the pellet dispenser within the specified time. When the animal's motion was not detected by any of the photosensors for longer than 1 min, the session was terminated and was considered as movement error. In the second version of the protocol, an additional possibility to end the trial was added. When the mouse chose the wrong arm and poked its head into the head detector in order to get a reward, the trial was finished and considered a decision error. Protocol was conducted in SOF-700RA-9 T-maze using training and testing software (Med Associates Inc., St.Albans, Vermont, USA), which was customized for our needs.

Each animal performed 5 trials per day with a 30 sec break in between. The surface of the maze was washed after each trial, in order to reduce the possibility of following their smell trace. On day 6, a single probe trial was performed. During this trial, the start box was situated on the opposite side to that used during the training. Mice had to perform exactly the same task, to find the correct arm but starting from the opposite direction. For the next five days, animals were trained again according to the previously described protocol and on day 12 they again performed the single probe trial. To check whether animals reached the level of overtraining, the following criteria were established:

- > 80% correct turns in average over 2 consecutive days
- overtraining until performance exceeded the criterion level in 10 consecutive days;

At the end of the experiment, data were transferred into an Excel file using SOF -731 Med-PC to Excel (Med Associates Inc., St.Albans, Vermont, USA). Protocol was adapted from (Packard & McGaugh 1996; Pittenger et al 2006).

6.2.8 Statistics

Behavioral data was analyzed for Univariate ANOVA (Field 2005) using SPSS-PASW Statistics version 18 (IBM, USA). Difference was considered to be significant at $P< 0.05$. All analysis was performed in consultation with a Prof. David Wolfer (Institute of Anatomy) and statistician Dr. Michal Okoniewski (Functional Genomic Centre Zurich).

7 References

Adams JA. 1971. A closed-loop theory of motor learning. *J Mot Behav* 3:111-49

Ader R, Cohen N. 1975. Behaviorally conditioned immunosuppression. *Psychosom Med* 37:333-40

Akaike M, Kato N, Ohno H, Kobayashi T. 1991. Hyperactivity and spatial maze learning impairment of adult rats with temporary neonatal hypothyroidism. *Neurotoxicol Teratol* 13:317-22

Albouy G, Sterpenich V, Balteau E, Vandewalle G, Desseilles M, et al. 2008. Both the hippocampus and striatum are involved in consolidation of motor sequence memory. *Neuron* 58:261-72

An XL, Zou JX, Wu RY, Yang Y, Tai FD, et al. 2011. Strain and Sex Differences in Anxiety-Like and Social Behaviors in C57BL/6J and BALB/cJ Mice. *Exp Anim* 60:111-23

Annies M, Bittcher G, Ramseger R, Loschinger J, Woll S, et al. 2006. Clustering transmembrane-agrin induces filopodia-like processes on axons and dendrites. *Mol Cell Neurosci* 31:515-24

Arikkath J. 2009. Regulation of dendrite and spine morphogenesis and plasticity by catenins. *Mol Neurobiol* 40:46-54

Auffret A, Gautheron V, Repici M, Kraftsik R, Mount HT, et al. 2009. Age-dependent impairment of spine morphology and synaptic plasticity in hippocampal CA1 neurons of a presenilin 1 transgenic mouse model of Alzheimer's disease. *J Neurosci* 29:10144-52

Bach ME, Barad M, Son H, Zhuo M, Lu YF, et al. 1999. Age-related defects in spatial memory are correlated with defects in the late phase of hippocampal long-term potentiation in vitro and are attenuated by drugs that enhance the cAMP signaling pathway. *Proc Natl Acad Sci U S A* 96:5280-5

Bagshaw MH, Benzies S. 1968. Multiple measures of the orienting reaction and their dissociation after amygdalectomy in monkeys. *Exp Neurol* 20:175-87

Baird AL, Meldrum A, Dunnett SB. 2001. The staircase test of skilled reaching in mice. *Brain Res Bull* 54:243-50

Barnes CA. 1999. Do synaptic markers provide a window on synaptic effectiveness in the aged hippocampus? *Neurobiol Aging* 20:349-51; discussion 59-60

Bartesaghi R, Raffi M, Severi S. 2003. Effects of early isolation on layer II neurons in the entorhinal cortex of the guinea pig. *Neuroscience* 120:721-32

Belzung C, Griebel G. 2001. Measuring normal and pathological anxiety-like behaviour in mice: a review. *Behav Brain Res* 125:141-9

Berger TW, Alger B, Thompson RF. 1976. Neuronal substrate of classical conditioning in the hippocampus. *Science* 192:483-5

Bezakova G, Ruegg MA. 2003. New insights into the roles of agrin. *Nat Rev Mol Cell Biol* 4:295-308

Black JE, Polinsky M, Greenough WT. 1989. Progressive failure of cerebral angiogenesis supporting neural plasticity in aging rats. *Neurobiol Aging* 10:353-8

Bliss TV, Gardner-Medwin AR. 1973. Long-lasting potentiation of synaptic transmission in the dentate area of the unanaestetized rabbit following stimulation of the perforant path. *J Physiol* 232:357-74

Blitzer RD, Wong T, Nouranifar R, Iyengar R, Landau EM. 1995. Postsynaptic cAMP pathway gates early LTP in hippocampal CA1 region. *Neuron* 15:1403-14

Bogdanovich S, McNally EM, Khurana TS. 2008. Myostatin blockade improves function but not histopathology in a murine model of limb-girdle muscular dystrophy 2C. *Muscle Nerve* 37:308-16

Bohlen M, Cameron A, Metten P, Crabbe JC, Wahlsten D. 2009. Calibration of rotational acceleration for the rotarod test of rodent motor coordination. *J Neurosci Methods* 178:10-4

Bose CM, Qiu D, Bergamaschi A, Gravante B, Bossi M, et al. 2000. Agrin controls synaptic differentiation in hippocampal neurons. *J Neurosci* 20:9086-95

Bourne HR, Nicoll R. 1993. Molecular machines integrate coincident synaptic signals. *Cell* 72 Suppl:65-75

Bourne JN, Harris KM. 2008. Balancing structure and function at hippocampal dendritic spines. *Annu Rev Neurosci* 31:47-67

Bradley H. Smith BSGM, William E. Pelham. 2002. The Clinically Meaningful Link Between Alcohol Use and Attention Deficit Hyperactivity Disorder. *Alcohol Research & Health* 26:122-9

Brindle PK, Montminy MR. 1992. The CREB family of transcription activators. *Curr Opin Genet Dev* 2:199-204

Buitrago MM, Ringer T, Schulz JB, Dichgans J, Luft AR. 2004a. Characterization of motor skill and instrumental learning time scales in a skilled reaching task in rat. *Behav Brain Res* 155:249-56

Buitrago MM, Schulz JB, Dichgans J, Luft AR. 2004b. Short and long-term motor skill learning in an accelerated rotarod training paradigm. *Neurobiol Learn Mem* 81:211-6

Burden SJ, Sargent PB, McMahan UJ. 1979. Acetylcholine receptors in regenerating muscle accumulate at original synaptic sites in the absence of the nerve. *J Cell Biol* 82:412-25

Burgess RW, Skarnes WC, Sanes JR. 2000. Agrin isoforms with distinct amino termini: differential expression, localization, and function. *J Cell Biol* 151:41-52

Butz M, Worgotter F, van Ooyen A. 2009. Activity-dependent structural plasticity. *Brain Res Rev* 60:287-305

Cajal Ry. 1893. Neue Darstellung vom Histologischen Bau des Centralnervensystems. *Archiv fur Anatomie und Entwickelungsgeschichte* Anatomische Abtheilung des Archives fur Anatome und Physiologie 319-428

Calabrese B, Wilson MS, Halpain S. 2006. Development and regulation of dendritic spine synapses. *Physiology (Bethesda)* 21:38-47

Calabresi P, Napolitano M, Centonze D, Marfia GA, Gubellini P, et al. 2000. Tissue plasminogen activator controls multiple forms of synaptic plasticity and memory. *Eur J Neurosci* 12:1002-12

Carlsson A. 1978. Age-dependent changes in central dopaminergic and other monoaminergic systems. *Adv Exp Med Biol* 113:1-13

Cavus I, Teyler T. 1996. Two forms of long-term potentiation in area CA1 activate different signal transduction cascades. *J Neurophysiol* 76:3038-47

Collen D, Schlott B, Engelborghs Y, Van Hoef B, Hartmann M, et al. 1993. On the mechanism of the activation of human plasminogen by recombinant staphylokinase. *J Biol Chem* 268:8284-9

Collingridge GL KS, McLennam H. . 1983. Activation of NMDA receptors blocks GABAergic inhibition in an in vitro model of epilepsy. *J Physiol.* 344

Comery TA, Harris JB, Willems PJ, Oostra BA, Irwin SA, et al. 1997. Abnormal dendritic spines in fragile X knockout mice: maturation and pruning deficits. *Proc Natl Acad Sci U S A* 94:5401-4

Cooke SF, Bliss TV. 2006. Plasticity in the human central nervous system. *Brain* 129:1659-73

Corbit LH, Balleine BW. 2000. The role of the hippocampus in instrumental conditioning. *J Neurosci* 20:4233-9

Costa RM, Cohen D, Nicolelis MA. 2004. Differential corticostriatal plasticity during fast and slow motor skill learning in mice. *Curr Biol* 14:1124-34

Countryman RA, Gold PE. 2007. Rapid forgetting of social transmission of food preferences in aged rats: relationship to hippocampal CREB activation. *Learn Mem* 14:350-8

Crawley J, Goodwin FK. 1980. Preliminary report of a simple animal behavior model for the anxiolytic effects of benzodiazepines. *Pharmacol Biochem Behav* 13:167-70

Criscimagna-Hemminger SE, Shadmehr R. 2008. Consolidation patterns of human motor memory. *J Neurosci* 28:9610-8

Cutler NR, Duara R, Creasey H, Grady CL, Haxby JV, et al. 1984. Brain Imaging - Aging and Dementia. *Ann Intern Med* 101:355-69

d'Houtaud S, Sztermer E, Buffenoir K, Giot JP, Wager M, et al. 2009. [Synapse formation and regeneration]. *Neurochirurgie* 55 Suppl 1:S49-62

Dash PK, Hochner B, Kandel ER. 1990. Injection of the cAMP-responsive element into the nucleus of Aplysia sensory neurons blocks long-term facilitation. *Nature* 345:718-21

De Paola V, Arber S, Caroni P. 2003. AMPA receptors regulate dynamic equilibrium of presynaptic terminals in mature hippocampal networks. *Nat Neurosci* 6:491-500

De Paola V, Holtmaat A, Knott G, Song S, Wilbrecht L, et al. 2006. Cell type-specific structural plasticity of axonal branches and boutons in the adult neocortex. *Neuron* 49:861-75

De Strooper B, Saftig P, Craessaerts K, Vanderstichele H, Guhde G, et al. 1998. Deficiency of presenilin-1 inhibits the normal cleavage of amyloid precursor protein. *Nature* 391:387-90

DeChiara TM, Bowen DC, Valenzuela DM, Simmons MV, Poueymirou WT, et al. 1996. The receptor tyrosine kinase MuSK is required for neuromuscular junction formation in vivo. *Cell* 85:501-12

Dekaban AS. 1978. Changes in brain weights during the span of human life: relation of brain weights to body heights and body weights. *Ann Neurol* 4:345-56

Devan BD, McDonald RJ, White NM. 1999. Effects of medial and lateral caudate-putamen lesions on place- and cue-guided behaviors in the water maze: relation to thigmotaxis. *Behav Brain Res* 100:5-14

Devenport L, Hill T, Wilson M, Ogden E. 1997. Tracking and averaging in variable environments: A transition rule. *J Exp Psychol Anim B* 23:450-60

Dickinson A, Balleine B. 1994. Motivational Control of Goal-Directed Action. *Anim Learn Behav* 22:1-18

Diekelmann S, Born J. 2010. The memory function of sleep. *Nat Rev Neurosci* 11:114-26

Diekelmann S, Wilhelm I, Born J. 2009. The whats and whens of sleep-dependent memory consolidation. *Sleep Med Rev* 13:309-21

Donald LT, Schmidt, R.P. 1999. *Motor control and learning emphasis*: Champaign, IL: Human Kinetics

Doyon J, Benali H. 2005. Reorganization and plasticity in the adult brain during learning of motor skills. *Curr Opin Neurobiol* 15:161-7

Dugbartey AT. 1998. Neurocognitive aspects of hypothyroidism. *Arch Intern Med* 158:1413-8

Dunaevsky A, Mason CA. 2003. Spine motility: a means towards an end? *Trends Neurosci* 26:155-60

Enari M, Sakahira H, Yokoyama H, Okawa K, Iwamatsu A, Nagata S. 1998. A caspase-activated DNase that degrades DNA during apoptosis, and its inhibitor ICAD. *Nature* 391:43-50

Engert F, Bonhoeffer T. 1999. Dendritic spine changes associated with hippocampal long-term synaptic plasticity. *Nature* 399:66-70

Everitt BJ, Dickinson A, Robbins TW. 2001. The neuropsychological basis of addictive behaviour. *Brain Res Brain Res Rev* 36:129-38

Ferreira TL, Moreira KM, Ikeda DC, Bueno OF, Oliveira MG. 2003. Effects of dorsal striatum lesions in tone fear conditioning and contextual fear conditioning. *Brain Res* 987:17-24

Fiala JC, Feinberg M, Popov V, Harris KM. 1998. Synaptogenesis via dendritic filopodia in developing hippocampal area CA1. *J Neurosci* 18:8900-11

Field A. 2005. *Discovering Statistics using SPSS*. London. 817 pp.

Fiumelli H, Jabaudon D, Magistretti PJ, Martin JL. 1999. BDNF stimulates expression, activity and release of tissue-type plasminogen activator in mouse cortical neurons. *Eur J Neurosci* 11:1639-46

Fricker RA, Annett LE, Torres EM, Dunnett SB. 1996. The placement of a striatal ibotenic acid lesion affects skilled forelimb use and the direction of drug-induced rotation. *Brain Res Bull* 41:409-16

Frischknecht R, Fejtova A, Viesti M, Stephan A, Sonderegger P. 2008. Activity-induced synaptic capture and exocytosis of the neuronal serine protease neurotrypsin. *J Neurosci* 28:1568-79

Gaffan D. 1994. Dissociated effects of perirhinal cortex ablation, fornix transection and amygdalectomy: evidence for multiple memory systems in the primate temporal lobe. *Exp Brain Res* 99:411-22

Garner CC, Zhai RG, Gundelfinger ED, Ziv NE. 2002. Molecular mechanisms of CNS synaptogenesis. *Trends Neurosci* 25:243-51

Gautam M, Noakes PG, Moscoso L, Rupp F, Scheller RH, et al. 1996. Defective neuromuscular synaptogenesis in agrin-deficient mutant mice. *Cell* 85:525-35

Gheysen F, Van Opstal F, Roggeman C, Van Waelvelde H, Fias W. 2010. Hippocampal contribution to early and later stages of implicit motor sequence learning. *Experimental Brain Research* 202:795-807

Gholamrezaei G, Whishaw IQ. 2009. Individual differences in skilled reaching for food related to increased number of gestures: evidence for goal and habit learning of skilled reaching. *Behavioral Neuroscience* 123:863-74

Giese KP, Fedorov NB, Filipkowski RK, Silva AJ. 1998. Autophosphorylation at Thr286 of the alpha calcium-calmodulin kinase II in LTP and learning. *Science* 279:870-3

Gilbert ME. 2004. Alterations in synaptic transmission and plasticity in area CA1 of adult hippocampus following developmental hypothyroidism. *Brain Res Dev Brain Res* 148:11-8

Gingras J, Rassadi S, Cooper E, Ferns M. 2007. Synaptic transmission is impaired at neuronal autonomic synapses in agrin-null mice. *Dev Neurobiol* 67:521-34

Gingrich MB, Traynelis SF. 2000. Serine proteases and brain damage - is there a link? *Trends Neurosci* 23:399-407

Glass DJ, Bowen DC, Stitt TN, Radziejewski C, Bruno J, et al. 1996. Agrin acts via a MuSK receptor complex. *Cell* 85:513-23

Glickstein M. 1992. The cerebellum and motor learning. *Curr Opin Neurobiol* 2:802-6

Gonzalez GA, Montminy MR. 1989. Cyclic AMP stimulates somatostatin gene transcription by phosphorylation of CREB at serine 133. *Cell* 59:675-80

Grant SG, O'Dell TJ, Karl KA, Stein PL, Soriano P, Kandel ER. 1992. Impaired long-term potentiation, spatial learning, and hippocampal development in fyn mutant mice. *Science* 258:1903-10

Graybiel AM. 2008. Habits, rituals, and the evaluative brain. *Annu Rev Neurosci* 31:359-87

Grutzendler J, Kasthuri N, Gan WB. 2002. Long-term dendritic spine stability in the adult cortex. *Nature* 420:812-6

Gschwend TP, Krueger SR, Kozlov SV, Wolfer DP, Sonderegger P. 1997. Neurotrypsin, a novel multidomain serine protease expressed in the nervous system. *Mol Cell Neurosci* 9:207-19

Hall SS, Burns DD, Lightbody AA, Reiss AL. 2008. Longitudinal changes in intellectual development in children with Fragile X syndrome. *J Abnorm Child Psychol* 36:927-39

Hanlon FM, Sutherland RJ. 2000. Changes in adult brain and behavior caused by neonatal limbic damage: implications for the etiology of schizophrenia. *Behav Brain Res* 107:71-83

Hannon R, Bader A. 1974. A comparison of frontal pole, anterior median and caudate nucleus lesions in the rat. *Physiol Behav* 13:513-21

Hanse E, Gustafsson B. 1994. TEA elicits two distinct potentiations of synaptic transmission in the CA1 region of the hippocampal slice. *J Neurosci* 14:5028-34

Hariri AR, Mattay VS, Tessitore A, Kolachana B, Fera F, et al. 2002. Serotonin transporter genetic variation and the response of the human amygdala. *Science* 297:400-3

Harris KM, Jensen FE, Tsao B. 1992. Three-dimensional structure of dendritic spines and synapses in rat hippocampus (CA1) at postnatal day 15 and adult ages: implications for the maturation of synaptic physiology and long-term potentiation. *J Neurosci* 12:2685-705

Harris KM, Kater SB. 1994. Dendritic spines: cellular specializations imparting both stability and flexibility to synaptic function. *Annu Rev Neurosci* 17:341-71

Harro J, Kiivet RA, Lang A, Vasar E. 1990. Rats with anxious or non-anxious type of exploratory behaviour differ in their brain CCK-8 and benzodiazepine receptor characteristics. *Behav Brain Res* 39:63-71

Hauptmann B, Karni A. 2002. From primed to learn: the saturation of repetition priming and the induction of long-term memory. *Brain Res Cogn Brain Res* 13:313-22

Hawkins CJ. 1897. Experiments on Memory Types. *Psychological Review* 4:289-94

Hawkins RD, Abrams TW, Carew TJ, Kandel ER. 1983. A cellular mechanism of classical conditioning in Aplysia: activity-dependent amplification of presynaptic facilitation. *Science* 219:400-5

Hebb D. 1994. Organization of Behavior. *New York: Wiley*

Henderson JM, Annett LE, Ryan LJ, Chiang W, Hidaka S, et al. 1999. Subthalamic nucleus lesions induce deficits as well as benefits in the hemiparkinsonian rat. *Eur J Neurosci* 11:2749-57

Hering H, Sheng M. 2001. Dendritic spines: structure, dynamics and regulation. *Nat Rev Neurosci* 2:880-8

Herry C, Ferraguti F, Singewald N, Letzkus JJ, Ehrlich I, Luthi A. 2010. Neuronal circuits of fear extinction. *Eur J Neurosci* 31:599-612

Hessl D, Nguyen DV, Green C, Chavez A, Tassone F, et al. 2009. A solution to limitations of cognitive testing in children with intellectual disabilities: the case of fragile X syndrome. *J Neurodev Disord* 1:33-45

Hilgenberg LG, Su H, Gu H, O'Dowd DK, Smith MA. 2006. Alpha3Na+/K+-ATPase is a neuronal receptor for agrin. *Cell* 125:359-69

Holtmaat A, De Paola V, Wilbrecht L, Knott GW. 2008. Imaging of experience-dependent structural plasticity in the mouse neocortex in vivo. *Behav Brain Res* 192:20-5

Holtmaat A, Wilbrecht L, Knott GW, Welker E, Svoboda K. 2006. Experience-dependent and cell-type-specific spine growth in the neocortex. *Nature* 441:979-83

Holtmaat AJ, Trachtenberg JT, Wilbrecht L, Shepherd GM, Zhang X, et al. 2005. Transient and persistent dendritic spines in the neocortex in vivo. *Neuron* 45:279-91

Huang YY, Malenka RC. 1993. Examination of TEA-induced synaptic enhancement in area CA1 of the hippocampus: the role of voltage-dependent Ca2+ channels in the induction of LTP. *J Neurosci* 13:568-76

Huber KM, Mauk MD, Kelly PT. 1995. Distinct LTP induction mechanisms: contribution of NMDA receptors and voltage-dependent calcium channels. *J Neurophysiol* 73:270-9

Hyman SE, Malenka RC, Nestler EJ. 2006. Neural mechanisms of addiction: the role of reward-related learning and memory. *Annu Rev Neurosci* 29:565-98

Iannacone EA, Yan AW, Gauger KJ, Dowling AL, Zoeller RT. 2002. Thyroid hormone exerts site-specific effects on SRC-1 and NCoR expression selectively in the neonatal rat brain. *Mol Cell Endocrinol* 186:49-59

Ingram DK, London ED, Reynolds MA, Waller SB, Goodrick CL. 1981. Differential effects of age on motor performance in two mouse strains. *Neurobiol Aging* 2:221-7

Irwin SA, Patel B, Idupulapati M, Harris JB, Crisostomo RA, et al. 2001. Abnormal dendritic spine characteristics in the temporal and visual cortices of patients with fragile-X syndrome: a quantitative examination. *Am J Med Genet* 98:161-7

Izquierdo I, Barros DM, Mello e Souza T, de Souza MM, Izquierdo LA, Medina JH. 1998. Mechanisms for memory types differ. *Nature* 393:635-6

Izquierdo I, Bevilaqua LR, Rossato JI, Bonini JS, Da Silva WC, et al. 2006. The connection between the hippocampal and the striatal memory systems of the brain: a review of recent findings. *Neurotox Res* 10:113-21

Johnston MV. 2004. Clinical disorders of brain plasticity. *Brain Dev* 26:73-80

Johnston MV, Nishimura A, Harum K, Pekar J, Blue ME. 2001. Sculpting the developing brain. *Adv Pediatr* 48:1-38

Jones KL. 2003. From recognition to responsibility: Josef Warkany, David Smith, and the fetal alcohol syndrome in the 21st century. *Birth Defects Res A Clin Mol Teratol* 67:13-20

Jontes JD, Smith SJ. 2000. Filopodia, spines, and the generation of synaptic diversity. *Neuron* 27:11-4

Joseph JA, Berger RE, Engel BT, Roth GS. 1978. Age-related changes in the nigrostriatum: a behavioral and biochemical analysis. *J Gerontol* 33:643-9

Ju W, Morishita W, Tsui J, Gaietta G, Deerinck TJ, et al. 2004. Activity-dependent regulation of dendritic synthesis and trafficking of AMPA receptors. *Nat Neurosci* 7:244-53

Karni A, Meyer G, Rey-Hipolito C, Jezzard P, Adams MM, et al. 1998. The acquisition of skilled motor performance: Fast and slow experience-driven changes in primary motor cortex. *P Natl Acad Sci USA* 95:861-8

Kerr AL, Steuer EL, Pochtarev V, Swain RA. 2010. Angiogenesis but not neurogenesis is critical for normal learning and memory acquisition. *Neuroscience* 171:214-26

Kim N, Stiegler AL, Cameron TO, Hallock PT, Gomez AM, et al. 2008. Lrp4 is a receptor for Agrin and forms a complex with MuSK. *Cell* 135:334-42

Knott GW, Holtmaat A, Wilbrecht L, Welker E, Svoboda K. 2006. Spine growth precedes synapse formation in the adult neocortex in vivo. *Nat Neurosci* 9:1117-24

Kogan JH, Frankland PW, Blendy JA, Coblentz J, Marowitz Z, et al. 1997. Spaced training induces normal long-term memory in CREB mutant mice. *Curr Biol* 7:1-11

Kojima N, Shirao T, Obata K. 1993. Molecular cloning of a developmentally regulated brain protein, chicken drebrin A and its expression by alternative splicing of the drebrin gene. *Brain Res Mol Brain Res* 19:101-14

Kopec CD, Li B, Wei W, Boehm J, Malinow R. 2006. Glutamate receptor exocytosis and spine enlargement during chemically induced long-term potentiation. *J Neurosci* 26:2000-9

Ksiazek I, Burkhardt C, Lin S, Seddik R, Maj M, et al. 2007. Synapse loss in cortex of agrin-deficient mice after genetic rescue of perinatal death. *J Neurosci* 27:7183-95

Laemmli UK. 1970. Cleavage of structural proteins during the assembly of the head of bacteriophage T4. *Nature* 227:680-5

Lanuza GM, Gosgnach S, Pierani A, Jessell TM, Goulding M. 2004. Genetic identification of spinal interneurons that coordinate left-right locomotor activity necessary for walking movements. *Neuron* 42:375-86

Larsen JO, Skalicky M, Viidik A. 2000. Does long-term physical exercise counteract age-related Purkinje cell loss? A stereological study of rat cerebellum. *J Comp Neurol* 428:213-22

Lee AS, Duman RS, Pittenger C. 2008. A double dissociation revealing bidirectional competition between striatum and hippocampus during learning. *Proc Natl Acad Sci U S A* 105:17163-8

Lepicard EM, Venault P, Negroni J, Perez-Diaz F, Joubert C, et al. 2003. Posture and balance responses to a sensory challenge are related to anxiety in mice. *Psychiatry Res* 118:273-84

Ling J, Heffernan TM, Luczakiewicz K, Stephens R. 2010. Subjective ratings of prospective memory deficits in chronic alcohol users. *Psychol Rep* 106:905-17

Lohmann C, Bonhoeffer T. 2008. A role for local calcium signaling in rapid synaptic partner selection by dendritic filopodia. *Neuron* 59:253-60

Luzhkov VB, Aqvist J. 2001. Mechanisms of tetraethylammonium ion block in the KcsA potassium channel. *FEBS Lett* 495:191-6

Lynch MA. 2004. Long-term potentiation and memory. *Physiol Rev* 84:87-136

M.F. Bear BWC, M.A. Paradiso. 2007. *Neuroscience: Exploring the Brain*: Lippincott Williams & Wilkins

M.L.P. F. 1830. Experiences sur les canaux semicirculares de l`oreille. *MemAcadSci* 9:455-75

Majewska AK, Newton JR, Sur M. 2006. Remodeling of synaptic structure in sensory cortical areas in vivo. *J Neurosci* 26:3021-9

Malenka RC, Bear MF. 2004. LTP and LTD: an embarrassment of riches. *Neuron* 44:5-21

Malenka RC, Kauer JA, Perkel DJ, Mauk MD, Kelly PT, et al. 1989. An essential role for postsynaptic calmodulin and protein kinase activity in long-term potentiation. *Nature* 340:554-7

Malenka RC, Lancaster B, Zucker RS. 1992. Temporal limits on the rise in postsynaptic calcium required for the induction of long-term potentiation. *Neuron* 9:121-8

Malenka RC, Nicoll RA. 1999. Long-term potentiation--a decade of progress? *Science* 285:1870-4

Maletic-Savatic M, Malinow R, Svoboda K. 1999. Rapid dendritic morphogenesis in CA1 hippocampal dendrites induced by synaptic activity. *Science* 283:1923-7

Malinow R, Schulman H, Tsien RW. 1989. Inhibition of postsynaptic PKC or CaMKII blocks induction but not expression of LTP. *Science* 245:862-6

Maren S, Aharonov G, Fanselow MS. 1997. Neurotoxic lesions of the dorsal hippocampus and Pavlovian fear conditioning in rats. *Behav Brain Res* 88:261-74

Matsumoto-Miyai K, Ninomiya A, Yamasaki H, Tamura H, Nakamura Y, Shiosaka S. 2003. NMDA-dependent proteolysis of presynaptic adhesion molecule L1 in the hippocampus by neuropsin. *J Neurosci* 23:7727-36

Matsumoto-Miyai K, Sokolowska E, Zurlinden A, Gee CE, Luscher D, et al. 2009. Coincident pre- and postsynaptic activation induces dendritic filopodia via neurotrypsin-dependent agrin cleavage. *Cell* 136:1161-71

Matsuzaki M, Honkura N, Ellis-Davies GC, Kasai H. 2004. Structural basis of long-term potentiation in single dendritic spines. *Nature* 429:761-6

Matus A. 2005. Growth of dendritic spines: a continuing story. *Curr Opin Neurobiol* 15:67-72

McCroskery S, Chaudhry A, Lin L, Daniels MP. 2006. Transmembrane agrin regulates filopodia in rat hippocampal neurons in culture. *Mol Cell Neurosci* 33:15-28

McDonald RJ, Devan BD, Hong NS. 2004. Multiple memory systems: the power of interactions. *Neurobiol Learn Mem* 82:333-46

McDonald RJ, White NM. 1993. A triple dissociation of memory systems: hippocampus, amygdala, and dorsal striatum. *Behav Neurosci* 107:3-22

Mitsui S, Osako Y, Yokoi F, Dang MT, Yuri K, et al. 2009. A mental retardation gene, motopsin/neurotrypsin/prss12, modulates hippocampal function and social interaction. *Eur J Neurosci* 30:2368-78

Miyachi S, Hikosaka O, Lu X. 2002. Differential activation of monkey striatal neurons in the early and late stages of procedural learning. *Exp Brain Res* 146:122-6

Mizoguchi K, Yuzurihara M, Ishige A, Sasaki H, Tabira T. 2002. Chronic stress impairs rotarod performance in rats: implications for depressive state. *Pharmacol Biochem Behav* 71:79-84

Mizui T, Takahashi H, Sekino Y, Shirao T. 2005. Overexpression of drebrin A in immature neurons induces the accumulation of F-actin and PSD-95 into dendritic filopodia, and the formation of large abnormal protrusions. *Mol Cell Neurosci* 30:630-8

Mizumori SJ, Cooper BG, Leutgeb S, Pratt WE. 2000. A neural systems analysis of adaptive navigation. *Mol Neurobiol* 21:57-82

Mizumori SJ, Williams JD. 1993. Directionally selective mnemonic properties of neurons in the lateral dorsal nucleus of the thalamus of rats. *J Neurosci* 13:4015-28

Molinari F, Rio M, Meskenaite V, Encha-Razavi F, Auge J, et al. 2002. Truncating neurotrypsin mutation in autosomal recessive nonsyndromic mental retardation. *Science* 298:1779-81

Montoya CP, Astell S, Dunnett SB. 1990. Effects of nigral and striatal grafts on skilled forelimb use in the rat. *Prog Brain Res* 82:459-66

Montoya CP, Campbell-Hope LJ, Pemberton KD, Dunnett SB. 1991. The "staircase test": a measure of independent forelimb reaching and grasping abilities in rats. *J Neurosci Methods* 36:219-28

Morgan SL, Teyler TJ. 1999. VDCCs and NMDARs underlie two forms of LTP in CA1 hippocampus in vivo. *J Neurophysiol* 82:736-40

Morris RG. 1981. Spatial localization does not require the presence of local cues. *Learn Motiv* 12:239-60

Morris RG, Anderson E, Lynch GS, Baudry M. 1986. Selective impairment of learning and blockade of long-term potentiation by an N-methyl-D-aspartate receptor antagonist, AP5. *Nature* 319:774-6

Nagerl UV, Eberhorn N, Cambridge SB, Bonhoeffer T. 2004. Bidirectional activity-dependent morphological plasticity in hippocampal neurons. *Neuron* 44:759-67

Nakazawa K, McHugh TJ, Wilson MA, Tonegawa S. 2004. NMDA receptors, place cells and hippocampal spatial memory. *Nat Rev Neurosci* 5:361-72

Napier RM, Macrae M, Kehoe EJ. 1992. Rapid reaquisition in conditioning of the rabbit's nictitating membrane response. *J Exp Psychol Anim Behav Process* 18:182-92

Negishi T, Kawasaki K, Sekiguchi S, Ishii Y, Kyuwa S, et al. 2005. Attention-deficit and hyperactive neurobehavioural characteristics induced by perinatal hypothyroidism in rats. *Behav Brain Res* 159:323-31

Newell KM. 1991. Motor skill acquisition. *Annu Rev Psychol* 42:213-37

Niemeijer AR, Frederiks BJ, Riphagen, II, Legemaate J, Eefsting JA, Hertogh CM. 2010. Ethical and practical concerns of surveillance technologies in residential care for people with dementia or intellectual disabilities: an overview of the literature. *Int Psychogeriatr* 22:1129-42

Nihei MK, Desmond NL, McGlothan JL, Kuhlmann AC, Guilarte TR. 2000. N-methyl-D-aspartate receptor subunit changes are associated with lead-induced deficits of long-term potentiation and spatial learning. *Neuroscience* 99:233-42

Nimchinsky EA, Sabatini BL, Svoboda K. 2002. Structure and function of dendritic spines. *Annu Rev Physiol* 64:313-53

Noguchi J, Matsuzaki M, Ellis-Davies GC, Kasai H. 2005. Spine-neck geometry determines NMDA receptor-dependent Ca2+ signaling in dendrites. *Neuron* 46:609-22

O'Doherty J, Dayan P, Schultz J, Deichmann R, Friston K, Dolan RJ. 2004. Dissociable roles of ventral and dorsal striatum in instrumental conditioning. *Science* 304:452-4

O'Keefe J. 1976. Place units in the hippocampus of the freely moving rat. *Exp Neurol* 51:78-109

O'Keefe J, Conway DH. 1978. Hippocampal place units in the freely moving rat: why they fire where they fire. *Exp Brain Res* 31:573-90

O'Keefe J, Dostrovsky J. 1971. The hippocampus as a spatial map. Preliminary evidence from unit activity in the freely-moving rat. *Brain Res* 34:171-5

O'Keefe JA, & Nadel, L. 1978. *The hippocampus as a cognitive map.* London

Okamoto K, Nagai T, Miyawaki A, Hayashi Y. 2004. Rapid and persistent modulation of actin dynamics regulates postsynaptic reorganization underlying bidirectional plasticity. *Nat Neurosci* 7:1104-12

Organization WWH. 2010. WHO Mental Health Gap Action Plan.

Ornoy A, Ergaz Z. 2010. Alcohol abuse in pregnant women: effects on the fetus and newborn, mode of action and maternal treatment. *Int J Environ Res Public Health* 7:364-79

Otmakhov N, Khibnik L, Otmakhova N, Carpenter S, Riahi S, et al. 2004. Forskolin-induced LTP in the CA1 hippocampal region is NMDA receptor dependent. *J Neurophysiol* 91:1955-62

Packard MG, Hirsh R, White NM. 1989. Differential effects of fornix and caudate nucleus lesions on two radial maze tasks: evidence for multiple memory systems. *J Neurosci* 9:1465-72

Packard MG, McGaugh JL. 1996. Inactivation of hippocampus or caudate nucleus with lidocaine differentially affects expression of place and response learning. *Neurobiol Learn Mem* 65:65-72

Pamela APaB. 2004. *Understanding Mental Retardation*: University Press of Mississippi

Parnass Z, Tashiro A, Yuste R. 2000. Analysis of spine morphological plasticity in developing hippocampal pyramidal neurons. *Hippocampus* 10:561-8

Paulus MP, Dulawa SC, Ralph RJ, Mark AG. 1999. Behavioral organization is independent of locomotor activity in 129 and C57 mouse strains. *Brain Res* 835:27-36

Pavlov IP. 1960. *Conditional Reflexes*. New York: Dover Publications

Pawlak R, Nagai N, Urano T, Napiorkowska-Pawlak D, Ihara H, et al. 2002. Rapid, specific and active site-catalyzed effect of tissue-plasminogen activator on hippocampus-dependent learning in mice. *Neuroscience* 113:995-1001

Pearce JM, Roberts AD, Good M. 1998. Hippocampal lesions disrupt navigation based on cognitive maps but not heading vectors. *Nature* 396:75-7

Peters A, Kaiserman-Abramof IR. 1970. The small pyramidal neuron of the rat cerebral cortex. The perikaryon, dendrites and spines. *Am J Anat* 127:321-55

Pisani A, Centonze D, Bernardi G, Calabresi P. 2005. Striatal synaptic plasticity: implications for motor learning and Parkinson's disease. *Mov Disord* 20:395-402

Pittenger C, Fasano S, Mazzocchi-Jones D, Dunnett SB, Kandel ER, Brambilla R. 2006. Impaired bidirectional synaptic plasticity and procedural memory formation in striatum-specific cAMP response element-binding protein-deficient mice. *J Neurosci* 26:2808-13

Pittenger C, Kandel ER. 2003. In search of general mechanisms for long-lasting plasticity: Aplysia and the hippocampus. *Philos Trans R Soc Lond B Biol Sci* 358:757-63

Powell RA, Symbaluk, D.G., Honey, P.L. 2009. *Introduction to Learning and Behavior*: Wadsworth Cengage Learning

Purpura DP. 1974. Dendritic spine "dysgenesis" and mental retardation. *Science* 186:1126-8

Pyter LM, Cochrane SF, Ouwenga RL, Patel PN, Pineros V, Prendergast BJ. 2010. Mammary tumors induce select cognitive impairments. *Brain Behav Immun* 24:903-7

Ramakers GM, Pasinelli P, van Beest M, van der Slot A, Gispen WH, De Graan PN. 2000. Activation of pre- and postsynaptic protein kinase C during tetraethylammonium-induced long-term potentiation in the CA1 field of the hippocampus. *Neurosci Lett* 286:53-6

Ranck JB, Jr. 1984. Head direction cells in the deep layer of dorsal presubiculum in freely moving rats

Soc. Neurosci. Abstr. 159

Reeves RR, Panguluri RL. 2011. Neuropsychiatric complications of traumatic brain injury. *J Psychosoc Nurs Ment Health Serv* 49:42-50

Reif R, Sales S, Hettwer S, Dreier B, Gisler C, et al. 2007. Specific cleavage of agrin by neurotrypsin, a synaptic protease linked to mental retardation. *FASEB J* 21:3468-78

Robbins SJ. 1990. Mechanisms Underlying Spontaneous-Recovery in Autoshaping. *J Exp Psychol Anim B* 16:235-49

Russell M, Dark KA, Cummins RW, Ellman G, Callaway E, Peeke HV. 1984. Learned histamine release. *Science* 225:733-4

Rustay NR, Wahlsten D, Crabbe JC. 2003. Influence of task parameters on rotarod performance and sensitivity to ethanol in mice. *Behav Brain Res* 141:237-49

Sanes JR, Marshall LM, McMahan UJ. 1978. Reinnervation of muscle fiber basal lamina after removal of myofibers. Differentiation of regenerating axons at original synaptic sites. *J Cell Biol* 78:176-98

Sassone-Corsi P. 1995. Transcription factors responsive to cAMP. *Annu Rev Cell Dev Biol* 11:355-77

Scarisbrick IA, Blaber SI, Lucchinetti CF, Genain CP, Blaber M, Rodriguez M. 2002. Activity of a newly identified serine protease in CNS demyelination. *Brain* 125:1283-96

Schaechter JD, Moore CI, Connell BD, Rosen BR, Dijkhuizen RM. 2006. Structural and functional plasticity in the somatosensory cortex of chronic stroke patients. *Brain* 129:2722-33

Schmidt RA. 1976. Control processes in motor skills. *Exerc Sport Sci Rev* 4:229-61

Schneider A, Hagerman RJ, Hessl D. 2009. Fragile X syndrome -- from genes to cognition. *Dev Disabil Res Rev* 15:333-42

Scoville WB, Milner B. 1957. Loss of recent memory after bilateral hippocampal lesions. *J Neurol Neurosurg Psychiatry* 20:11-21

Sekino Y, Kojima N, Shirao T. 2007. Role of actin cytoskeleton in dendritic spine morphogenesis. *Neurochem Int* 51:92-104

Serpinskaya AS, Feng G, Sanes JR, Craig AM. 1999. Synapse formation by hippocampal neurons from agrin-deficient mice. *Dev Biol* 205:65-78

Sheline YI, Gado MH, Kraemer HC. 2003. Untreated depression and hippocampal volume loss. *Am J Psychiatry* 160:1516-8

Shiosaka S, Yoshida S. 2000. Synaptic microenvironments--structural plasticity, adhesion molecules, proteases and their inhibitors. *Neurosci Res* 37:85-9

Siegler RS, Svetina M. 2006. What leads children to adopt new strategies? A microgenetic/cross-sectional study of class inclusion. *Child Dev* 77:997-1015

Silva AJ, Kogan JH, Frankland PW, Kida S. 1998. CREB and memory. *Annu Rev Neurosci* 21:127-48

Skinner BF. 1935. The Generic Nature of the Concepts of Stimulus and Response. *J Gen Psychol* 12:40-65

Skoff RP, Hamburger V. 1974. Fine structure of dendritic and axonal growth cones in embryonic chick spinal cord. *J Comp Neurol* 153:107-47

Slane JM, Lee HS, Vorhees CV, Zhang J, Xu M. 2000. DNA fragmentation factor 45 deficient mice exhibit enhanced spatial learning and memory compared to wild-type control mice. *Brain Res* 867:70-9

Sorra KE, Fiala JC, Harris KM. 1998. Critical assessment of the involvement of perforations, spinules, and spine branching in hippocampal synapse formation. *J Comp Neurol* 398:225-40

Stackman RW, Taube JS. 1998. Firing properties of rat lateral mammillary single units: head direction, head pitch, and angular head velocity. *J Neurosci* 18:9020-37

Stephan A, Mateos JM, Kozlov SV, Cinelli P, Kistler AD, et al. 2008. Neurotrypsin cleaves agrin locally at the synapse. *FASEB J* 22:1861-73

Stern M. BJ, Elek SD., Fleck DG. 1969. Microbial causes of mental retardation. The role of prenatal infections with cytomegalovirus, rubella virus, and toxoplsma. *Lancet.* 30

Sutherland RJ, & Rudy, J. W. . 1988. Place learning in the Morris place navigation task is impaired by damage to the hippocampal formation even if the temporal demands are reduced. *Psychobiology*:129-44

Tada T, Sheng M. 2006. Molecular mechanisms of dendritic spine morphogenesis. *Curr Opin Neurobiol* 16:95-101

Takahashi H, Sekino Y, Tanaka S, Mizui T, Kishi S, Shirao T. 2003. Drebrin-dependent actin clustering in dendritic filopodia governs synaptic targeting of postsynaptic density-95 and dendritic spine morphogenesis. *J Neurosci* 23:6586-95

Tang YP, Shimizu E, Dube GR, Rampon C, Kerchner GA, et al. 1999. Genetic enhancement of learning and memory in mice. *Nature* 401:63-9

Taube JS, Muller RU, Ranck JB, Jr. 1990a. Head-direction cells recorded from the postsubiculum in freely moving rats. I. Description and quantitative analysis. *J Neurosci* 10:420-35

Taube JS, Muller RU, Ranck JB, Jr. 1990b. Head-direction cells recorded from the postsubiculum in freely moving rats. II. Effects of environmental manipulations. *J Neurosci* 10:436-47

Terman LM. 1916. The Binet Scale and the Diagnosis of Feeble-Mindedness. *J Am Inst Crim Law C* 7:530-43

Thompson RF, Krupa DJ. 1994. Organization of memory traces in the mammalian brain. *Annu Rev Neurosci* 17:519-49

Thorndike EL. 1927. The Law of Effect. *The American Journal of Psychology* 39:212-22

Thorndike EL. 1933. A Proof of the Law of Effect. *Science* 77:173-5

Toni N, Teng EM, Bushong EA, Aimone JB, Zhao C, et al. 2007. Synapse formation on neurons born in the adult hippocampus. *Nat Neurosci* 10:727-34

Topliss DJ, Eastman CJ. 2004. 5: Diagnosis and management of hyperthyroidism and hypothyroidism. *Med J Aust* 180:186-93

Toscano CD, Guilarte TR. 2005. Lead neurotoxicity: from exposure to molecular effects. *Brain Res Brain Res Rev* 49:529-54

Vaughn JE, Henrikson CK, Grieshaber JA. 1974. A quantitative study of synapses on motor neuron dendritic growth cones in developing mouse spinal cord. *J Cell Biol* 60:664-72

Verina T, Rohde CA, Guilarte TR. 2007. Environmental lead exposure during early life alters granule cell neurogenesis and morphology in the hippocampus of young adult rats. *Neuroscience* 145:1037-47

Ward MT, Oler JA, Markus EJ. 1999. Hippocampal dysfunction during aging I: deficits in memory consolidation. *Neurobiol Aging* 20:363-72

Weinberger NM. 1965. Effect of Detainment on Extinction of Avoidance Responses. *J Comp Physiol Psychol* 60:135-8

Weinert D, Waterhouse J. 1999. Daily activity and body temperature rhythms do not change simultaneously with age in laboratory mice. *Physiol Behav* 66:605-12

Weiss T, Miltner WH, Liepert J, Meissner W, Taub E. 2004. Rapid functional plasticity in the primary somatomotor cortex and perceptual changes after nerve block. *Eur J Neurosci* 20:3413-23

Wiener SI. 1993. Spatial and behavioral correlates of striatal neurons in rats performing a self-initiated navigation task. *J Neurosci* 13:3802-17

Wines M. 2006. Malnutrition Is Cheating Its Survivors, and Africa's Future. *The New York Times*

Winnepenninckx B. RL, Kooy F. 2003. Mental Retardation: a review of the genetic causes. *The British Journal of Developmental Disabilities* 49:29-44

Wolfer DP, Lang R, Cinelli P, Madani R, Sonderegger P. 2001. Multiple roles of neurotrypsin in tissue morphogenesis and nervous system development suggested by the mRNA expression pattern. *Mol Cell Neurosci* 18:407-33

Wolff JR, Missler M. 1992. Synaptic reorganization in developing and adult nervous systems. *Ann Anat* 174:393-403

Wood ER, Dudchenko PA, Robitsek RJ, Eichenbaum H. 2000. Hippocampal neurons encode information about different types of memory episodes occurring in the same location. *Neuron* 27:623-33

Xu T, Yu X, Perlik AJ, Tobin WF, Zweig JA, et al. 2009. Rapid formation and selective stabilization of synapses for enduring motor memories. *Nature* 462:915-9

Yang G, Pan F, Gan WB. 2009. Stably maintained dendritic spines are associated with lifelong memories. *Nature* 462:920-4

Yerkes RM, Dodson JD. 1908. The relation of strength of stimulus to rapidity of habit-formation. *J Comp Neurol Psycho* 18:459-82

Yin HH, Knowlton BJ. 2006. The role of the basal ganglia in habit formation. *Nat Rev Neurosci* 7:464-76

Yin HH, Ostlund SB, Balleine BW. 2008. Reward-guided learning beyond dopamine in the nucleus accumbens: the integrative functions of cortico-basal ganglia networks. *Eur J Neurosci* 28:1437-48

Yin HH, Ostlund SB, Knowlton BJ, Balleine BW. 2005. The role of the dorsomedial striatum in instrumental conditioning. *Eur J Neurosci* 22:513-23

Yuste R, Bonhoeffer T. 2001. Morphological changes in dendritic spines associated with long-term synaptic plasticity. *Annu Rev Neurosci* 24:1071-89

Yuste R, Bonhoeffer T. 2004. Genesis of dendritic spines: insights from ultrastructural and imaging studies. *Nat Rev Neurosci* 5:24-34

Zhou Q, Homma KJ, Poo MM. 2004. Shrinkage of dendritic spines associated with long-term depression of hippocampal synapses. *Neuron* 44:749-57

Zierath D, Hadwin J, Savos A, Carter KT, Kunze A, Becker KJ. 2010. Anamnestic recall of stroke-related deficits: an animal model. *Stroke* 41:2653-60

Ziv NE, Smith SJ. 1996. Evidence for a role of dendritic filopodia in synaptogenesis and spine formation. *Neuron* 17:91-102

Curriculum vitae

First name	Ewa
Surname	Sokolowska
Date of birth	30.12.1981
Nationality	Polish

EDUCATION

09. 1996 – 06. 2000 **Adam Mickiewicz High School**, Olsztyn, Poland

10. 2000 – 06. 2005 **University of Warmia and Mazury**, Olsztyn, Poland

Faculty of Biology

MSc Degree in Biotechnology

Supervisor: Prof. Bozena Szafranska

Project: "Amplicons Production of the PAG (Pregnancy-Associated Glycoprotein) Gene Family as Potential Genetic Markers"

03. 2006 – 11. 2006 **European Molecular Biology Laboratory**,

Mouse Biology Unit

Monterotondo Outstation, Italy

Trainee

Supervisors: Dr. Cornelius Gross, Dr. Giovanni Frazzetto

Project: "Identification of genes underlying anxiety related behavior in mouse and human by environmental interaction."

12.2006 – 09.2011 **University of Zurich**

Department of Biochemistry

PhD Student

Supervisor: Prof. Peter Sonderegger

Project: "Physiological and Behavioral Consequences of Activity-Dependent Agrin Cleavage by Neurotrypsin"

Acknowledgments

First of all I want to express my gratitude to **Peter Sonderegger,** who believed in my capabilities and provided me with the opportunity to do doctoral studies in his laboratory. I thank him for his patience, interest and the abundance good advices that he has contributed over the last five years.

Special thanks to **Kazumasa Matsumoto-Miyai** who took good care of me at the beginning of my thesis, introduced me to a broad spectrum of technical knowledge and who was always open to receiving my questions.

I want to thank **David Wolfer** for all his advice, fruitful discussions and constructive criticism concerning the behavioral part of my thesis.

I am also obliged to **Beat Kunz** for his wonderful and efficient organization of our laboratory work and his constant help concerning animal breeding and their preparation for future experiments.

I greatly acknowledge the contribution of **Inger Drescher** and **Claudia Meyer** for all their help with mice and setting up various behavioral tests, and of **Michal Okoniewski** for his help with statistics.

I would like to thank all current and former members of our group for their various contributions, for many interesting discussions and for providing a friendly working atmosphere.

Last but not least, I want to express my gratitude to my family for their constant belief in me and their moral support in difficult situations. Special thanks to my friends who all shared good and bad moments with me during my doctorate and who always found time to share spare time with me.

APPENDIX

The following chapter includes detailed statistical analyses of the behavioral studies conducted on wild-type and NT-deficient mice.

Table 1. Statistical calculation for the 1st series of the Rotarod test.

Tests of Between-Subjects Effects

Dependent Variable:Latency to Fall (sec)

TestPhase	Source	Type III Sum of Squares	df	Mean Square	F	Sig.
before the break	Corrected Model	4379717.875	18	243317.660	65.135	.000
	Intercept	31526958.31	1	31526958.31	8439.680	.000
	Genotype	568482.476	1	568482.476	152.181	.000
	Sex	38399.247	1	38399.247	10.279	.001
	Weight	155217.215	1	155217.215	41.551	.000
	Trial	378701.309	9	42077.923	11.264	.000
	Day	3328263.850	6	554710.642	148.495	.000
	Error	6443846.374	1725	3735.563		
	Total	58245941.58	1744			
	Corrected Total	10823564.24	1743			
after the break	Corrected Model	232522.011[b]	13	17886.309	3.840	.000
	Intercept	10696432.44	1	10696432.44	2296.302	.000
	Genotype	34627.953	1	34627.953	7.434	.007
	Sex	22117.367	1	22117.367	4.748	.030
	Weight	50035.534	1	50035.534	10.742	.001
	Trial	128573.862	9	14285.985	3.067	.001
	Day	19870.334	1	19870.334	4.266	.039
	Error	2263842.100	486	4658.111		
	Total	18647444.69	500			
	Corrected Total	2496364.112	499			

a. R Squared = .405 (Adjusted R Squared = .398)
b. R Squared = .093 (Adjusted R Squared = .069)

Table 2. Statistical calculation for the 2nd series of the Rotarod test.

Tests of Between-Subjects Effects

Dependent Variable:Latency to Fall (sec)

Source	Type III Sum of Squares	df	Mean Square	F	Sig.
Corrected Model	427015.205[a]	23	18565.878	25.845	.000
Intercept	4647874.960	1	4647874.960	6470.109	.000
Trial	110885.721	9	12320.636	17.151	.000
Day	219281.580	12	18273.465	25.438	.000
Stage	.000	0	.	.	.
Sex	20241.730	1	20241.730	28.178	.000
Error	183900.469	256	718.361		
Total	5509188.552	280			
Corrected Total	610915.674	279			

a. R Squared = .699 (Adjusted R Squared = .672)

Table 3. Statistical calculation for the 3rd series of the Rotarod test.

Tests of Between-Subjects Effects

Dependent Variable:Latency to Fall (sec)

TestPhase	Source	Type III Sum of Squares	df	Mean Square	F	Sig.
before the break	Corrected Model	4729425.476	20	236471.274	45.111	.000
	Intercept	59618886.82	1	59618886.82	11373.276	.000
	Genotype	1142980.193	1	1142980.193	218.042	.000
	Weight	157733.991	1	157733.991	30.090	.000
	Day	3054188.888	9	339354.321	64.737	.000
	Trial	462259.621	9	51362.180	9.798	.000
	Error	11731630.52	2238	5242.015		
	Total	82616595.78	2259			
	Corrected Total	16461055.99	2258			
after the break	Corrected Model	345910.441[b]	14	24707.889	4.199	.000
	Intercept	29201411.63	1	29201411.63	4962.763	.000
	Genotype	266947.140	1	266947.140	45.368	.000
	Weight	24.352	1	24.352	.004	.949
	Day	12084.697	3	4028.232	.685	.562
	Trial	62918.220	9	6990.913	1.188	.299
	Error	5236852.516	890	5884.104		
	Total	37606919.74	905			
	Corrected Total	5582762.957	904			

a. R Squared = .287 (Adjusted R Squared = .281)
b. R Squared = .062 (Adjusted R Squared = .047)

Table 4. Statistical calculation of the muscle strength difference between wild-type and Nt-deficient mice.

Independent Samples Test

age			Levene's Test for Equality of Variances		t-test for Equality of Means						
										95% Confidence Interval of the Difference	
			F	Sig.	t	df	Sig. (2-tailed)	Mean Difference	Std. Error Difference	Lower	Upper
5-7 months old	result	Equal variances assumed	.160	.694	-1.575	18	.133	-7.96000	5.05376	-18.57755	2.65755
		Equal variances not assumed			-1.575	17.743	.133	-7.96000	5.05376	-18.58860	2.66860
9-11 months old	result	Equal variances assumed	3.761	.060	-2.409	38	.021	-13.27879	5.51202	-24.43729	-2.12028
		Equal variances not assumed			-2.314	28.348	.028	-13.27879	5.73967	-25.02946	-1.52812
12-14 months old	result	Equal variances assumed	1.103	.300	-.629	42	.533	-3.70000	5.88385	-15.57409	8.17409
		Equal variances not assumed			-.629	41.295	.533	-3.70000	5.88385	-15.58010	8.18010

Table 5. Statistical calculation of the general locomotor activity during the 1st series of activity test.

Tests of Between-Subjects Effects

Dependent Variable:Activity

Source	Type III Sum of Squares	df	Mean Square	F	Sig.
Corrected Model	737425.678[a]	9	81936.186	12.732	.000
Intercept	3290977.252	1	3290977.252	511.396	.000
Genotype	153635.886	1	153635.886	23.874	.000
Age	492209.787	4	123052.447	19.122	.000
Genotype * Age	153706.343	4	38426.586	5.971	.000
Error	965292.228	150	6435.282		
Total	5819163.241	160			
Corrected Total	1702717.906	159			

a. R Squared = .433 (Adjusted R Squared = .399)

Table 6. Statistical calculation of the general locomotor activity during the 2nd series of activity test.

Tests of Between-Subjects Effects

Dependent Variable:Activity

Source	Type III Sum of Squares	df	Mean Square	F	Sig.
Corrected Model	562317.237[a]	9	62479.693	9.719	.000
Intercept	3512749.829	1	3512749.829	546.419	.000
Genotype	33577.520	1	33577.520	5.223	.024
AgeCode	508763.623	4	127190.906	19.785	.000
Genotype * AgeCode	11444.501	4	2861.125	.445	.776
Error	964301.918	150	6428.679		
Total	6240352.591	160			
Corrected Total	1526619.155	159			

a. R Squared = .368 (Adjusted R Squared = .330)

Table 7. Statistical calculation of general locomotor activity change over time.

Tests of Between-Subjects Effects

Dependent Variable:Activity

Age	Source	Type III Sum of Squares	df	Mean Square	F	Sig.
6 mold	Corrected Model	150300.364[a]	1	150300.364	103.427	.000
	Intercept	946325.086	1	946325.086	651.200	.000
	Genotype	150300.364	1	150300.364	103.427	.000
	Error	31970.454	22	1453.202		
	Total	982820.651	24			
	Corrected Total	182270.818	23			
7 mo old	Corrected Model	124615.923[b]	1	124615.923	6.767	.013
	Intercept	1986142.019	1	1986142.019	107.856	.000
	Genotype	124615.923	1	124615.923	6.767	.013
	Error	699762.234	38	18414.796		
	Total	2691177.314	40			
	Corrected Total	824378.157	39			
8 mo old	Corrected Model	24368.229[c]	1	24368.229	4.556	.041
	Intercept	803824.164	1	803824.164	150.274	.000
	Genotype	24368.229	1	24368.229	4.556	.041
	Error	160471.827	30	5349.061		
	Total	1451336.775	32			
	Corrected Total	184840.056	31			
9 mo old	Corrected Model	430.453[d]	1	430.453	1.612	.225
	Intercept	110152.100	1	110152.100	412.574	.000
	Genotype	430.453	1	430.453	1.612	.225
	Error	3737.821	14	266.987		
	Total	114320.375	16			
	Corrected Total	4168.274	15			
10 mo old	Corrected Model	614.547[e]	1	614.547	.408	.526
	Intercept	509543.688	1	509543.688	337.982	.000
	Genotype	614.547	1	614.547	.408	.526
	Error	69349.891	46	1507.606		
	Total	579508.126	48			
	Corrected Total	69964.438	47			

a. R Squared = .825 (Adjusted R Squared = .817)
b. R Squared = .151 (Adjusted R Squared = .129)
c. R Squared = .132 (Adjusted R Squared = .103)
d. R Squared = .103 (Adjusted R Squared = .039)
e. R Squared = .009 (Adjusted R Squared = -.013)

Table 8. Statistical calculation of the fear response during Fear Conditioning training.

Tests of Between-Subjects Effects

Dependent Variable:Freezing Level

Source	Type III Sum of Squares	df	Mean Square	F	Sig.
Corrected Model	1686.123[a]	3	562.041	1.491	.222
Intercept	22069.851	1	22069.851	58.543	.000
Genotype	403.531	1	403.531	1.070	.304
Experiment	1425.429	1	1425.429	3.781	.055
Genotype * Experiment	23.008	1	23.008	.061	.805
Error	33928.934	90	376.988		
Total	59328.345	94			
Corrected Total	35615.058	93			

a. R Squared = .047 (Adjusted R Squared = .016)

Table 9. Statistical calculation of the response to the context during Fear Conditioning.

Tests of Between-Subjects Effects

Dependent Variable:Freezing Level

Source	Type III Sum of Squares	df	Mean Square	F	Sig.
Corrected Model	151.145[a]	3	50.382	.137	.938
Intercept	20310.761	1	20310.761	55.342	.000
Genotype	137.206	1	137.206	.374	.542
Experiment	3.547	1	3.547	.010	.922
Genotype * Experiment	4.027	1	4.027	.011	.917
Error	33030.605	90	367.007		
Total	54139.887	94			
Corrected Total	33181.749	93			

a. R Squared = .005 (Adjusted R Squared = -.029)

Table 10. Statistical calculation of the response to the cue during Fear Conditioning.

Tests of Between-Subjects Effects

Dependent Variable:Freezing Level

Source	Type III Sum of Squares	df	Mean Square	F	Sig.
Corrected Model	2284.549[a]	3	761.516	1.522	.214
Intercept	46295.849	1	46295.849	92.529	.000
Genotype	1057.508	1	1057.508	2.114	.149
Experiment	1470.632	1	1470.632	2.939	.090
Genotype * Experiment	142.402	1	142.402	.285	.595
Error	45030.371	90	500.337		
Total	97513.537	94			
Corrected Total	47314.919	93			

a. R Squared = .048 (Adjusted R Squared = .017)

Table 11. Statistical calculation of the improvement in reaching and grasping abilities during Staircase test.

Tests of Between-Subjects Effects

Dependent Variable:PelletNR

Source	Type III Sum of Squares	df	Mean Square	F	Sig.
Corrected Model	213.509[a]	10	21.351	3.204	.001
Intercept	11111.653	1	11111.653	1667.531	.000
Genotype	.853	1	.853	.128	.721
Day	212.270	9	23.586	3.539	.000
Error	1119.474	168	6.664		
Total	12487.000	179			
Corrected Total	1332.983	178			

a. R Squared = .160 (Adjusted R Squared = .110)

Table 12. Statistical calculation for the Two-cue water-maze test/Distance to cue (m).

ANOVA Table for dc-patt-dayP
Inclusion criteria: IN from NtkoWmHVccall-AB.svd

	DF	Sum of Squares	Mean Square	F-Value	P-Value	Lambda	Power
grp	1	1.317E-4	1.317E-4	.020	.8898	.020	.052
vers	1	.009	.009	1.401	.2486	1.401	.195
grp * vers	1	8.928E-5	8.928E-5	.013	.9092	.013	.051
Subject(Group)	23	.154	.007				
patt	1	.081	.081	7.576	.0113	7.576	.758
patt * grp	1	8.862E-5	8.862E-5	.008	.9284	.008	.051
patt * vers	1	3.322E-4	3.322E-4	.031	.8619	.031	.053
patt * grp * vers	1	2.909E-4	2.909E-4	.027	.8707	.027	.053
patt * Subject(Group)	23	.247	.011				
dayP	2	.010	.005	1.127	.3329	2.253	.228
dayP * grp	2	.005	.003	.574	.5670	1.149	.136
dayP * vers	2	.009	.005	1.011	.3719	2.021	.208
dayP * grp * vers	2	.003	.002	.387	.6814	.774	.107
dayP * Subject(Group)	46	.207	.004				
patt * dayP	2	.002	.001	.292	.7483	.584	.092
patt * dayP * grp	2	.001	3.987E-4	.098	.9067	.196	.064
patt * dayP * vers	2	.002	.001	.191	.8264	.383	.078
patt * dayP * grp * vers	2	.006	.003	.775	.4667	1.550	.169
patt * dayP * Subject(Group)	46	.187	.004				

Table 13. Statistical calculation for the Two-cue water-maze test/Escape latency (s) during 2nd - 5th day (one cue).

ANOVA Table for tim-dayC
Inclusion criteria: IN from NtkoWmHVccall-AB.svd

	DF	Sum of Squares	Mean Square	F-Value	P-Value	Lambda	Power
grp	1	37.017	37.017	.907	.3508	.907	.143
vers	1	26.268	26.268	.644	.4306	.644	.116
grp * vers	1	37.874	37.874	.928	.3454	.928	.145
Subject(Group)	23	938.629	40.810				
dayC	3	3815.758	1271.919	43.266	<.0001	129.799	1.000
dayC * grp	3	48.341	16.114	.548	.6511	1.644	.154
dayC * vers	3	4.100	1.367	.046	.9866	.139	.058
dayC * grp * vers	3	113.674	37.891	1.289	.2851	3.867	.321
dayC * Subject(Group)	69	2028.427	29.397				

Table 14. Statistical calculation for the Two-cue water-maze test/Escape latency (s) during 8th-14th day (cue discrimination, only training trials).

ANOVA Table for tim-dayD
Inclusion criteria: IN from NtkoWmHVccall-AB.svd

	DF	Sum of Squares	Mean Square	F-Value	P-Value	Lambda	Power
grp	1	6.484	6.484	.153	.6995	.153	.066
vers	1	101.456	101.456	2.390	.1358	2.390	.302
grp * vers	1	104.977	104.977	2.473	.1295	2.473	.311
Subject(Group)	23	976.309	42.448				
dayD	6	92.117	15.353	1.564	.1623	9.382	.582
dayD * grp	6	37.697	6.283	.640	.6981	3.839	.245
dayD * vers	6	53.479	8.913	.908	.4913	5.447	.344
dayD * grp * vers	6	15.418	2.570	.262	.9537	1.570	.118
dayD * Subject(Group)	138	1354.920	9.818				

Table 15. Statistical calculation for the Two-cue water-maze test/Time near wall (%) during 2nd-5th day (one cue).

ANOVA Table for wti-dayC
Inclusion criteria: IN from NtkoWmHVccall-AB.svd

	DF	Sum of Squares	Mean Square	F-Value	P-Value	Lambda	Power
grp	1	68.033	68.033	1.408	.2475	1.408	.196
vers	1	80.283	80.283	1.661	.2102	1.661	.223
grp * vers	1	.002	.002	5.061E-5	.9944	5.061E-5	.050
Subject(Group)	23	1111.349	48.320				
dayC	3	3637.510	1212.503	22.488	<.0001	67.463	1.000
dayC * grp	3	435.863	145.288	2.695	.0527	8.084	.627
dayC * vers	3	18.677	6.226	.115	.9508	.346	.070
dayC * grp * vers	3	24.200	8.067	.150	.9296	.449	.076
dayC * Subject(Group)	69	3720.392	53.919				

Table 16. Statistical calculation for the 4th series of the Classical Morris water-maze test/Escape latency (s).

Tests of Between-Subjects Effects

Dependent Variable:Escape latency / swim time (s)

Learning	Source	Type III Sum of Squares	df	Mean Square	F	Sig.
aqusition	Corrected Model	48522.071[a]	7	6931.724	25.210	.000
	Intercept	85728.997	1	85728.997	311.787	.000
	Genotype	1001.153	1	1001.153	3.641	.058
	WeightCode	678.794	1	678.794	2.469	.118
	AgeCode	2300.398	4	575.099	2.092	.085
	Day	44587.422	1	44587.422	162.160	.000
	Error	40694.064	148	274.960		
	Total	262936.350	156			
	Corrected Total	89216.135	155			
reversal learning	Corrected Model	16907.264[b]	7	2415.323	11.557	.000
	Intercept	25089.227	1	25089.227	120.043	.000
	Genotype	846.300	1	846.300	4.049	.046
	WeightCode	248.857	1	248.857	1.191	.277
	AgeCode	1505.883	4	376.471	1.801	.131
	Day	14179.216	1	14179.216	67.843	.000
	Error	36366.224	174	209.001		
	Total	127366.378	182			
	Corrected Total	53273.488	181			

a. R Squared = .544 (Adjusted R Squared = .522)
b. R Squared = .317 (Adjusted R Squared = .290)

Table 17. Statistical calculation for the 4th series of the Classical Morris water-maze test/Absolute direction error (°).

Tests of Between-Subjects Effects

Dependent Variable:Absolute direction error (*)

Learning	Source	Type III Sum of Squares	df	Mean Square	F	Sig.
aqusition	Corrected Model	5633.344[a]	7	804.763	5.566	.000
	Intercept	47093.269	1	47093.269	325.713	.000
	Genotype	73.735	1	73.735	.510	.476
	WeightCode	138.316	1	138.316	.957	.330
	AgeCode	408.770	4	102.193	.707	.588
	Day	4973.117	1	4973.117	34.396	.000
	Error	21398.586	148	144.585		
	Total	233936.864	156			
	Corrected Total	27031.930	155			
reversal learning	Corrected Model	14049.181[b]	7	2007.026	14.884	.000
	Intercept	31075.168	1	31075.168	230.459	.000
	Genotype	1802.652	1	1802.652	13.369	.000
	WeightCode	276.904	1	276.904	2.054	.154
	AgeCode	927.319	4	231.830	1.719	.148
	Day	11131.223	1	11131.223	82.551	.000
	Error	23462.212	174	134.840		
	Total	234447.507	182			
	Corrected Total	37511.392	181			

a. R Squared = .208 (Adjusted R Squared = .171)
b. R Squared = .375 (Adjusted R Squared = .349)

Table 18. Statistical calculation for the 4th series of the Classical Morris water-maze test/Path efficiency (%).

Tests of Between-Subjects Effects

Dependent Variable:Path efficiency (%)

Learning	Source	Type III Sum of Squares	df	Mean Square	F	Sig.
aqusition	Corrected Model	9808.658[a]	7	1401.237	18.539	.000
	Intercept	12238.412	1	12238.412	161.916	.000
	Genotype	116.350	1	116.350	1.539	.217
	WeightCode	517.881	1	517.881	6.852	.010
	AgeCode	365.688	4	91.422	1.210	.309
	Day	8447.514	1	8447.514	111.762	.000
	Error	11186.576	148	75.585		
	Total	222744.500	156			
	Corrected Total	20995.234	155			
reversal learning	Corrected Model	10191.141[b]	7	1455.877	10.799	.000
	Intercept	822.809	1	822.809	6.103	.014
	Genotype	735.957	1	735.957	5.459	.021
	WeightCode	488.211	1	488.211	3.621	.059
	AgeCode	583.128	4	145.782	1.081	.367
	Day	8264.251	1	8264.251	61.298	.000
	Error	23458.913	174	134.821		
	Total	360940.750	182			
	Corrected Total	33650.055	181			

a. R Squared = .467 (Adjusted R Squared = .442)
b. R Squared = .303 (Adjusted R Squared = .275)

Table 19. Statistical calculation for the 4th series of the Classical Morris water-maze test/Time in current goal quadrant (s).

Tests of Between-Subjects Effects

Dependent Variable:Time in current goal quadrant

Learning	Source	Type III Sum of Squares	df	Mean Square	F	Sig.
aqusition	Corrected Model	9854.003[a]	7	1407.715	13.568	.000
	Intercept	12342.946	1	12342.946	118.968	.000
	Genotype	613.940	1	613.940	5.917	.016
	WeightCode	3.414	1	3.414	.033	.856
	AgeCode	754.937	4	188.734	1.819	.128
	Day	8563.689	1	8563.689	82.542	.000
	Error	15354.999	148	103.750		
	Total	245838.290	156			
	Corrected Total	25209.002	155			
reversal learning	Corrected Model	20612.502[b]	7	2944.643	24.531	.000
	Intercept	211.584	1	211.584	1.763	.186
	Genotype	606.578	1	606.578	5.053	.026
	WeightCode	200.641	1	200.641	1.671	.198
	AgeCode	584.407	4	146.102	1.217	.305
	Day	18523.424	1	18523.424	154.312	.000
	Error	20886.688	174	120.038		
	Total	382495.390	182			
	Corrected Total	41499.190	181			

a. R Squared = .391 (Adjusted R Squared = .362)
b. R Squared = .497 (Adjusted R Squared = .476)

Table 20. Statistical calculation for the 4th series of the Classical Morris water-maze test/Distance to current goal quadrant (m).

Tests of Between-Subjects Effects

Dependent Variable:Distance to current goal (m)

Learning	Source	Type III Sum of Squares	df	Mean Square	F	Sig.
aqusition	Corrected Model	.686[a]	7	.098	25.124	.000
	Intercept	7.946	1	7.946	2035.924	.000
	Genotype	.016	1	.016	3.993	.048
	WeightCode	.002	1	.002	.625	.430
	AgeCode	.025	4	.006	1.628	.170
	Day	.637	1	.637	163.319	.000
	Error	.578	148	.004		
	Total	37.938	156			
	Corrected Total	1.264	155			
reversal learning	Corrected Model	1.010[b]	7	.144	25.584	.000
	Intercept	4.137	1	4.137	733.451	.000
	Genotype	.061	1	.061	10.786	.001
	WeightCode	.001	1	.001	.131	.718
	AgeCode	.052	4	.013	2.309	.060
	Day	.890	1	.890	157.769	.000
	Error	.981	174	.006		
	Total	39.251	182			
	Corrected Total	1.991	181			

a. R Squared = .543 (Adjusted R Squared = .521)
b. R Squared = .507 (Adjusted R Squared = .487)

Table 21. Statistical calculation for the 4th series of the Classical Morris water-maze test/Beeline start-goal (m).

Tests of Between-Subjects Effects

Dependent Variable:Beeline start-goal (m)

Learning	Source	Type III Sum of Squares	df	Mean Square	F	Sig.
aqusition	Corrected Model	.087[a]	7	.012	6.444	.000
	Intercept	12.864	1	12.864	6688.789	.000
	Genotype	.003	1	.003	1.367	.244
	WeightCode	.005	1	.005	2.453	.119
	AgeCode	.014	4	.004	1.847	.123
	Day	.061	1	.061	31.497	.000
	Error	.285	148	.002		
	Total	81.271	156			
	Corrected Total	.371	155			
reversal learning	Corrected Model	.039[b]	7	.006	1.116	.355
	Intercept	4.180	1	4.180	846.537	.000
	Genotype	.011	1	.011	2.269	.134
	WeightCode	.021	1	.021	4.199	.042
	AgeCode	.014	4	.004	.716	.582
	Day	.006	1	.006	1.310	.254
	Error	.859	174	.005		
	Total	105.550	182			
	Corrected Total	.898	181			

a. R Squared = .234 (Adjusted R Squared = .197)
b. R Squared = .043 (Adjusted R Squared = .004)

Table 22. Statistical calculation for the 4th series of the Classical Morris water-maze test/Swim path (s).

Tests of Between-Subjects Effects

Dependent Variable:Swim path (m)

Learning	Source	Type III Sum of Squares	df	Mean Square	F	Sig.
aqusition	Corrected Model	1231.698[a]	7	175.957	22.440	.000
	Intercept	2344.601	1	2344.601	299.004	.000
	Genotype	18.051	1	18.051	2.302	.131
	WeightCode	26.629	1	26.629	3.396	.067
	AgeCode	38.643	4	9.661	1.232	.300
	Day	1142.666	1	1142.666	145.723	.000
	Error	1160.521	148	7.841		
	Total	7429.017	156			
	Corrected Total	2392.219	155			
reversal learning	Corrected Model	600.171[b]	7	85.739	12.716	.000
	Intercept	952.431	1	952.431	141.251	.000
	Genotype	23.595	1	23.595	3.499	.063
	WeightCode	7.733	1	7.733	1.147	.286
	AgeCode	37.664	4	9.416	1.396	.237
	Day	530.648	1	530.648	78.698	.000
	Error	1173.252	174	6.743		
	Total	4566.816	182			
	Corrected Total	1773.423	181			

a. R Squared = .515 (Adjusted R Squared = .492)
b. R Squared = .338 (Adjusted R Squared = .312)

Table 23. Statistical calculation for the 4th series of the Classical Morris water-maze test/Time near wall (%).

Tests of Between-Subjects Effects

Dependent Variable:Time near wall (%)

Learning	Source	Type III Sum of Squares	df	Mean Square	F	Sig.
aqusition	Corrected Model	3123.294[a]	7	446.185	13.318	.000
	Intercept	7008.274	1	7008.274	209.182	.000
	Genotype	.489	1	.489	.015	.904
	WeightCode	.114	1	.114	.003	.954
	AgeCode	84.450	4	21.113	.630	.642
	Day	3019.948	1	3019.948	90.139	.000
	Error	4958.475	148	33.503		
	Total	21772.838	156			
	Corrected Total	8081.769	155			
reversal learning	Corrected Model	853.627[b]	7	121.947	3.582	.001
	Intercept	915.800	1	915.800	26.899	.000
	Genotype	55.365	1	55.365	1.626	.204
	WeightCode	146.762	1	146.762	4.311	.039
	AgeCode	638.125	4	159.531	4.686	.001
	Day	196.311	1	196.311	5.766	.017
	Error	5924.073	174	34.046		
	Total	12901.572	182			
	Corrected Total	6777.700	181			

a. R Squared = .386 (Adjusted R Squared = .357)

b. R Squared = .126 (Adjusted R Squared = .091)

Table 24. Statistical calculation for the Fear extinction test/Response to training.

Tests of Between-Subjects Effects

Dependent Variable:Freezing level / Training

Source	Type III Sum of Squares	df	Mean Square	F	Sig.
Corrected Model	3165.719[a]	7	452.246	7.986	.000
Intercept	982.381	1	982.381	17.348	.000
Genotype	.054	1	.054	.001	.975
Stage	527.365	1	527.365	9.313	.004
Experiment	634.351	1	634.351	11.202	.002
Genotype * Stage	.001	1	.001	.000	.996
Genotype * Experiment	1.826	1	1.826	.032	.858
Stage * Experiment	541.355	1	541.355	9.560	.003
Genotype * Stage * Experiment	2.611	1	2.611	.046	.831
Error	2604.897	46	56.628		
Total	8624.091	54			
Corrected Total	5770.616	53			

a. R Squared = .549 (Adjusted R Squared = .480)

Table 25. Statistical calculation for the Fear extinction test/Response to context.

Tests of Between-Subjects Effects

Dependent Variable:Freezing level / Context

Source	Type III Sum of Squares	df	Mean Square	F	Sig.
Corrected Model	976.359[a]	7	139.480	4.480	.001
Intercept	373.976	1	373.976	12.013	.001
Genotype	.067	1	.067	.002	.963
Stage	373.976	1	373.976	12.013	.001
Experiment	66.281	1	66.281	2.129	.151
Genotype * Stage	.067	1	.067	.002	.963
Genotype * Experiment	4.753E-5	1	4.753E-5	.000	.999
Stage * Experiment	66.281	1	66.281	2.129	.151
Genotype * Stage * Experiment	4.753E-5	1	4.753E-5	.000	.999
Error	1432.020	46	31.131		
Total	3231.925	54			
Corrected Total	2408.380	53			

a. R Squared = .405 (Adjusted R Squared = .315)

Table 26. Statistical calculation for the Fear extinction test/Response to cue.

Tests of Between-Subjects Effects

Dependent Variable:Freezing level / Cue

Source	Type III Sum of Squares	df	Mean Square	F	Sig.
Corrected Model	6005.317[a]	7	857.902	5.977	.000
Intercept	2430.425	1	2430.425	16.933	.000
Genotype	105.861	1	105.861	.738	.395
Stage	2058.826	1	2058.826	14.344	.000
Experiment	451.313	1	451.313	3.144	.083
Genotype * Stage	81.473	1	81.473	.568	.455
Genotype * Experiment	227.498	1	227.498	1.585	.214
Stage * Experiment	399.141	1	399.141	2.781	.102
Genotype * Stage * Experiment	187.313	1	187.313	1.305	.259
Error	6602.321	46	143.529		
Total	18511.263	54			
Corrected Total	12607.638	53			

a. R Squared = .476 (Adjusted R Squared = .397)

Table 27. Statistical calculation for the Fear extinction test/Fear extinction.

Tests of Between-Subjects Effects

Dependent Variable:Freezing level / Extinction

Source	Type III Sum of Squares	df	Mean Square	F	Sig.
Corrected Model	8742.060[a]	23	380.090	3.667	.000
Intercept	4034.755	1	4034.755	38.925	.000
Genotype	66.091	1	66.091	.638	.426
Experiment	680.504	1	680.504	6.565	.011
Block	2003.406	5	400.681	3.866	.003
Genotype * Experiment	3.196	1	3.196	.031	.861
Genotype * Block	87.941	5	17.588	.170	.973
Experiment * Block	1548.682	5	309.736	2.988	.014
Genotype * Experiment * Block	56.884	5	11.377	.110	.990
Error	14304.408	138	103.655		
Total	32000.811	162			
Corrected Total	23046.469	161			

a. R Squared = .379 (Adjusted R Squared = .276)

Table 28. Statistical calculation for the Fear extinction test/Fear recovery.

Tests of Between-Subjects Effects

Dependent Variable:Freezing level / Recovery

Source	Type III Sum of Squares	df	Mean Square	F	Sig.
Corrected Model	1871.030[a]	23	81.349	2.244	.002
Intercept	2126.140	1	2126.140	58.638	.000
Genotype	7.874	1	7.874	.217	.642
Experiment	52.467	1	52.467	1.447	.231
Block	558.149	5	111.630	3.079	.011
Genotype * Experiment	9.265	1	9.265	.256	.614
Genotype * Block	43.128	5	8.626	.238	.945
Experiment * Block	289.780	5	57.956	1.598	.165
Genotype * Experiment * Block	76.340	5	15.268	.421	.833
Error	5003.685	138	36.259		
Total	9637.217	162			
Corrected Total	6874.715	161			

a. R Squared = .272 (Adjusted R Squared = .151)

Table 29. Statistical calculation for the T-maze test/Time to goal during 1st series.

Tests of Between-Subjects Effects

Dependent Variable:AverTime

DayCateg	Source	Type III Sum of Squares	df	Mean Square	F	Sig.
training 1-6 day	Corrected Model	3419.142[a]	6	569.857	1.440	.206
	Intercept	64448.486	1	64448.486	162.806	.000
	Day	555.159	1	555.159	1.402	.239
	Genotype	554.483	1	554.483	1.401	.239
	AgeCode	2669.435	2	1334.718	3.372	.038
	Genotype * AgeCode	970.499	2	485.250	1.226	.297
	Error	43544.554	110	395.860		
	Total	342775.534	117			
	Corrected Total	46963.696	116			
1st probe trial	Corrected Model	3523.915[b]	5	704.783	1.025	.449
	Intercept	.000	0	.	.	.
	Day	.000	0	.	.	.
	Genotype	15.073	1	15.073	.022	.885
	AgeCode	1635.299	2	817.650	1.189	.341
	Genotype * AgeCode	2353.196	2	1176.598	1.712	.225
	Error	7562.043	11	687.458		
	Total	29664.356	17			
	Corrected Total	11085.958	16			
training 8-11day	Corrected Model	5163.022[c]	6	860.504	1.138	.350
	Intercept	6400.857	1	6400.857	8.465	.005
	Day	995.391	1	995.391	1.316	.255
	Genotype	4.760	1	4.760	.006	.937
	AgeCode	3815.974	2	1907.987	2.523	.088
	Genotype * AgeCode	49.036	2	24.518	.032	.968
	Error	51418.533	68	756.155		
	Total	263823.781	75			
	Corrected Total	56581.555	74			
2nd probe trial	Corrected Model	734.314[d]	4	183.578	.763	.573
	Intercept	.000	0	.	.	.
	Day	.000	0	.	.	.
	Genotype	.594	1	.594	.002	.961
	AgeCode	474.005	2	237.003	.985	.407
	Genotype * AgeCode	170.687	1	170.687	.710	.419
	Error	2405.295	10	240.530		
	Total	9508.718	15			
	Corrected Total	3139.609	14			

a. R Squared = .073 (Adjusted R Squared = .022)

b. R Squared = .318 (Adjusted R Squared = .008)

c. R Squared = .091 (Adjusted R Squared = .011)

d. R Squared = .234 (Adjusted R Squared = -.073)

Table 30. Statistical calculation for the T-maze test/Number of successfully reached goals during 1st series.

Tests of Between-Subjects Effects

Dependent Variable:GoalReached

DaysCateg	Source	Type III Sum of Squares	df	Mean Square	F	Sig.
training 1-6 day	Corrected Model	54.011[a]	6	9.002	4.603	.000
	Intercept	415.356	1	415.356	212.395	.000
	Day	15.858	1	15.858	8.109	.005
	Genotype	13.889	1	13.889	7.102	.009
	Age	3.905	2	1.953	.999	.372
	Genotype * Age	3.705	2	1.852	.947	.391
	Error	220.981	113	1.956		
	Total	1823.000	120			
	Corrected Total	274.992	119			
1st probe trial	Corrected Model	.600[b]	5	.120	.862	.530
	Intercept	.000	0	.	.	.
	Day	.000	0	.	.	.
	Genotype	.161	1	.161	1.159	.300
	Age	.118	2	.059	.425	.662
	Genotype * Age	.118	2	.059	.425	.662
	Error	1.950	14	.139		
	Total	17.000	20			
	Corrected Total	2.550	19			
training 8-11 day	Corrected Model	24.125[c]	6	4.021	1.673	.140
	Intercept	7.249	1	7.249	3.016	.087
	Day	.250	1	.250	.104	.748
	Genotype	14.690	1	14.690	6.113	.016
	Age	12.601	2	6.301	2.622	.080
	Genotype * Age	2.023	2	1.011	.421	.658
	Error	175.425	73	2.403		
	Total	1006.000	80			
	Corrected Total	199.550	79			
2nd probe trial	Corrected Model	1.067[d]	5	.213	.953	.478
	Intercept	.000	0	.	.	.
	Day	.000	0	.	.	.
	Genotype	.153	1	.153	.685	.422
	Age	1.019	2	.510	2.277	.139
	Genotype * Age	.120	2	.060	.267	.769
	Error	3.133	14	.224		
	Total	14.000	20			
	Corrected Total	4.200	19			

a. R Squared = .196 (Adjusted R Squared = .154)

b. R Squared = .235 (Adjusted R Squared = -.038)

c. R Squared = .121 (Adjusted R Squared = .049)

d. R Squared = .254 (Adjusted R Squared = -.012)

Table 31. Statistical calculation for the T-maze test/Time to goal during 2nd series.

Tests of Between-Subjects Effects

Dependent Variable:TimeToGoal

DayCateg	Source	Type III Sum of Squares	df	Mean Square	F	Sig.
training 1-5 day	Corrected Model	29101.604[a]	10	2910.160	3.628	.000
	Intercept	82508.655	1	82508.655	102.851	.000
	Day	232.902	1	232.902	.290	.591
	Genotype	4032.648	1	4032.648	5.027	.026
	Age	15344.010	4	3836.002	4.782	.001
	Genotype * Age	9979.974	4	2494.993	3.110	.016
	Error	196542.520	245	802.214		
	Total	869359.501	256			
	Corrected Total	225644.124	255			
1st probe trial	Corrected Model	2048.735[b]	9	227.637	.876	.576
	Intercept	.000	0	.	.	.
	Day	.000	0	.	.	.
	Genotype	558.286	1	558.286	2.149	.177
	Age	1357.750	4	339.438	1.306	.338
	Genotype * Age	541.149	4	135.287	.521	.723
	Error	2338.476	9	259.831		
	Total	17035.920	19			
	Corrected Total	4387.212	18			
training 7-11 day	Corrected Model	14737.051[c]	10	1473.705	1.820	.060
	Intercept	7837.006	1	7837.006	9.679	.002
	Day	954.446	1	954.446	1.179	.279
	Genotype	1183.781	1	1183.781	1.462	.228
	Age	6932.024	4	1733.006	2.140	.078
	Genotype * Age	10000.764	4	2500.191	3.088	.017
	Error	143311.420	177	809.669		
	Total	673086.633	188			
	Corrected Total	158048.471	187			
2nd probe trial	Corrected Model	1114.354[d]	7	159.193	5.911	.034
	Intercept	.000	0	.	.	.
	Day	.000	0	.	.	.
	Genotype	399.500	1	399.500	14.834	.012
	Age	601.284	4	150.321	5.582	.044
	Genotype * Age	174.513	2	87.257	3.240	.125
	Error	134.657	5	26.931		
	Total	5733.851	13			
	Corrected Total	1249.010	12			

a. R Squared = .129 (Adjusted R Squared = .093)

b. R Squared = .467 (Adjusted R Squared = -.066)

c. R Squared = .093 (Adjusted R Squared = .042)

d. R Squared = .892 (Adjusted R Squared = .741)

Table 32. Statistical calculation for the T-maze test/Number of successfully reached goals during 2nd series.

Tests of Between-Subjects Effects

Dependent Variable:Goal

DayCateg	Source	Type III Sum of Squares	df	Mean Square	F	Sig.
training 1-5 day	Corrected Model	54.762[a]	15	3.651	4.023	.000
	Intercept	86.891	1	86.891	95.750	.000
	Day	.005	1	.005	.006	.941
	Genotype	.417	1	.417	.460	.500
	Weight	2.381	2	1.190	1.312	.275
	Age	14.669	4	3.667	4.041	.005
	Genotype * Weight	.000	0	.	.	.
	Genotype * Age	23.814	2	11.907	13.121	.000
	Weight * Age	4.817	1	4.817	5.308	.024
	Genotype * Weight * Age	.000	0	.	.	.
	Error	76.228	84	.907		
	Total	751.000	100			
	Corrected Total	130.990	99			
1st probe trial	Corrected Model	.950[b]	14	.068	8.106E29	.000
	Intercept	.000	0	.	.	.
	Day	.000	0	.	.	.
	Genotype	.000	1	.000	.000	1.000
	Weight	.355	2	.177	2.118E30	.000
	Age	.278	4	.070	8.311E29	.000
	Genotype * Weight	.000	0	.	.	.
	Genotype * Age	.000	2	.000	.000	1.000
	Weight * Age	.000	1	.000	.000	1.000
	Genotype * Weight * Age	.000	0	.	.	.
	Error	4.185E-31	5	8.371E-32		
	Total	19.000	20			
	Corrected Total	.950	19			
training 7-11 day	Corrected Model	62.970[c]	15	4.198	4.420	.000
	Intercept	1.665	1	1.665	1.753	.189
	Day	1.620	1	1.620	1.706	.195
	Genotype	.593	1	.593	.625	.432
	Weight	21.967	2	10.983	11.564	.000
	Age	13.201	4	3.300	3.475	.011
	Genotype * Weight	.000	0	.	.	.
	Genotype * Age	40.930	2	20.465	21.548	.000
	Weight * Age	1.350	1	1.350	1.421	.237
	Genotype * Weight * Age	.000	0	.	.	.
	Error	79.780	84	.950		
	Total	485.000	100			
	Corrected Total	142.750	99			
2nd probe trial	Corrected Model	3.383[d]	14	.242	1.036	.529
	Intercept	.000	0	.	.	.
	Day	.000	0	.	.	.
	Genotype	.028	1	.028	.119	.744
	Weight	.788	2	.394	1.689	.275
	Age	1.395	4	.349	1.495	.331
	Genotype * Weight	.000	0	.	.	.
	Genotype * Age	.986	2	.493	2.112	.216
	Weight * Age	.750	1	.750	3.214	.133
	Genotype * Weight * Age	.000	0	.	.	.
	Error	1.167	5	.233		
	Total	13.000	20			
	Corrected Total	4.550	19			

a. R Squared = .418 (Adjusted R Squared = .314)

b. R Squared = 1.000 (Adjusted R Squared = 1.000)

c. R Squared = .441 (Adjusted R Squared = .341)

d. R Squared = .744 (Adjusted R Squared = .026)